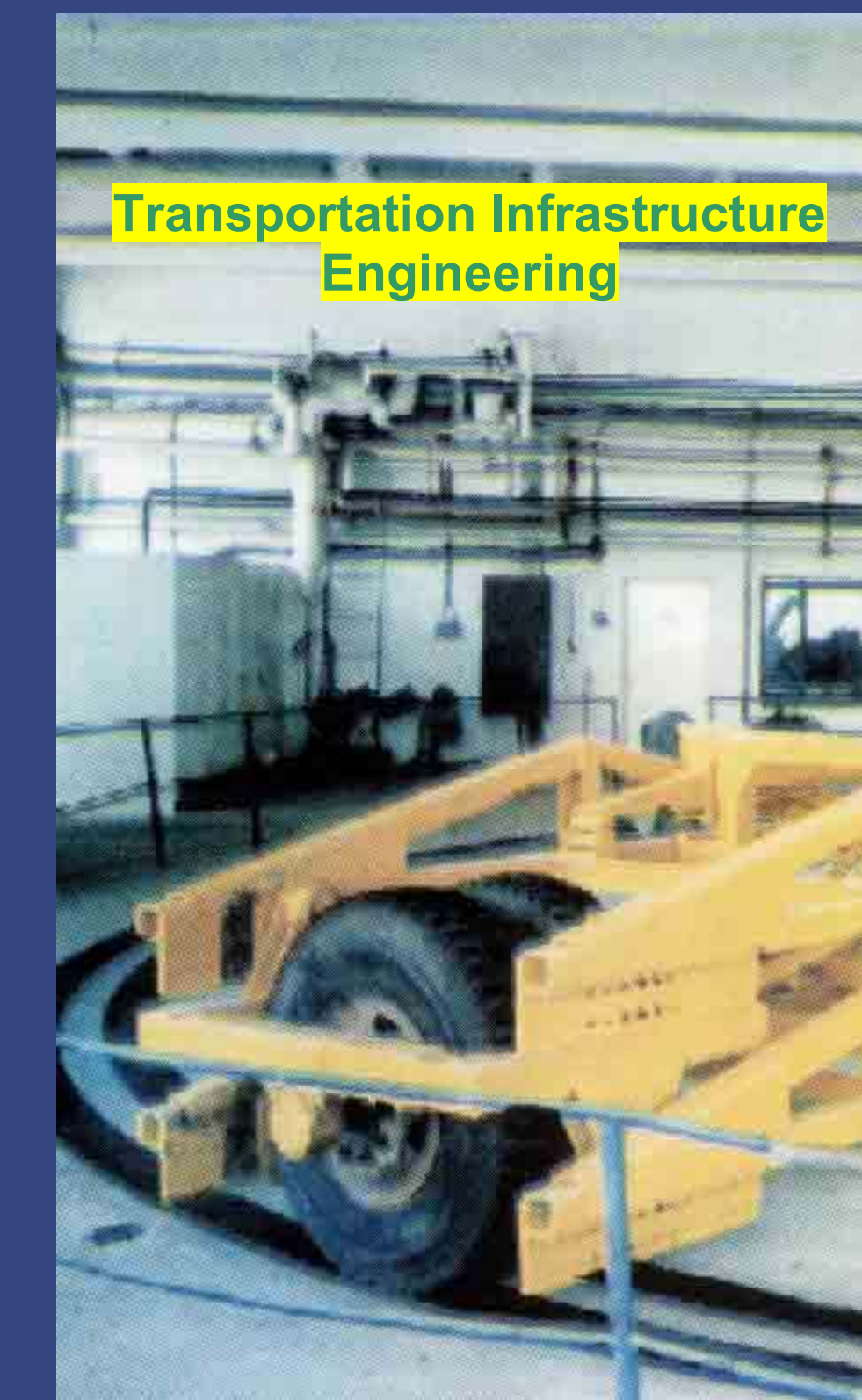


SZO

Volume 4, No.1, 2006

SERSECTII

ш S **M** 田 ト ス



INTERSECTII http://www.ce.tuiasi.ro/intersections

Rodian SCINTEIE Issue Editor

Executive Director, CERT-CESTRIN Bucharest rodian.scinteie@gmail.com

Radu ANDREI Team Leader

Department of Soil Mechanics and Transportation Infrastructures Faculty of Civil Engineering Technical University "Gh. Asachi" of Iaşi, România randrei@catv.embit.ro

Horia Gh. ZAROJANU

Department of Soil Mechanics and Transportation Infrastructures Faculty of Civil Engineering Technical University "Gh. Asachi" of Iaşi, România zarojanu@ce.tuiasi.ro

Nicolae Vladimir VLAD

Department of Soil Mechanics and Transportation Infrastructures Faculty of Civil Engineering Technical University "Gh. Asachi" of Iaşi, România vladnic03@yahoo.fr

Vasile BOBOC

Department of Soil Mechanics and Transportation Infrastructures Faculty of Civil Engineering Technical University "Gh. Asachi" of Iaşi, România vboboc@ce.tuiasi.ro

Gheorghe GUGIUMAN

Department of Soil Mechanics and Transportation Infrastructures Faculty of Civil Engineering Technical University "Gh. Asachi" of Iaşi, România gugiuman@ce.tuiasi.ro

Dan POPOVICI

Department of Soil Mechanics and Transportation Infrastructures Faculty of Civil Engineering Technical University "Gh. Asachi" of Iaşi, România popovicid@ce.tuiasi.ro

Benonia COSOSCHI

Department of Soil Mechanics and Transportation Infrastructures Faculty of Civil Engineering Technical University "Gh. Asachi" of Iaşi, România bcososchi@ce.tuiasi.ro



INTERSECTII http://www.ce.tuiasi.ro/intersections

Diana Irinel VRÂNCIANU

Department of Soil Mechanics and Transportation Infrastructures Faculty of Civil Engineering Technical University "Gh. Asachi" of Iaşi, România diana_tuna@yahoo.co.uk

Aura GAVRILUŢĂ

Department of Soil Mechanics and Transportation Infrastructures Faculty of Civil Engineering Technical University "Gh. Asachi" of Iaşi, România aura_gavriluta@yahoo.com

Cristina LUCACHE

Department of Soil Mechanics and Transportation Infrastructures Faculty of Civil Engineering Technical University "Gh. Asachi" of Iaşi, România cristina_lucache@yahoo.com

INSERSECTII http://www.ce.tuiasi.ro/intersections

Analysis of dynamic parameters of rail fastening by Rihaczek transformation	
by J. Smutny, L. Pazdera	pp.5-14
Wind Dynamic Response of a Suspension Pedestrian Br by O.M. Stan	ridge pp.15-24
Discrete model for the stability of continuous welded ra by A. Dósa, V.V. Ungureanu	il pp.25-34
Non-linear effects in traffic simulations by T. Apeltauer, P. Holcner, M. Kysely, J. Macur	pp.35-48
The Structural Expertise of Steel Cables by L.G. Kopenetz, F-Zs. Gobesz	pp.49-62
Quality costs in Bridge Engineering by A. Nicuță, C. Ionescu	pp.63-70
Sensitivity study of a model for the stability analysis of continuous welded rail by V.V. Ungureanu, M. Comanici	pp.71-78
The Generalized Mohr-Coulomb (GMC) Yield Criterion	n and



pp.79-85

some implications on characterization of pavement materials

by M. Balcu, Ş.M. Lazăr

INTERSECTII http://www.ce.tuiasi.ro/intersections

The use of the bi-spectrum for analysis dynamic parameters of rail fastening by J. Smutny, L. Pazdera pp.86-93

1 Parametrical study of the effect of the torsional resistance of the fastenings on the stability of continuous welded rail pp.94-102 by V.V. Ungureanu, A. Dósa



INTERSECTII http://www.ce.tuiasi.ro/inters

Analysis of dynamic parameters of rail fastening by Rihaczek transformation

Jaroslav Smutny¹, Lubos Pazdera²

¹Department of Railway Constructions and Structures, Faculty of Civil Engineering, University of Technology Brno, Brno, 602 00, Czech Republic ²Department of Physics, Faculty of Civil Engineering, University of Technology Brno, Brno, 602 00, Czech Republic

Summary

For evaluation of response signals obtained by rail fastening analysis a new method using time and frequency related transformations has been developed. In the paper the laboratory measurements and dynamic parameter analyses of flexible fastening of Vossloh SKL14 type have been described. The method can also be used for designing new rail fastening systems and their parts.

KEYWORDS: Rail fastening, dynamic test, time frequency transform

1. INTRODUCTION

The basis for the selection and comparison of new components of rail superstructure are also theoretical analysis (simulation) and static and dynamic tests carried out in the laboratory and in the field (directly on the railway) [9]. It is necessary to mention that theoretical analysis of application of mathematical simulation is often based on idealized assumptions. Hence, when the real conditions on the railway or tramway superstructure are encountered, the model may be inaccurate.

For testing the railway superstructure construction, different methods and different criterions were applied. Dynamic testing [4] often uses the method of exciting the structure by mechanical shock. Exciting by shock is useful for the setting up a given set of frequencies as the shock, according to the theory, stimulates all frequencies, mainly resonant. Mechanical shock is often stimulated by a special hammer, which has an incorporated power sensor in radial direction to the railhead.

The response is measured by accelerometer sensors at different points of the rail structure (rail foot, clip plate, clamp, sleeper etc). This method makes it possible to record frequency components in the range 1 Hz to 10 kHz. Recorded data are often recalculated and presented in the form of the frequency transfer function. This



INTERSECTII http://www.ce.tuiasi.ro/intersections

J. Smutny, L. Pazdera

shows important frequency components (mainly resonant) that include information about dynamic properties of particular parts of tested structure.

Often in the experimental investigation of dynamic properties [5] of rail fastening, the measurement and calculation of the transfer function is called accelerance (inverse function of dynamic weight). It is for that reason that the acceleration transducer is the most suitable electromechanical measurement device for the measuring of oscillation. Accelerance is defined by the relation

$$H_{aF}(f) = \frac{S_{aF}(f)}{S_{FF}(f)} \tag{1}$$

where $S_{aF}(f)$ is cross spectrum of response and entry signal, S_{FF} is auto-spectrum of entry signal. From the relation (1) it can be seen that measured acceleration is standardized for power measured during the shock.

In spite of the advantages, it is not possible to localize the time behavior of frequency components included in the signal. Therefore for the evaluation of response signals when analyzing the rails fastenings, the authors supplemented the methods of the measurements by utilizing progressive processes of signal analysis, i.e. by utilizing time frequency transformations.

One possible procedure to analyze time occurrence of frequency components of transfer and non-stationary signals, is the use of the so-called time frequency proceedings (transformations). These can be distributed according to two basic groups [3]:

- linear (including mainly Short Time Fourier Transformation, Wavelet Transformation etc.)
- non-linear (including mainly quadratic Cohen Transformations, Affine and Hyperbolic Transformation, eventually further special proceedings)

2. THEORY OF TIME FREQUENCY ANALYSIS

Given a time series, x(t), it can readily be seen how the "energy" of the signal is distributed in time. By performing a Fourier transform to obtain the spectrum, X (ω), it can also be seen how the "energy" of the signal is distributed in frequency. For a stationary signal, there is usually no need to go beyond the time or frequency domains. However, most real world signals have characteristics that change over time, and the individual domains of time and frequency do not provide a means for extracting this information. The general goal of this contribution is to demonstrate some lesser-known methods for creating functions that represent the energy of the signal simultaneously in time and frequency.



INTERSECTII http://www.ce.tuiasi.ro/inters

Analysis of dynamic parameters of rail fastening by Rihaczek transformation

Example of linear time-frequency distributions is the Short Time Fourier Transformation. The main idea of the Short Time Fourier Transform (STFT) is to split a non-stationary signal into fractions within which stationary assumptions apply and to carry out a Fourier transform on each of these fractions. The STFT is defined by equation [3, 4]

$$STFT(\tau, f) = \int_{-\infty}^{\infty} [x(t) \cdot g^*(t - \tau)] \cdot e^{-j \cdot 2 \cdot \pi \cdot f \cdot t} \cdot dt$$
 (2)

where '*' denotes the complex conjugate, g is the short time window, x(t) is the signal, τ is the time location parameter, f is frequency and t is time. In the two dimensional time-frequency joint representation, the vertical stripes of the complex valued STFT coefficients STFT(τ , f) correspond to the Fourier spectra of the windowed signal with the window shifted to given times τ . The main disadvantage of linear time-frequency transform is that the time frequency resolution is limited to the Heisenberg bound. This is due to the imposition of local time window g(t). If this window is more resolved in time, the frequency resolution suffers because the effective width of its Fourier transform G(f) increases, and vice-versa.

Quadratic (non-linear) methods present the second fundamental class of time frequency distributions. Quadratic methods are based upon estimating an instantaneous power (or energy) spectrum using a bilinear operation on the signal x(t) itself. The class of all quadratic time-frequency distributions to time shifts and frequency-shift is called Cohen's class. Similarly, the class of all quadratic timefrequency distributions covariant to time-shift and scales is called the Affine class. The intersection of these two classes contains time-frequency distributions, like the Wigner-Ville distribution, that are covariant to all operators.

Cohen [1] generalized the definition of the time frequency distributions in such a way as to include a wide variety of different distributions. These different distributions can be represented in several ways. Cohen's class definition like the Fourier Transformation, with respect to τ , of the generalized local correlation function is most common. With a two-dimensional kernel, the bilinear time frequency distribution of the Cohen's class is defined according to equation [2]:

$$C_{x}(t,f) = \iiint e^{-j\cdot 2\pi\cdot\theta\cdot t'-j\cdot 2\pi\cdot f\cdot \tau+j\cdot 2\pi\cdot\theta\cdot t} \cdot \psi(\theta,\tau) \cdot x\left(t+\frac{\tau}{2}\right) \cdot x^{*}\left(t-\frac{\tau}{2}\right) \cdot d\theta \cdot dt \cdot d\tau$$
(3)

where x is the signal, t(t') is the time, τ is the time location parameter, ω is angular frequency, θ is shift frequency parameter, $\psi(\theta, \tau)$ is called the kernel of the time frequency distribution. A distribution C_x (t, f) from Cohen's class can be interpreted as the two-dimensional Fourier Transformation of a weighted version of the ambiguity function of the signal



INTERSECTII http://www.ce.tuiasi.ro/inters

J. Smutny, L. Pazdera

$$C_{x}(t,f) = \iint A_{x}(\theta,\tau) \cdot \psi(\theta,\tau) \cdot e^{-j \cdot 2\pi \cdot f \cdot \tau} \cdot e^{-j \cdot 2\pi \cdot \theta \cdot t} \cdot d\tau \cdot d\theta \tag{4}$$

where $A_x(\theta, \tau)$ is the ambiguity function of the signal x(t), given by equation:

$$A(\theta, \tau) = \int x \left(t + \frac{\tau}{2} \right) \cdot x^* \left(t - \frac{\tau}{2} \right) \cdot e^{-j \cdot \theta \cdot t} \cdot dt$$
 (5)

We note that all integrals run from $-\infty$ to ∞ . The weighted function $\psi(\theta, \tau)$ is called the kernel. It determines the specific properties of the distribution. The product $A_x(\theta, \tau) \cdot \psi(\theta, \tau)$ is known as the characteristic function.

Since the ambiguity function is a bilinear function of the signal, it exhibits cross components, which, if allowed to pass into time frequency distribution, can reduce auto-component resolution, obscure the true signal feature, and make interpretation of the distribution difficult. Therefore, the kernel is often selected to weight the ambiguity function such that the auto-components, which are centered at the origin of the (θ, τ) ambiguity plane, are passed, while the cross-components, which are located away from origin, are suppressed. This means that the suppression of crosscomponents might be understood as the frequency response of a two-dimensional low-pass filter.

When a low pass kernel is employed, there is a trade-off between crosscomponents suppression and auto-component concentration. Generally, as the band-pass region of the kernel is made smaller, the amount of cross-component suppression increases, but at the expense of auto-component concentration. There is definition of the kernel for Rihaczek Transformation in equation 6

$$\psi(\theta,\tau) = e^{\frac{j\cdot\theta\cdot\tau}{2}}. (6)$$

Equation 4 can also be rewritten into the following form [5]

$$C_{x}(t,f) = \int_{-\infty}^{\infty} \int_{-\infty}^{\infty} \Pi(\tau - t,\theta - f) \cdot WVT(\tau,\theta) \cdot d\tau \cdot d\theta$$
 (7)

where

$$\Pi(t,f) = \int_{-\infty}^{\infty} \int_{-\infty}^{\infty} \psi(\theta,\tau) e^{-j\cdot 2\cdot \pi\cdot (f\cdot \tau - \theta\cdot t)} \cdot dt \cdot d\omega$$
 (8)

is the two-dimensional Fourier transform of the kernel w and WVT presents Wigner-Ville transform. Cohen's class has a simple interpretation as a smoothed Wigner-Ville distribution [5].



INTERSECTII http://www.ce.tuiasi.ro/intersections

Analysis of dynamic parameters of rail fastening by Rihaczek transformation

3. ANALYSIS OF DYNAMIC PARAMETERS

The model used for laboratory measurements and analysis of dynamic parameters of a sample of rail fastening is presented below. The rail grid model was constructed of concrete sleepers B 91, on which there were fastened rails of construction shape UIC 60 by flexible fastening Vossloh SKL14.

For the testing of the dynamic properties of the sample, the method of measuring the response to mechanical shock was used. Mechanical shock was stimulated by a special hammer in the radial direction on the railhead. A part of this hammer is a force detector.

The response was measured by accelerometers at different points of the rail structure, on the rail foot and sleepers (10 cm from fastening). Figure 1 show the location of detectors. From the response time signals frequency transfer functions (accelerance) were calculated in order to obtain standardized responses [5].

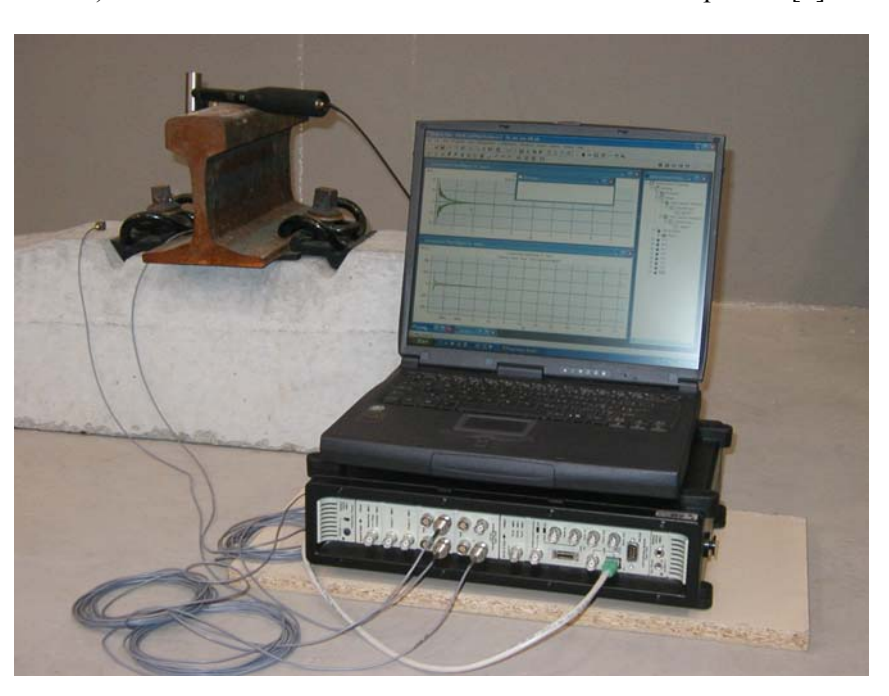


Figure 1 General view of the working place

Signals from measurements on the rail and sleepers were used for the presentation of particular analyses in this contribution. The measuring system consisted of a Brüel and Kjaer PULSE modular analyses for recording the vibration parameters together with B&k cubic acceleration detector and a B&k shock stimulation hammer (Figure 1).



INTERSECTI http://www.ce.tuiasi.ro/inte

http://www.ce.tuiasi.ro/intersections

J. Smutny, L. Pazdera

The accelerometers were fastened to the measured construction by means of bee wax. The results were recorded digitally.

The analysis of the response to mechanical shock was evaluated by means of the following methods and parameters [5]:

- Time records of the duration of impulse response function (in principle standardized acceleration value)
- Frequency analysis with the use of frequency response function (according to equation 1)
- Time-frequency method of spectral analysis (for the transfer from time to time- frequency domain, the algorithm of Short Time Fourier Transformation and Rihaczek Transformation was used)

Time histories of the impulse response function, recorded by accelerometers, located on the rail foot, are depicted on the upper graph of Figure 2. The maximum positive value of acceleration of 300 m·s⁻² is reached 1 ms from the observed beginning. The maximum negative value of acceleration of -300 m·s⁻² is reached 2 ms from the beginning. Damping of the signal from the acceleration 300 m·s⁻² to the acceleration lower than 30 m·s⁻² took 15 ms.

In the left graph of Figure 2 is depicted the amplitude spectrum of this frequency response function calculated according to equation 1. In the graph, six important frequencies (0.2 kHz, 0.7 kHz, 1.9 kHz, 2.4 kHz, 3.3 kHz and 3.7 kHz), are visible. The important values are taken as those which have the damping up to 20 dB from the maximum value of amplitude spectrum.

Time frequency amplitude spectrum estimated by application of Short Time Fourier Transformation to the impulse response function is depicted in the middle graph in Figure 2. As shown on this graph, the time history of important frequency components essentially differ.

Frequency component 1.9 kHz reaches the highest values for a relatively long time (compared to other frequency components). It appears in the signal nearly in its full history, i.e. approximately 40 ms by damping up to 40 dB. The second most important component is the frequency 3.3 kHz. This appears in signal up to the time of 20 ms from the above. Other notable frequencies 2.4 kHz and 3.7 kHz are in the signal for the time of 5 ms up to 15 ms.

Similar conclusions are visible from the middle graph of Figure 3, which present the analysis of impulse response function on the rail foot by the use of Rihaczek Transformation. This transform belong to the category of non-linear time frequency proceedings from the Cohen class.



INTERSECTII

http://www.ce.tuiasi.ro/intersections

Analysis of dynamic parameters of rail fastening by Rihaczek transformation

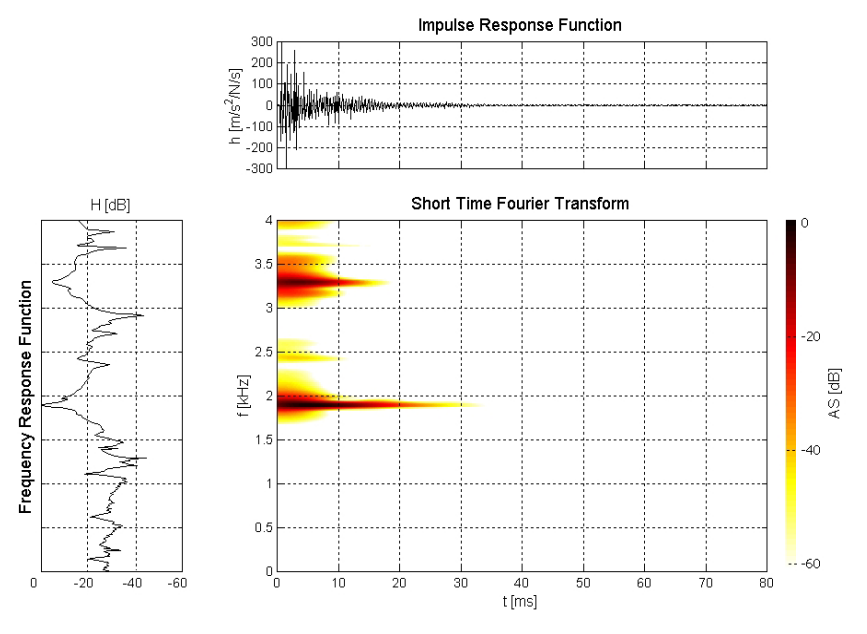


Figure 2 Accelerometric detector located on the rail foot, time frequency analysis by Short Time Fourier Transformation

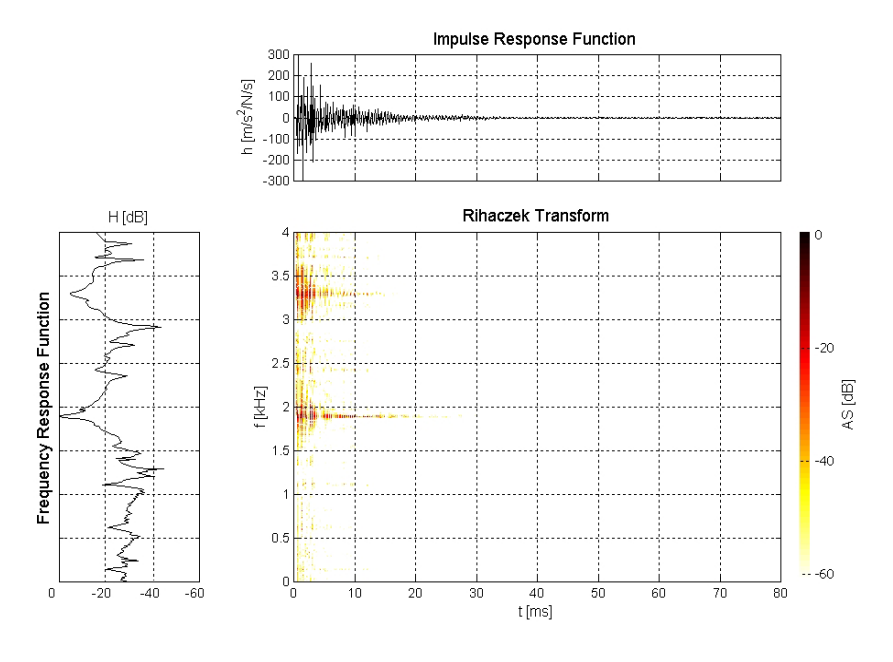


Figure 3 Accelerometric detector located on the rail foot, time frequency analysis by Rihaczek Transformation



INTERSECTII

http://www.ce.tuiasi.ro/intersections

J. Smutny, L. Pazdera

Signals (impulse response function) taken by a second transducer, located on the concrete sleeper, have different character. From the time record (see upper graph of Figure 4) it is apparent that the maximum impulse response function amplitude acquires lower frequency values as a result of the influence of the transformation of the signal through the fastening of rail, clip plate, sleeper to the accelerometer and reaches values of 50 m·s⁻². These values were reached 2 ms from the first rise time from "amplitude pack". Values of acceleration are considerably lower than those by the transducer located on the rail foot which was located nearer to the source of mechanical impulse.

In the left graph of Figure 4 is depicted the amplitude spectrum of frequency response function. The form of spectrum considerably differs from the characteristics measured by the first transducer located on the rail foot. The most important components appear in the lower frequencies from the transducer located on the rail foot: in the interval of 0.2 kHz up to 2 kHz, there are also more in number.

Similar conclusions are given by the middle graph of Figure 4 which presents the time frequency amplitude spectrum estimated by the application of the Short Time Fourier Transformation. From this graph it can be seen that time occurrence of significant components included in signal is considerably shorter (the longest is approx. 20 ms from the imaginary beginning) than it is from the signal from transducer located on the rail foot.

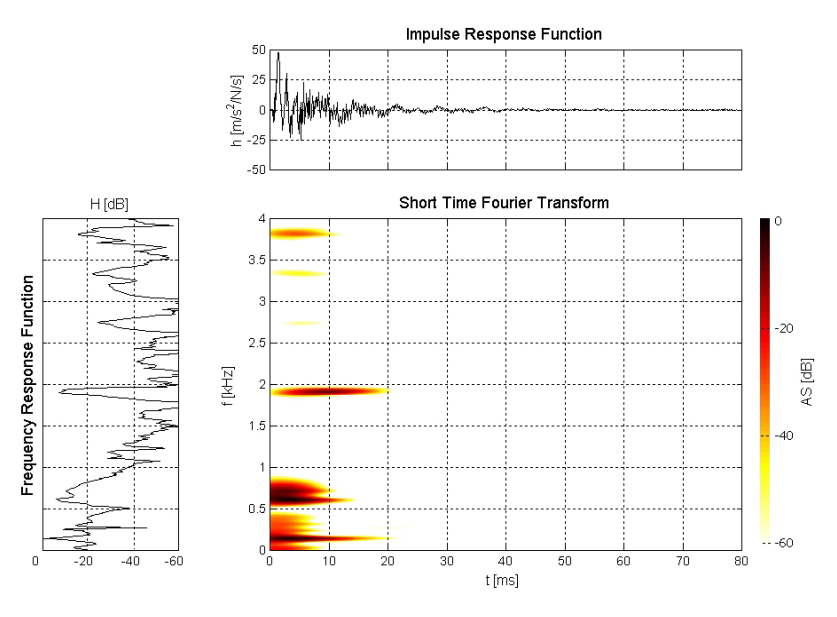


Figure 4 Accelerometric detector located on concrete sleeper, time frequency analysis by Short Time Fourier Transformation

INTERSECTII

http://www.ce.tuiasi.ro/intersections

Analysis of dynamic parameters of rail fastening by Rihaczek transformation

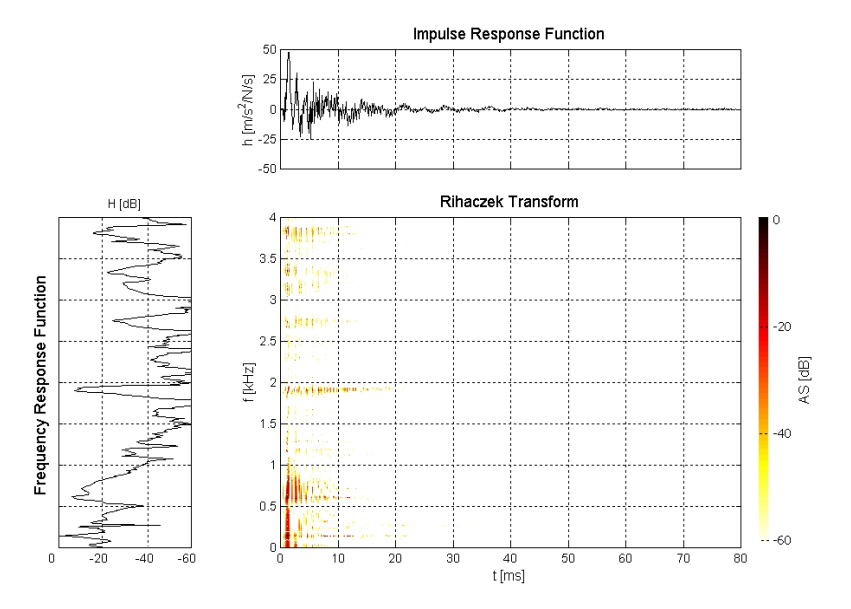


Figure 5 Accelerometric detector located on concrete sleeper, time frequency analysis by Rihaczek Transformation

Similar conclusions apply to the middle graphs of Figure 5 which present the analysis of signals from transducers located on the sleeper by the use of Rihaczek Transformation. The significant frequency components which are calculated by the Rihaczek Transformation (Figure 6) are frequencies of 0.2 kHz, 0.7 kHz, 1.9 kHz, 2.7 kHz, 3.2 kHz, 3.4 kHz and 3.7 kHz. The most significant spectrum component is the frequency component 0.2 kHz which appears within this spectrum for a relatively long time in relation to the activity of other components.

On the whole, it is possible to state from the middle graphs in Figure 2 to Figure 5 that in contrast to linear methods whose ability to resolve the frequency elements in the time region is limited by certain window functions, quadratic methods can achieve this objective. Higher distinguishing makes more favorable localization of significant frequency components in time possible.

The quality of time and frequency achieved by measuring the signal response to mechanical shock and applying by these transformations is a good choice.

4. CONCLUSIONS

Based on measurements and analyses, it is possible to state that the methods presented above are very good for the measurement of dynamic parameters of rail

INTERSECTII http://www.ce.tuiasi.ro/inters

http://www.ce.tuiasi.ro/intersections

J. Smutny, L. Pazdera

fastenings. The use of these methods enables the testing of new types of rail fastenings and different types of rail washers under rails and the opportunity to optimize the geometric location of damping elements on rail etc. From the mathematical means of signal analysis it is possible to utilize both Short Time Fourier Transformation and Rihaczek Transformation for time-localization of the occurrence of frequency elements of stationary and non-stationary signals.

Based on the experience acquired, it is of great advantage for the analysis of real signals to utilize the properly selected time and frequency sections. This procedure seems to be more suitable than the spatial arrangement. It is possible for more precise localization of time records to separate significant frequency components or to depict all important frequencies. Analysis of signals, acquired by measurement and analysis of response to mechanical shock gives new, more detailed insights to transition characteristics of railway and tramway structures. Hence, it grants valuable knowledge for a thorough analysis of these constructions, which can be important for consequent optimization of construction and operational conditions. Also the fact that by time frequency proceedings analysis of dynamic load of railway and tramway constructions provides real data for consequent formulation of mathematical models. From this point of view, both linear and non-linear time frequency transformations are applicable. These methods give a fast and accurate localization of frequency components included in the measured signal. It is possible to apply the described method successfully not only on samples of several constructions of railway and tramway superstructure but also directly in the field on real tracks.

Acknowledgements

This research has been supported by the research project 103/07/0183 ("The investigation of dynamic effects due to the rail transport by the method of quadratic time and frequency invariant transformations ") and by research project MSM 0021630519 ("Progressive reliable and durable load-bearing structural constructions")

References

- 1. Cohen L., Time-frequency distributions, Proc. IEEE, 1989, vol. 77 no. 7, pp. 941-981
- 2. O'Neill J.C., Quartic Functions for Time-Frequency Analysis with Applications to Signal Adaptive Kernel Design, SPIE - Advanced Signal Processing Algorithms, 1997
- 3. Poularikas A. D.: The Transform and Applications Handbook, IEEE Press, 1996
- 4. Melcer, J., Kucharova, D.: Mechanical properties of rubber pads under static and dynamic load, proceedings of International Conference on Materials Science and Engineering, BRAMAT 2003, Romania, Brasov, 3/2003, University of Brasov, 2003, pp. 18-314.
- 5. Smutný J., Pazdera L.: New techniques in analysis of dynamic parameters rail fastening, InSight, The Journal of The British Institute of Non-Destructive Testing, Vol 46, No 10, October, 2004, pp. 612-615, ISSN 13542575



INTERSECTII http://www.ce.tuiasi.ro/intersections

Wind Dynamic Response of a Suspension Pedestrian Bridge

Oana Mihaela Stan

Department of Mechanics, Statics and Dynamics of Structures, Technical University of Civil Engineering, Bucharest, Zip code 72302, Romania

Summary

The paper presents wind dynamic response of a suspension pedestrian bridge. Dynamic response of the structure was obtained by performing two analyses: modal superposition (linear analysis) and direct integration of equation of motion (geometric nonlinear analysis). The aerodynamic instability of the suspension structure was studied too. All the analysis was carried out by LUSAS (FEM) program.

KEYWORDS: Geometric nonlinear analysis, Dynamic response

1. INTRODUCTION

After the disaster of Tacoma Narrows Bridge in 1940 attention focused on the dynamic problems of suspension bridges. The great span length of suspension bridges makes their static and dynamic behavior under the action of lateral forces an important problem. The most significant forces are due to wind and to the earthquakes.

In order to obtain a correct response of the structure subjected to dynamic loads it is absolute necessary to carry out nonlinear dynamic analysis.

Time history response of the suspension bridge will be obtained in two load cases: mean velocity wind action and for gust of wind.

2. PEDESTRIAN SUSPENSION BRIDGE

Pedestrian Suspension Bridge was designed as a link between Burjuc and Tisa, over Mures River.

The superstructure consist in a steel continuous lattice girder over three spans (40,00 m + 120,00 m + 40,00 m) (Figure 1.).

The deck is a triangular system with 1,55 m high and 2,20 m width and stiffening frame at superior and inferior sole.



INTERSECTII http://www.ce.tuiasi.ro/intersections

O.M. Stan

The suspension system is formed by the main parabolic suspension cables and vertical hangers. Each main suspension cable is it made from three steel carrying cables with 60 mm in diameter. The vertical hangers are made from 6 round steel bars with 21 mm in diameter, placed at 5,00 m one to another along the central span.

The steel towers has A shape in longitudinal and transversal plane. The high of the towers is 25,40 m. The towers are supported on two caisson indirect column foundations.

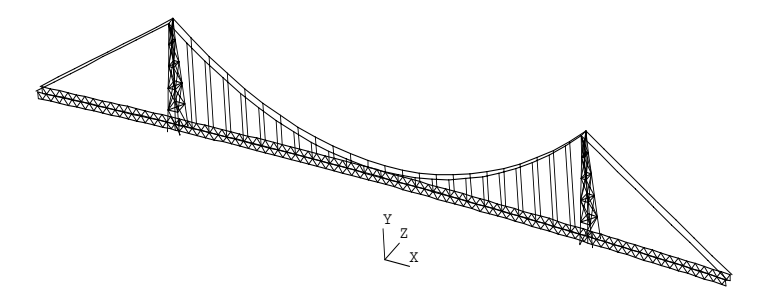


Figure 1. Finite element model

3. FINITE ELEMENT MODEL

The structure has a pronounced spatially behavior. This is the reason that lead to a discrete spatially model. The finite elements (3D beam) were chosen to allow running nonlinear geometric analysis. Discrete model of the structure has 3088 nodal points and 1330 beam finite elements, [6].

4. STRUCTURE ANALYSIS

4.1. Static analysis

The geometric nonlinearity of the suspension system of the structure require static nonlinear analysis (modified Newton – Raphson), [3].

The wind pressure acting in global direction Z is 2 kN/m² according to the standards.

A comparative study between linear and nonlinear geometric static analysis is illustrated in Figure 2. Lateral flexibility of the suspension system is revealed by



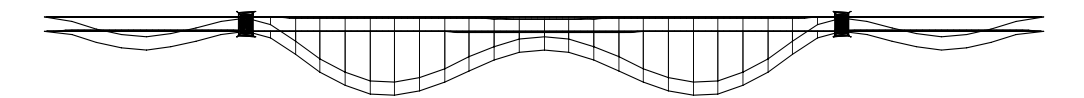
INTERSECTII

http://www.ce.tuiasi.ro/intersections

Wind Dynamic Response of a Suspension Pedestrian Bridge

the evaluation of the displacements of the main suspension cables in both linear and geometric nonlinear static analysis.

Maximum displacement for the middle of central span 0,248 m – linear static analysis 0,246 m – geometric nonlinear static analysis



Maximum displacement for the cables 5,300 m – linear static analysis 1,206 m – geometric nonlinear static analysis

Figure 2. Maximum displacement for wind pressure

4.2. Modal analysis

The necessity of running a modal analysis result from the prescription of different European codes for vibration response of the suspension structure, [1], [4].

The 3D discrete model was subjected to modal analysis is order to obtain the first 15 eigenvalues and mode shapes.

In Figure 3. are presented the most significant mode shape of the suspension bridge: the first symmetric mode of lateral vibration of the deck (Mode No. 1), the first anti-symmetric mode of vertical vibration (Mode No. 2), the first symmetric mode of lateral vibrations of the towers (Mode no. 9) and the first mode of torsional vibrations (Mode no. 11).

4.3. Wind effect according to different European prescription

Once eigenvalues and mode shape obtained from modal analysis, it can be use to evaluate wind velocity corresponding to specific dynamic effects.

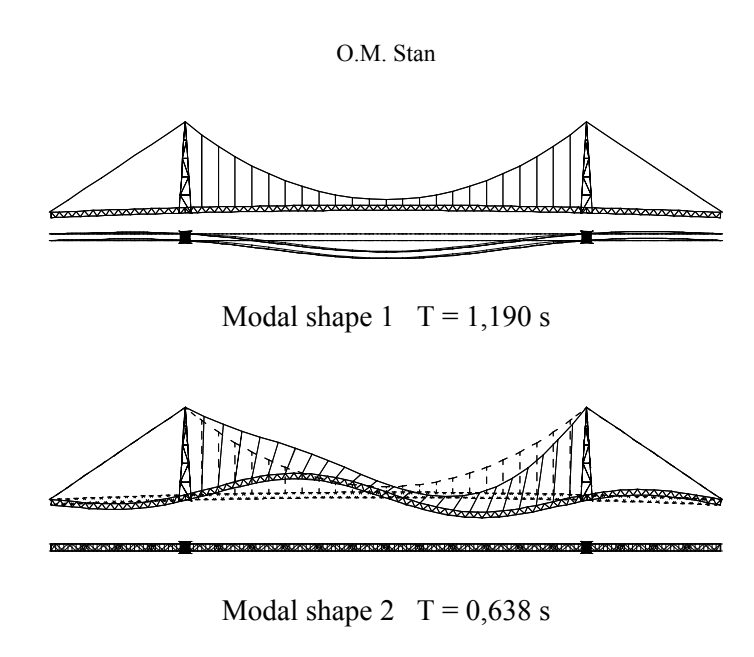
Not all the specific effects were reflected in European prescription. This is the reason that wind critical values are evaluated only according to some prescription.

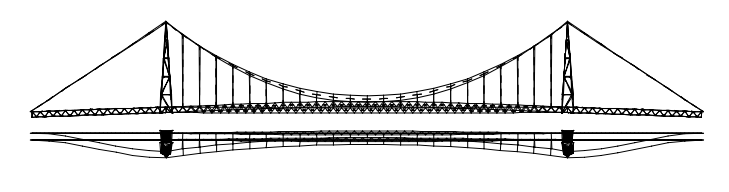
Evaluation of wind response involve studies about limited amplitude oscillations, divergent amplitude oscillations and non-oscillatory divergent movements, [1], [4], [8], [9].



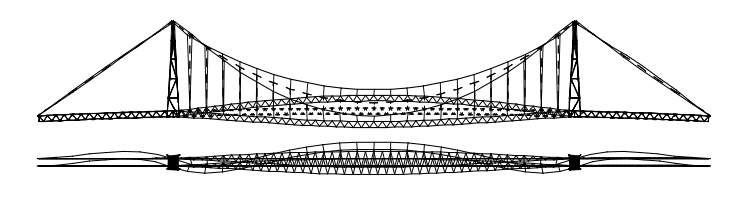
INTERSECTII

http://www.ce.tuiasi.ro/intersections





Modal shape 9 T = 0.228 s



Modal shape 11 T = 0.218 s

Figure 3. The most significant modal shapes

Conclusion: Pedestrian suspension bridge present aerodynamic stability for wind turbulence, for von Karman gust and flutter effect (the most dangerous dynamic effect of the wind acting on suspension bridges), [6].



INTERSECTION

http://www.ce.tuiasi.ro/intersections

Wind Dynamic Response of a Suspension Pedestrian Bridge

4.4. Resonance amplitude

The first 15 natural frequencies of the structure were in the range of 0.00 - 6.00 Hz. Wind response will be studied in the same range of frequency.

The structure response is presented for two nodal points which offer the most significant information.

For the tower - the maximum lateral displacement of a nodal point lead to the top of the tower.

For the deck - the maximum lateral displacement of a nodal point corresponding to the middle of the central span.

The structure response in frequency domain due to wind excitation is presented in Figure 4. and Figure 5.

The resonance amplitude of 4,39 Hz at the top of the tower is related to the first natural frequency of symmetric lateral vibration mode (Mode no. 9). In the same way, the resonance amplitude of 0,84 Hz at the middle of the central span is related to the first natural frequency of symmetric lateral vibration mode (Mode no. 1). The amplitude in X and Y global directions can be neglected instead of Z global direction.

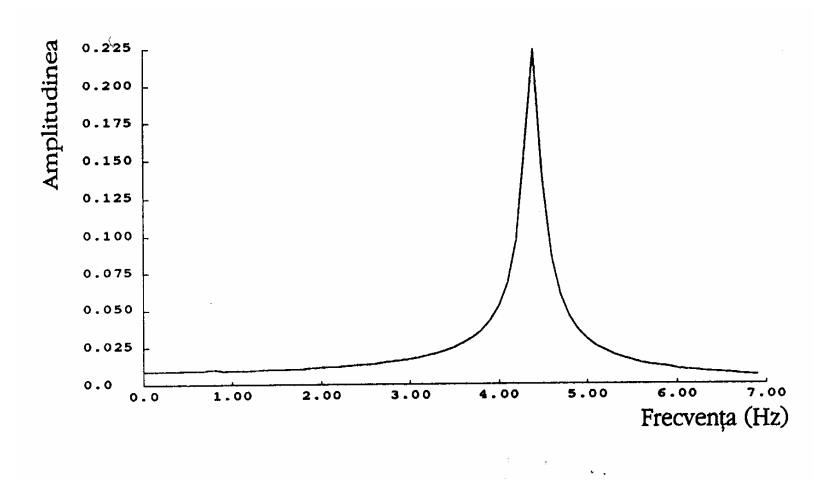


Figure 4. Resonance amplitude for the top of the tower due to wind excitation

INTERSECTII

http://www.ce.tuiasi.ro/intersections

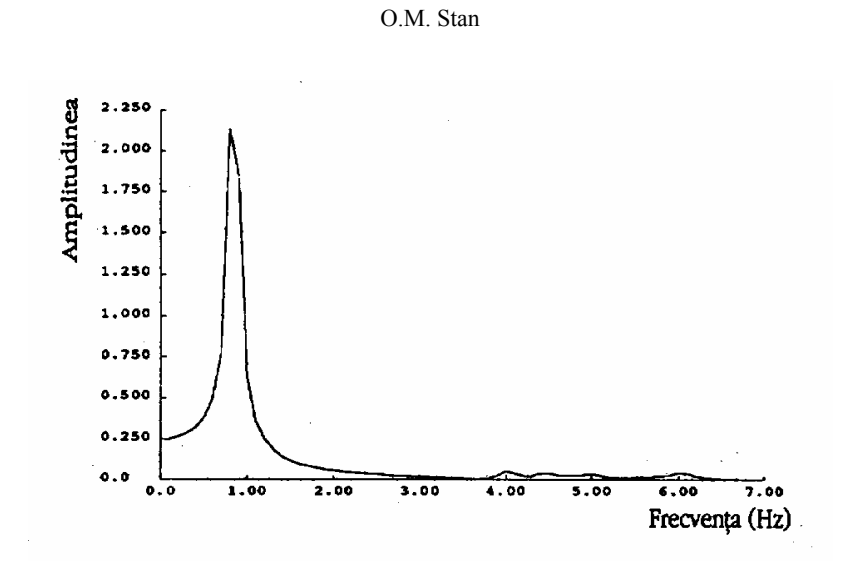


Figure 5. Resonance amplitude for the middle of the central span due to wind excitation

4.5. DYNAMIC WIND ANALYSIS

4.5.1. Wind mean pressure

The real wind forces were considered acting in one step. Time history response of the structure is presented in Figure 6 and Figure 7 for the same nodal point (top of the tower and middle of the central span). Lateral displacements of nodal points oscillating around the same values obtained in static analysis for wind pressure.

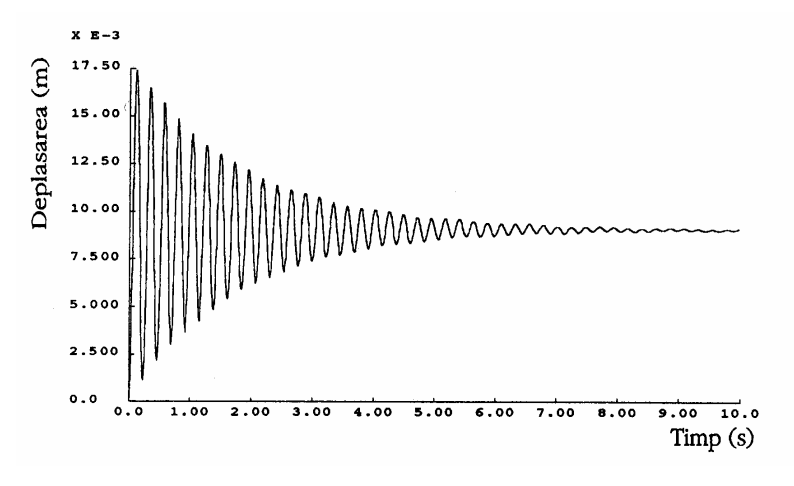


Figure 6. Time history response in displacements for the top of the tower.



INTERSECTII

http://www.ce.tuiasi.ro/intersections

Wind Dynamic Response of a Suspension Pedestrian Bridge

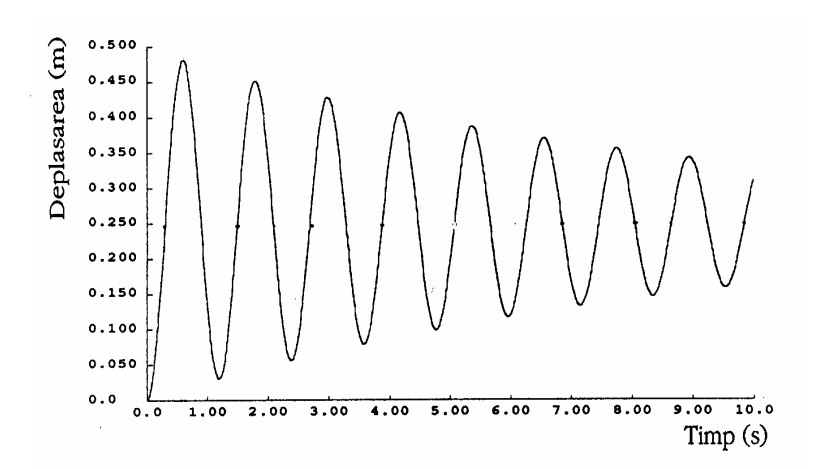


Figure 7. Time history response in displacements for the middle of the central span.

4.5.2. Gusty wind

The real wind velocity is permanently changing in time and space. A result of different study and measurements on wind velocity is illustrated in Figure 8.

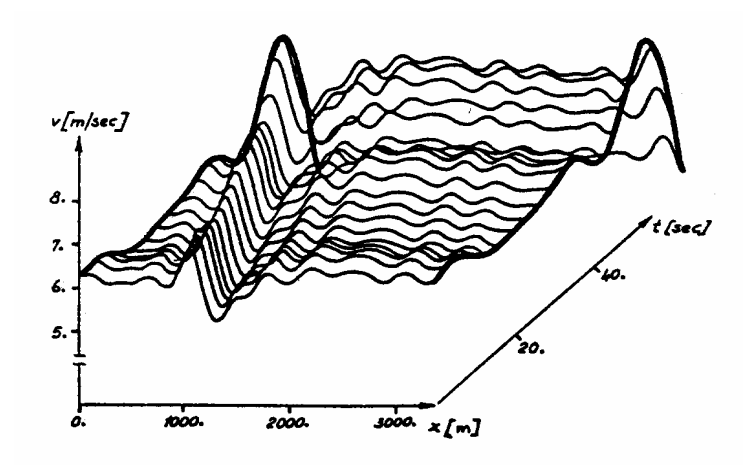


Figure 8. Wind velocity space and time distribution

Dynamic response on wind excitation can be obtained by experimental or by analytical approach.

Mathematical method can be a stochastic approach in frequency domain – unacceptable for suspension bridges (cannot evidence the flutter effect) or a deterministic approach in time domain – which require time history of air flow in

INTERSECTION

http://www.ce.tuiasi.ro/intersections

O.M. Stan

time and space for direct integration of equation of motion at different moment of time.

Suspension bridge was subjected on a deterministic approach. Air flow was modeled in time steps of 0,05 s for 12,0 s range (Figure 9). The 12,0 s range is long enough to cover the dynamic response of the structure which has first natural period 1,19 s.

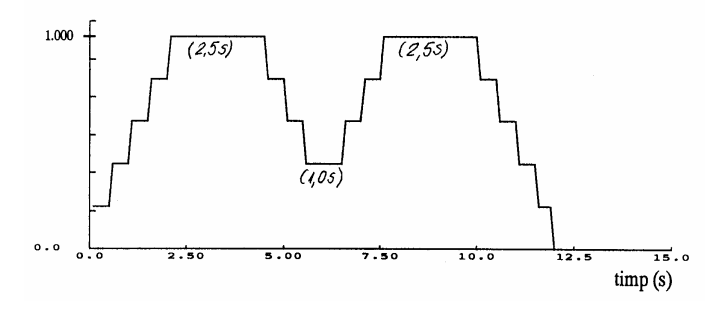


Figure 9. Wind velocity time distribution

Space air flow was neglected – considering constant pressure of the wind along the bridge.

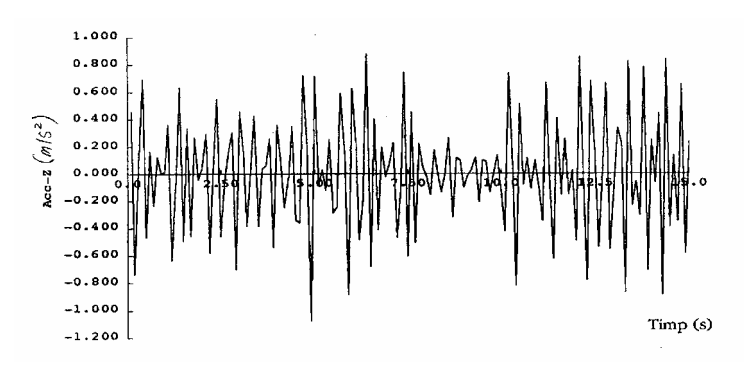


Figure 10. Time history in acceleration of the top of the tower in global direction Z shows a maximum acceleration of 0,12g.

Dynamic analysis include 12,0 s of wind pressure and 3,0 s without any excitation.

For gusty wind it was defined a specific load function which multiplied static wind load for all the members of the structure (Figure 9.).

Time history response of the structure is illustrated in Figures 10 - 13 for different quantities.

INTERSECTII

http://www.ce.tuiasi.ro/intersections

Wind Dynamic Response of a Suspension Pedestrian Bridge

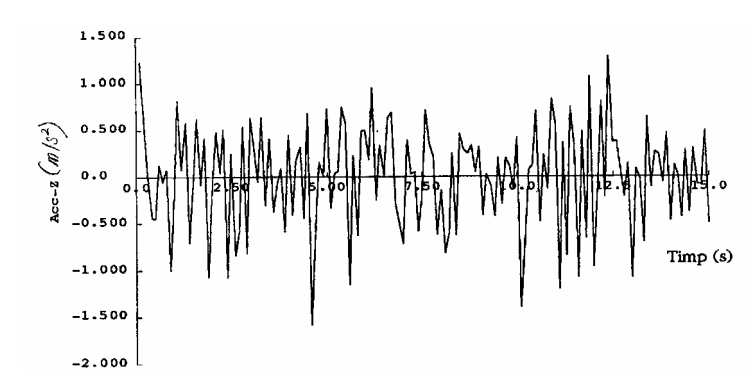


Figure 11. Time history in acceleration of the middle of the central span in global direction Z shows a maximum acceleration of 0,15g.

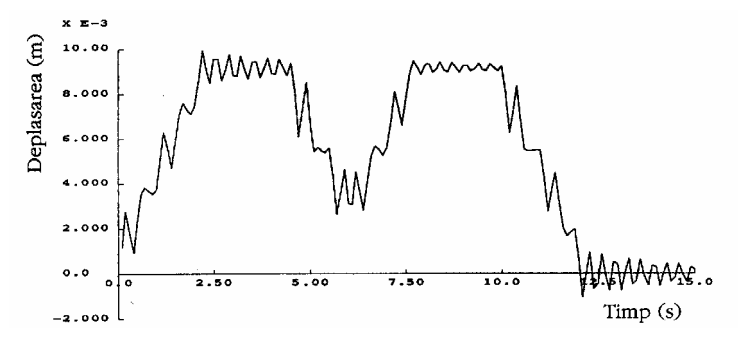


Figure 12. Time history displacement shows an oscillation around displacement value evaluated in static analysis for top of the tower.

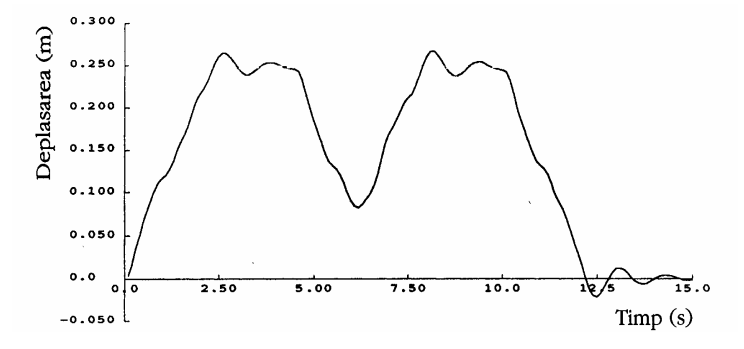


Figure 13. Time history displacement shows an oscillation around displacement value evaluated in static analysis for middle of the central span.



INTERSECTII

http://www.ce.tuiasi.ro/intersections

O.M. Stan

5. CONCLUSIONS

The geometric nonlinearity of the suspension system requires static nonlinear analysis.

Dynamic response of suspension bridges is highly influenced by the damping ratio. Choosing a wrong value for damping ratio can corrupt the response.

Geometric nonlinearity has to be taken into account for dynamic analysis too. Direct integration of equation of motion is the solution for flexible structure.

The pedestrian suspension bridge is well conformed from static and dynamic point of view.

References

- 1. W. C. ARROL Implications of the Rules on Bridge Design Past and Future, Bridge Aerodynamics, London, March, 1981.
- J. M. W. BROWNJOHN Estimation of Damping in Suspension Bridges Proc. Instn. Civ. Engrs Structs & Bldgs, Vol. 104, Nov., 1994.
- 3. M. A. CRISFIELD Nonlinear Finite Element Analysis of Solids and Structures, Vol. 1 Esentials; John Wiley & Sons, 1997.
- 4. EUROCODE 1: Basis of Design and Actions on Structures, 1994.
- D. GHIOCEL, D. Lungu Acțiunea vântului, zăpezii şi a variațiilor de temperatură în construcții, Ed. Tehnică București, 1972. (in Romanian)
- O. M. STAN Efecte dinamice specifice la poduri de mare deschidere Teză de doctorat, U.T.C.B., 1998. (in Romanian)
- 7. Shigeki UNJOH, Yukio ADACHI Damping Characteristics of Long Span Bridges, IABSE SYMPOSIUM, KOBE 1998 (Long Span and High Rise Structures), p.335-340.
- 8. T. A. WYAT The Effect of Wind on Slender Long Span Bridges, Symposium on Wind Effects on Buildings and Structures, Paper 36, London, 1984.
- T. A. WYATT, C. SCRUTON A Brief Survey of the Aerodynamic Stability Problems of Bridges, Bridge Aerodynamics, London, March, 1981.



INTERSECTII http://www.ce.tuiasi.ro/inters

Discrete model for the stability of continuous welded rail

Adam Dósa, Valentin-Vasile Ungureanu

Department of civil engineering, "TRANSILVANIA" UNIVERSITY, Braşov, Romania

Summary

In this paper a discrete model is developed for the buckling analysis of continuous welded rail subjected to temperature load. The model is based on a nonlinear analysis in total lagrangean formulation. The structure consists of beam elements and lateral, longitudinal and torsional spring elements. The source of nonlinearity is due to the geometric nonlinearity of the rail high axial forces and also to the nonlinearity of material type for the lateral and longitudinal resistance of the ballast and the torsional resistance of the fasteners. The use of a displacement control algorithm leads the analysis beyond the critical point and permits a more realistic computation of the structural safety. The track model is encoded into a special purpose program which allows a parametric study of the influence of vehicle loading, the stiffness properties of the structure and of the geometric imperfections on the track stability.

The validity of the present model is verified through a series of comparative analyses with other author's results.

KEYWORDS: Continuous welded rail, Non-linear stability analysis, Temperature loading, Structural safety.

1. INTRODUCTION

The first computational models of the buckling of the continuous welded rail (CWR) were developed at the beginning of the 1930 years. These models can take into account the main parameters which control the stability of CWR like the horizontal and vertical stiffness of the rail, the longitudinal and transversal resistance of the rail, the torsional resistance of the fasteners, the stresses induced by the vehicle and temperature loading, the geometry and the misalignment of the rail. In the SCFJ model presented in this paper the structure consists of beam elements and lateral, longitudinal and torsional spring elements. The beam elements are modeling the rail and have geometric nonlinear characteristics due to high compressive thermal stresses. The spring elements are describing the material nonlinear behavior of the ballast and the fasteners.



INTERSECTII

http://www.ce.tuiasi.ro/intersections

A. Dósa, V.V. Ungureanu

2. DEVELOPMENT OF THE TRACK MODEL

2.1. The longitudinal ballast behavior

In the SCFJ model the longitudinal resistance of the ballast is introduced by spring elements having the, linear or bilinear displacement-force curves given in figure 1. In the case of vehicle loading, the bilinear curve is corrected [6] by the equation (1) taking into account the vertical force Q on each sleeper.

$$U_{\nu}^{c} = U_{\nu} + Q \cdot \tan \phi_{L} , \quad U_{\nu}^{c} \ge \frac{2}{3} U_{\nu}$$
 (1)

In the above equation U_{ν} is the reference value of the longitudinal resistance (without vehicle loading), U_{ν}^{c} is the corrected value of this resistance and ϕ_{L} is the angle of the longitudinal friction between the sleeper and the ballast.

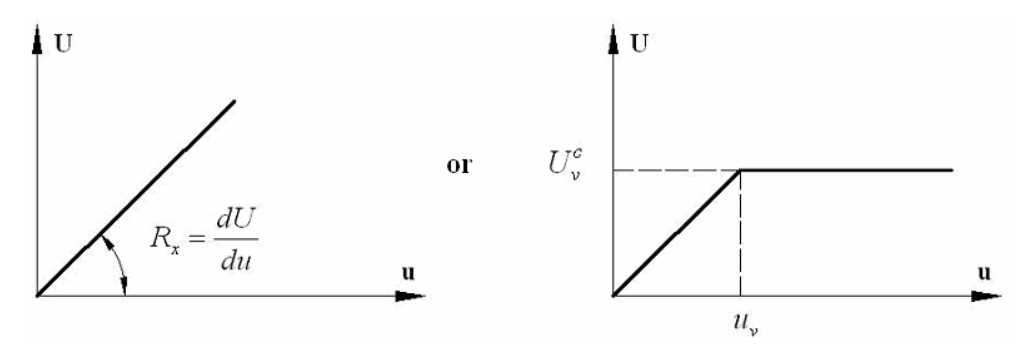


Figure 1. Longitudinal resistance versus longitudinal displacement of the ballast

2.2. The transversal ballast behavior

The transversal resistance of the ballast is introduced by spring elements having the displacement-force curves given in figure 2. In both cases the elasto-plastic model includes softening. This kind of ballast behavior has been measured for consolidated ballast. In the case of vehicle loading, the bilinear curve is corrected [6] by the equation (1) taking into account the vertical force Q on each sleeper using equations (2), (3) or (4).

$$V_{\nu}^{c} = V_{\nu} + Q \cdot \tan \phi_{T} , \quad V_{\nu}^{c} \ge \frac{2}{3} V_{\nu}$$
 (2)

$$V_r^c = V_r \cdot V_v^c / V_v \tag{3}$$

INTERSECTII

http://www.ce.tuiasi.ro/intersections

Discrete model for the stability of continuous welded rail

for
$$tipV=1: V = V_r^c + (V_v^c - V_r^c) \cdot 2^{-2\frac{v - v_v}{v_r - v_v}}$$
 (if $v > v_v$) (4)

In the above equations V_{ν} is the reference value of the peak transversal resistance (without vehicle loading), V_{ν}^{c} is the corrected value of this resistance, ϕ_{T} is the angle of the transversal friction between the sleeper and the ballast, V_{r} is the reference value of the residual transversal resistance (without vehicle loading), and V_{r}^{c} is the corrected value of this resistance. In the case of exponential softening the difference $V_{\nu}^{c} - V_{r}^{c}$ is half at the middle of $v_{\nu}^{c} - v_{r}^{c}$ interval.

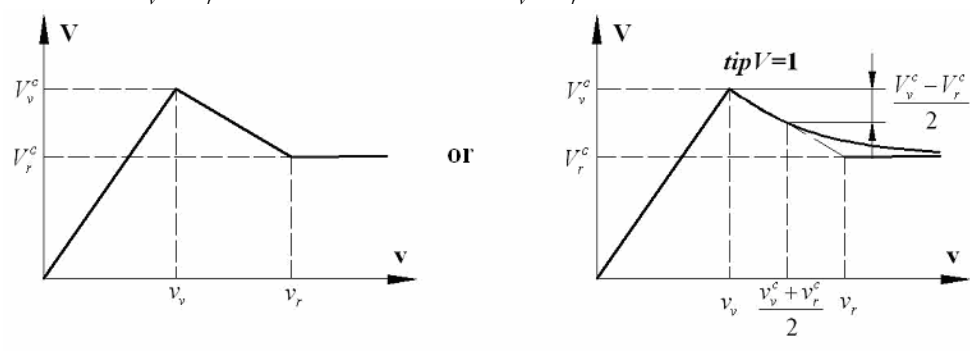


Figure 2. Transversal resistance versus transversal displacement of the ballast

2.3. The torsional stiffness of the fasteners

The resistance of the fasteners is introduced by torsional springs having the linear or tri-linear behavior shown in figure 3. In the case of loaded rail this behavior also can be corrected taking into account the vertical force acting on each sleeper.

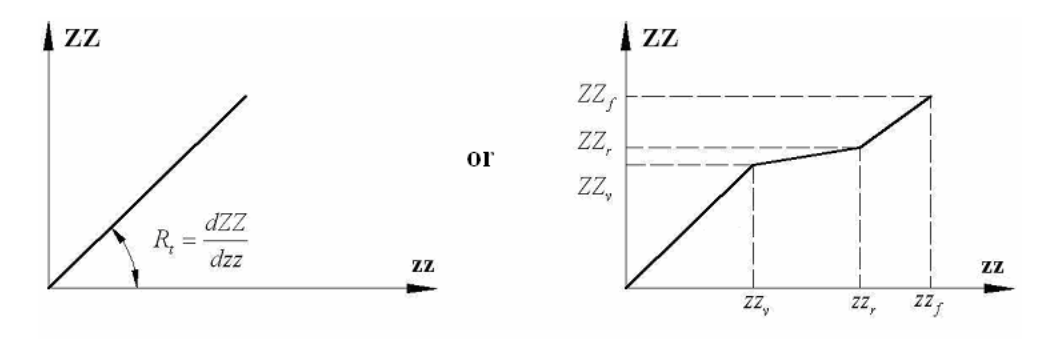


Figure 3. The torsional stiffness of the fasteners



INTERSECTII http://www.ce.tuiasi.ro/intersections

A. Dósa, V.V. Ungureanu

2.4. The geometrical and physical characteristics of the rail

The rail is modeled by beam elements having area of the cross section A, second order moment about the vertical and horizontal axes I_z and I_v respectively. The Young modulus and the thermal expansion coefficient of the material are E and respectively α In the model the misalignment of the rail can be described by two types of curves: a complete or a half cosine wave having the total length λ and the amplitude δ (figure 6). The length of the model is an input of the program. At the end of the model special infinite boundary elements are introduced -equivalent with the theoretical infinite rail [6]. This elements lead to the reduction of the length of the model and hence the computational effort. Further reduction can be obtained by using the symmetric half structure.

3. THE NUMERICAL ALGORITHM

Since in a simplified manner, the horizontal and vertical behavior are considered decoupled, the numerical algorithm has two phases.

3.1. The computational model for vertical loadings

This model is linear elastic consisting of a beam on elastic springs. The nodes of the structure are considered at the sleepers. Each node has two degrees of freedom: the vertical translation w and the rotation θ_v . The system of equations of equilibrium is:

$$\mathbf{K}\mathbf{a} = \mathbf{F} \,. \tag{5}$$

where:

K is the stiffness matrix of the structure and results by assembling the stiffness matrices \mathbf{k} of the beams and the vertical stiffness of the fasteners.

a is the displacement vector of the nodes of the structure.

F is the vector of forces at the nodes of the structure, which (in this case) results by assembling the vectors \mathbf{f}_0 of the forces on the beams.

The stiffness matrix $\mathbf{k}_{(4x4)}$ of a beam is given by the equation:

Here $\mathbf{B}_{(2 \times 4)}$ is a transformation vector, which links the vector of displacements of the beam and the reduced vector of displacements of the beam. The reduced vector of displacements does not contain the rigid body displacements.



INTERSECTII

http://www.ce.tuiasi.ro/intersections

Discrete model for the stability of continuous welded rail

$$\mathbf{a}_{el}^{d} = \begin{cases} \boldsymbol{\theta}_{yi}^{d} \\ \boldsymbol{\theta}_{yi+1}^{d} \end{cases} = \mathbf{B} \cdot \mathbf{a}_{el} = \begin{bmatrix} 1/L & 1 & -1/L & 0 \\ 1/L & 0 & -1/L & 1 \end{bmatrix} (w_i \quad \boldsymbol{\theta}_{yi} \quad w_{i+1} \quad \boldsymbol{\theta}_{yi+1})^T$$
 (7)

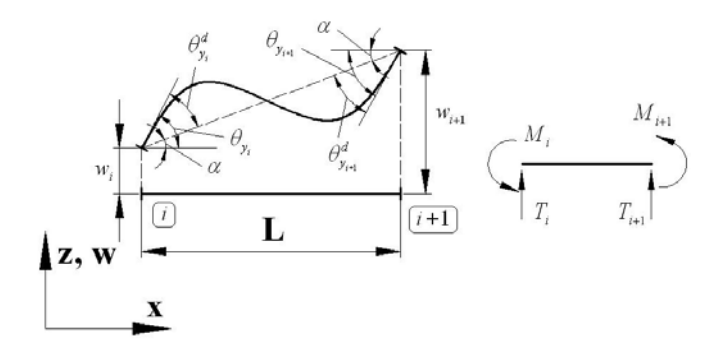


Figure 4. The displacements of the beam in the vertical plane

 $\mathbf{k}^{d}_{(2 \times 2)}$ is the reduced stiffness matrix of the beam.

$$\mathbf{k}^d = \frac{EI_y}{L} \begin{bmatrix} 4 & 2\\ 2 & 4 \end{bmatrix} \tag{8}$$

If the beam is loaded, the vector \mathbf{f}_{θ} of equivalent forces in the nodes is given by equations (9).

Error! Objects cannot be created from editing field codes. (9)

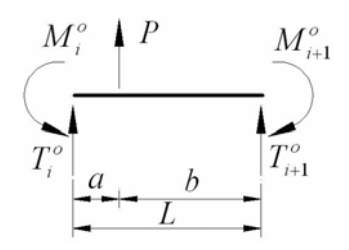


Figure 5. Equivalent nodal forces of the beam

The stiffness matrices and the load vectors of the beams are assembled by the relation (10).

$$\mathbf{K}_{ind\ ind} = \mathbf{K}_{ind\ ind} + \mathbf{k}, \quad \mathbf{F}_{ind} = \mathbf{F}_{ind} + \mathbf{f}_{0}. \tag{10}$$

Here *ind* is the vector of the indices of the displacements of the current beam.

The stiffness of the sleepers is assembled with the help of the equation (11).

INTERSECTII http://www.ce.tuiasi.ro/intersections

A. Dósa, V.V. Ungureanu

$$\mathbf{K}_{ind,ind} = \mathbf{K}_{ind,ind} + R_z L \tag{11}$$

In the above equation *ind* is the set of indices of vertical displacements of the nodes jnd=1, 3, ..., 2nnd-1. The constraints of the structure are introduced by setting to zero the displacements of the supports. The free displacements of the nodes result by solving the system of linear equations:

$$\mathbf{a}_{id} = (\mathbf{K}_{id,id})^{-1} \mathbf{F}_{id}. \tag{12}$$

In equation (12) id is the set of the free displacements of the structure.

Using the vertical displacements, the vertical force on each sleeper can be computed by the equation (13)

$$Q = -wR_z L + G_{sleeper}. (13)$$

The transversal, longitudinal and torsional resistances are corrected taking into account the forces Q on each sleeper using equations (1) to (4).

3.2. The computational model in the horizontal plane

The model is a straight or curved beam on elastic supports with misalignments (figure 6). The nodes of the structure are considered at the sleepers. At each node are introduced longitudinal, transversal and rotational spring elements which are modeling the sleepers. The infinite boundary elements at the ends of the model have equivalent characteristics (Young modulus and thermal expansion coefficient) in order to replace the theoretical infinite rail [6]. The loading of the model is an increase of the temperature in the rail. The characteristics of the beams and of the springs correspond to the two rails of the track panel. A node has three degrees of freedom: two linear displacements in the horizontal plane, u and v and the rotation θ_z around the vertical axis. In the analysis of the structure the goal is to obtain the displacement-temperature curve. The problem is solved by a displacement control based incremental process. The behavior of the system is determined as a sequence of increments of state parameters (forces and displacements). In the current increment j characterized by the small control displacement δv_{cj} , the nonlinear behavior of the system can be approximated by a linear relation between the successive increments of the state parameters:

$$\mathbf{a}_{j+1} = \mathbf{a}_j + \delta \mathbf{a}_j, \quad \delta \mathbf{F}_j = \mathbf{K}_j \delta \mathbf{a}_j. \tag{14}$$

In the above equation \mathbf{a}_i is the displacement vector in the current configuration, $\delta \mathbf{a}_i$ is the increment of the displacements, $\delta \mathbf{F}_i$ is the incremental load vector and \mathbf{K}_i is the incremental (tangent) stiffness matrix of the structure.

INTERSECTII

http://www.ce.tuiasi.ro/intersections

Discrete model for the stability of continuous welded rail

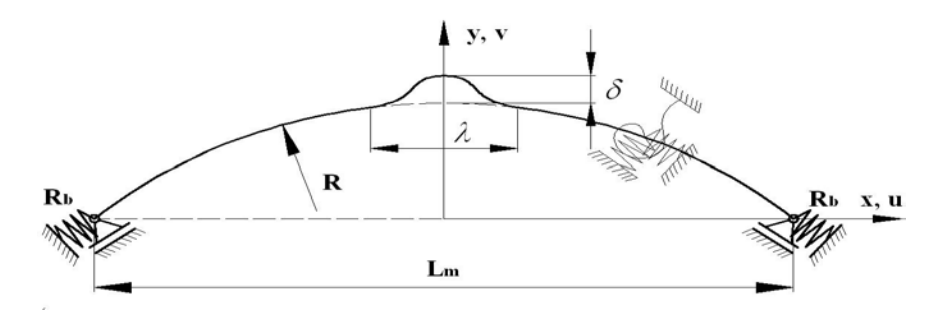


Figure 6. The model for horizontal displacements

By using equations (14), the following incremental scheme results:

$$\delta \mathbf{a}_{j} = (\mathbf{K}_{j})^{-1} \delta \mathbf{F}_{j}, \quad \mathbf{a}_{j+1} = \mathbf{a}_{j} + \delta \mathbf{a}_{j}.$$
 (15)

In this paper an improved scheme is used, known as Heun's or midpoint rule:

$$\mathbf{a}_{j+1/2} = \mathbf{a}_{j} + 1/2 (\mathbf{K}_{j})^{-1} \delta \mathbf{F}_{j},$$

$$\mathbf{K}_{j+1/2} = \mathbf{K} (\mathbf{a}_{j+1/2}),$$

$$\delta \mathbf{F}_{j+1/2} = \delta \mathbf{F} (\mathbf{a}_{j+1/2}),$$

$$\mathbf{a}_{j+1} = \mathbf{a}_{j} + 1/2 (\mathbf{K}_{j+1/2})^{-1} \delta \mathbf{F}_{j+1/2}.$$
(16)

The incremental load vector $\delta \mathbf{F}_j$ is not computed. The incremental displacement $\delta \mathbf{a}_j$ is the result of a yet unknown increment of the temperature produced by a known increment δv_{cj} of the control displacement. For simplicity, in the next equations indices j of the current configuration are dropped. The displacement control consists of loading the system with displacement increments δv_c in a specific node. As a rule in this paper: the control displacement is taken as the maximum transversal displacement of the node on the symmetry axe of the structure. The phases of the computation are the following:

- It is adopted a base system with the control displacement fixed at zero.
- This base system is loaded with two load cases:
- i) Load 1 is a temperature increase $\delta T = I$, which produces displacements $\delta a^{(I)}$ at the free nodes and reaction $R^{(I)}$ in the artificial support.
- ii) Load 2 is a displacement δv_c of the artificial support, which produces displacements $\delta \mathbf{a}^{(2)}$ at the free nodes and reaction $R^{(2)}$ in the artificial support.

http://www.ce.tuiasi.ro/inters

A. Dósa, V.V. Ungureanu

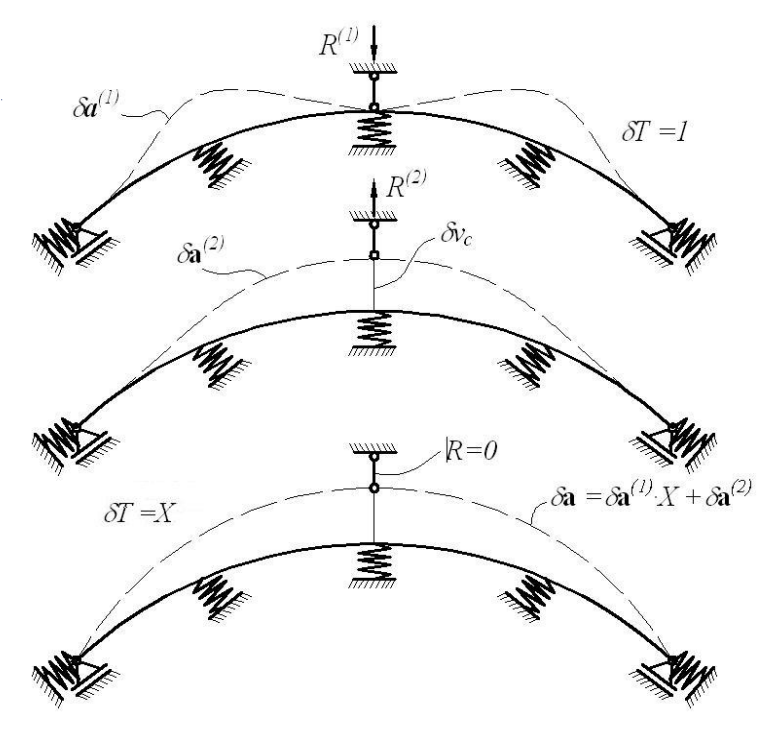


Figure 7. The determination of the temperature and displacement increments

The base system and the initial system are identical if the total reaction in the artificial support is zero. $R = R^{(1)} \delta T + R^{(2)} = 0$. This equation yields the unknown variation δT of temperature and the incremental displacements δa of the free nodes.

$$\delta T = -R^{(2)} / R^{(1)}, \tag{17}$$

$$\delta \mathbf{a} = \delta \mathbf{a}^{(1)} \cdot \delta T + \delta \mathbf{a}^{(2)}. \tag{18}$$

The tangent stiffness matrix \mathbf{K}_i in the j increment depends on the parameters of the system in the current step and results by assembling the stiffness matrices $\mathbf{k}_{t(6 x 6)}$ of the beams and of the springs which model the sleepers.

$$\mathbf{k}_{t} = EA/L \cdot \mathbf{r}^{T} \mathbf{r} + \mathbf{B}^{T} (\mathbf{k}^{d} + \mathbf{k}_{G}^{d}) \mathbf{B} + N_{j}/L \cdot \mathbf{z}^{T} \mathbf{z}.$$
 (19)

In this equation $\mathbf{r} = (-\cos\beta - \sin\beta \ 0 \ \cos\beta \ \sin\beta \ 0)$, $z = (\sin\beta - \cos\beta \ 0 - \sin\beta \cos\beta \ 0),$

$$\mathbf{B} = \begin{bmatrix} 0 & 0 & 1 & 0 & 0 & 0 \\ 0 & 0 & 0 & 0 & 1 \end{bmatrix} - \frac{1}{L} \begin{bmatrix} \mathbf{z} \\ \mathbf{z} \end{bmatrix}, \quad \mathbf{k}^d = \frac{EI_z}{L} \begin{bmatrix} 4 & 2 \\ 2 & 4 \end{bmatrix}, \quad \mathbf{k}^d_G = \frac{N_j L}{30} \begin{bmatrix} 4 & -1 \\ -1 & 4 \end{bmatrix},$$

INTERSECTII

http://www.ce.tuiasi.ro/intersections

Discrete model for the stability of continuous welded rail

and N_j is the axial force in the beam in the *j*-th incremental step: $N_j = EA \Delta L_j / L_j$, $\Delta L_j = L_j - L_0$, $L_0 = \sqrt{(\mathbf{x}_{i+1}^0 - \mathbf{x}_i^0)^2}$, $L_j = \sqrt{(\mathbf{x}_{i+1}^j - \mathbf{x}_i^j)^2}$.

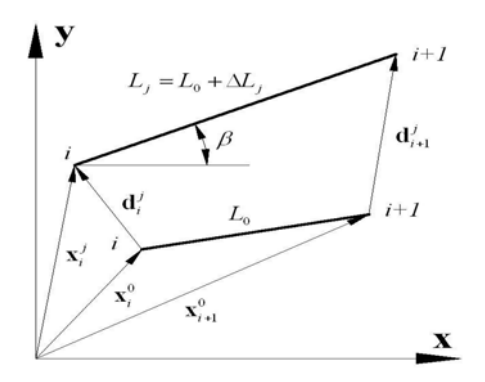


Figure 8. The axial deformation of the beam

Matrices \mathbf{k}^d and \mathbf{k}_G^d are the material and geometric stiffness matrices respectively. They are expressed with the reduced set of displacements which produce deformations and they are not containing the rigid body displacements of the beam. This reduced form of the stiffness matrices needs less computational effort and speeds up significantly the computation. Equation (19) introduces the non-linear effect of the axial force N_j . The complete tangent stiffness matrix in the updated lagrangean formulation used here has two more terms corresponding to the variation of the length of the beam in bending and to the effect of the shear force [1], [2], [3], [4], [5]. Since in the current cases the structure is divided in a sufficient number of beams, the errors are very small, when neglecting these two terms. In a study using the complete tangent stiffness matrix and equation (19) the differences between the resulting limit temperatures were only at the fifth digit.

4. NUMERICAL EXPERIMENTS

The validity of the present model is verified through a series of comparative analyses with other author's results. The numerical example presented here corresponds with one given in [1]. The track length is L=24.359/2 m corresponding to 21 sleepers on the symmetric half of the structure. The curvature radius is R=400 m. The horizontal misalignment is characterized by a half wave cosine with a length λ =9.144 m and an amplitude δ =0.0381 m. The rails have the characteristics of two AREA 136 rails. The vertical stiffness of the ballast elements is R_z =68900 kN/m per meter of track. The longitudinal stiffness is R_x =1378 kN/m per meter of track. The torsional stiffness of the fasteners is 111.250 kNm/rad per meter of

INTERSECTII

http://www.ce.tuiasi.ro/intersections

A. Dósa, V.V. Ungureanu

track. Laterally the ballast is modeled by the tri-linear constitutive behavior given in figure 2. The reference values of the lateral peak resistance and residual resistance are V_v =17.508 and V_r =9.630 kN per meter of track. These values are corrected with the vertical forces resulting from the vehicle loading. The lateral displacement at the peak value is v_v =0.00635 m and at the limit value is v_r =0.0381 m. The model is vertically loaded by a vehicle with two bogies represented by four vertical loads of 293 kN each. The centre spacing between the bogies is 12.85 m. The spacing between the axles in a bogie is 1.78 m. The centre of the misalignment is located in the middle between the bogies. The track is loaded by a temperature increase from zero to a maximal value corresponding to the buckling of the rail. The lateral displacement of the middle node versus the resulting temperature increase is shown in figure 9.

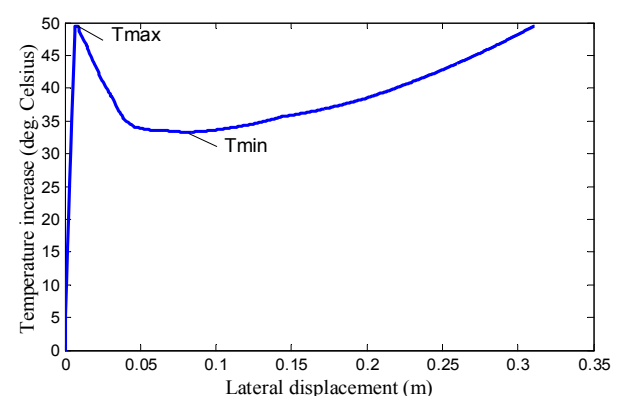


Figure 9. Lateral displacement versus temperature increase

The curve in the figure 9 is characterized by two points: T_{max} - the maximum increase of temperature for which the buckling certainly starts, and T_{min} - the minimum increase of temperature which occurs in the post-buckling domain. The values computed by the SCFJ model - T_{max} =49.5 °C and T_{min} =33.3 °C - are in a good agreement with those given in [1].

References

- 1. Bănuț, V. Calculul neliniar al structurilor, Editura tehnică, București, 1981.
- 2. Crisfield, M.A. Non-linear Finite Element Analysis of Solids and Structures, Wiley, 1991.
- 3. Dósa,A., Litră E. Elemente de bară încovoiată cu precizie îmbunătățită pentru calculul neliniar și de stabilitate, *Revista Construcțiilor*, 2006.
- 4. Dósa, A., Popa L. High order beam elements for the stability and non-linear analysis of frame structures, "Computational Civil Engineering 2006", Iași, România.
- Felippa C.A., Nonlinear Finite Element Methods, www.colorado.edu/engineering/CAS/courses.d/NFEM.d.
- 6. Van, M.A., Stability of Continuous Welded Rail Track, Delft University Press, 1997.



INTERSECTII http://www.ce.tuiasi.ro/inters

Non-linear effects in traffic simulations

Tomas Apeltauer, Petr Holcner, Martin Kyselv and Jiri Macur Faculty of Civil Engineering, Brno University of Technology, Brno, CZ-602 00, Czech Republic

Summary

Growing requirements on transport of passengers and goods have a principle impact on life and economy. It is not need not intricately needed to search accurate formulation of economic consequences, on the contrary would be enough to quote, for example, United States Secretary of Transportation Norman Mineta, according to which local drivers lose in traffic jams almost 4 billions hours and 2 billions gallons of fuel each year. Upward trend is perceptible especially on highways, where some out of traffic jams affects two-thirds drivers every day, which is double compared to situation twenty years ago.

In Los Angeles at that time transportation problem lasted 4.5 hours every day, about two decade later in the same town transport breaks down for 7 hours every day. It is evident it is not always possible extend capacity carriage according to their users needs and is necessary to search alternative manners. One of these is transition to description of traffic flow via nonlinear dynamics, which explains the behavior of very complicated systems.

If we explain properties of the traffic flow, we can try to describe emergency of traffic jams and search manners, how those situation precede at least in part.

KEYWORDS: non-linear dynamics; traffic flow; congestions; traffic modeling; simulations

1. TRAFFIC CHAOS AS A TECHNICAL TERM

Nonlinear dynamics as a tool for understanding chaos emergency already gets through wide spectra branch. Presently it is perceptible that we cannot apply the clean deterministic look even on very simple system, whereas the meaning of nonlinear system features grows with their complexity. One of such dynamic systems is the traffic flow. A group of German physicists headed by Dirk Helbing, Boris Kerner and Michael Schreckenberg published in top class magazines like Physical Review Letters, Journal of Physics and Nature results of computer simulations of the vehicle movement. They noticed following interesting matter: while using equations for a gas molecule movement, supplemented by some specific characteristics of the human driver (among others the effort to avoid



INTERSECTII http://www.ce.tuiasi.ro/inters

http://www.ce.tuiasi.ro/intersections

T. Apeltauer, P. Holcner, M. Kysely, J. Macur

collision), they discovered special effects which truly copies real characteristics of traffic. For example in places of bottlenecks traffic started compression, whereas this perturbation expands as a density wave against the direction of traffic flow. It is the exact analogy of known retardation and accumulation out in fronts before bottlenecks - as soon as vehicles near bottleneck slow down, other vehicles will slow down too, which causes the wave of "stop-and-go" spreading upstream.

At all the biggest surprise was the following result: the traffic jam can emerge in certain circumstances spontaneously, without bottlenecks, traffic accident or other at first sight obvious causes. Traffic flow is able to flow freely, and nevertheless suddenly will change to the slowly ridden flow. Under certain condition the "negligible" fluctuation in the vehicle velocity or headway can lead to the system collapse, which last for long hours after primary impulse.

In spite of it is relatively cheerless inquest, it is absolutely in agreement with results of mathematical models of many physical and biological systems. All these studied systems have the common emergency of phenomenon known from popular literature as the "chaos". Simply: in every complex system with many parts which influences each other a weak fluctuations can lead to big consequences. But we cannot predict the emergency of such turnover. Scientists these phenomena describe like non-linear - seemingly unimportant change in one characteristic might have unreasonably extensive incidence on entire system. Non-linear characteristics were detected in weather, biological systems or chemistry. And during recent decades it is also mentioned in transport.

2. REAL TRAFFIC DYNAMICS OBSERVING

Every correct physical theory requires agreement with experimental data. Good theory had to reproduce known system behavior as also predict its future. It will be shown further that selection of the right method for data collection on road is a very idyllic business with comparison to the construction of the right theory.

2.1. Measuring of the traffic variables

Probably the oldest and at the same time most complicated technology of traffic detection is aerial photography, by the help of whose we can obtain total view of the situation on tracked section. If we need to obtain concrete traffic variable such as traffic flow velocity, we have to use digital picture analysis. Problems of visual analysis generally belongs to the most complicated tasks, it is very time consuming and not balanced with corresponding result accuracy. Its usage in current traffic research is therefore rather border. But some advantage aerial photograph has further: emergency of traffic jam and its progress is apparent at the first sight.



INTERSECTII

http://www.ce.tuiasi.ro/intersections

Non-linear effects in traffic simulations

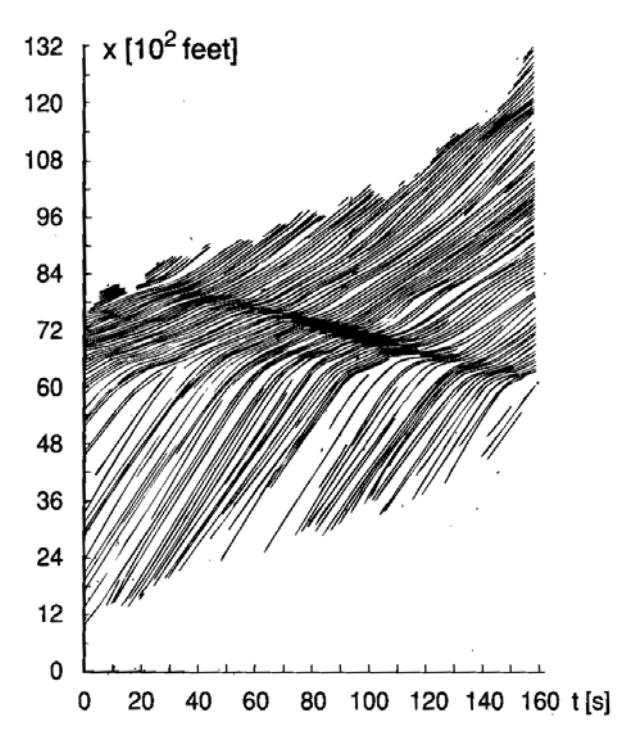


Figure 1. The traffic jam behavior, derived from aerial photography [17].

The second way can be taken with *floating vehicle*, which works as a movable detector. But the biggest data sets are now collected by detectors placed on concrete fixed place on the motorway. Most widespread is the *induction loop* placed closely below the road surface. Incoming vehicle turns its inductance and creates a weak signal.

From a simple induction loop we can obtain especially information about vehicles that passed tracked place during definite time, which matches the definition of *traffic intensity*. Today double induction loops ale placed in the most cases, which make possible to measure in addition vehicle lengths and its velocity. Combination of these values finally makes it possible to determine *traffic density* like second crucial traffic variable. Correlation between traffic intensity and its density is a very basic tool in the traffic research.

2.2. Measurement with induction loops

We can obtain a good notion about possibilities of detection via induction loops from A5-Nord highway nearby German Frankfurt.



INTERSECTII

http://www.ce.tuiasi.ro/intersections

T. Apeltauer, P. Holcner, M. Kysely, J. Macur

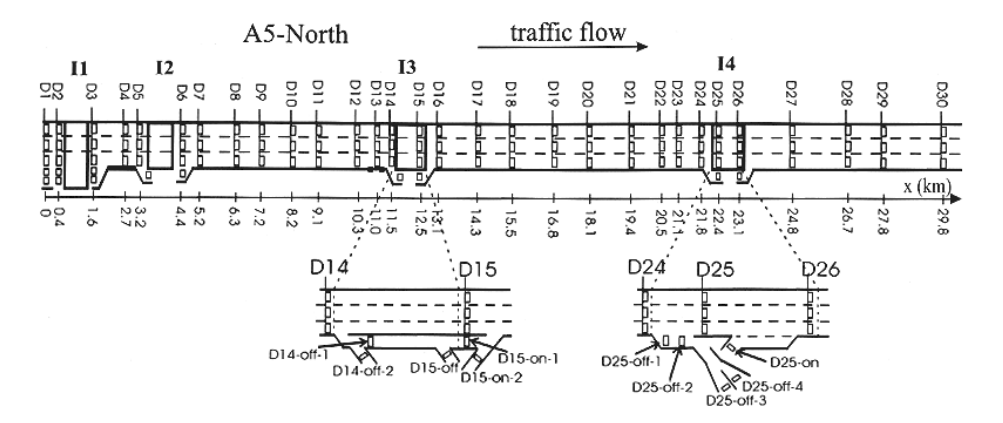


Figure 2. Location of induction loops on the part of A5-Nord highway [5].

Described section of highway has on the whole four intersections which join it on next communications. On that section there are deployed about thirty double induction loops with labels from D1 to D30. Each set of loops includes three detectors for every lane, special cases are slip and trunk roads.

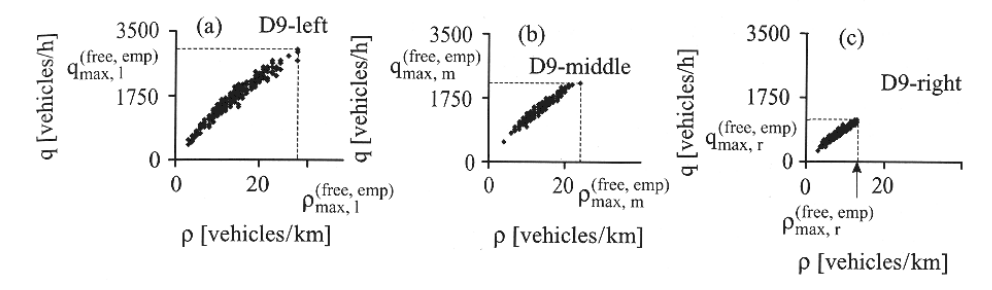


Figure 3. Data collected on A5-Nord highway. We can see one minute averages of traffic densities and intensities from lanes on the place od detector D6. Measurement was on 9th October 1992 between 7.00 – 12.00 [5].

We can see results on selected detectors on fig. 3. Three graphs a) to c) shows the dependence of traffic flow intensity on traffic density for every of the three lanes. How we will see further, in all cases this values correspond to *free traffic flow* and at first sight there are perceptible expressive differences in maximal measured values. Here we have to remark that the on German motorways there is a big asymmetry in vehicle types among lanes. Trucks here usually do not move in the left lane, only use the right one in some cases the middle one for overtaking.

INTERSECTII

http://www.ce.tuiasi.ro/intersections

Non-linear effects in traffic simulations

2.3. Free flow and congestions

As mentioned above, there are three basic variables which characterize traffic flow in specific time and place: *traffic density* (number of vehicles in one kilometer), *velocity* (in most cases km.h⁻¹) and *traffic intensity* (number of vehicles which passed specific point in some period of time, one hour generally). It holds in steady traffic flow the traffic intensity is a product of its velocity and density. Unfortunately both these variables are not mutually independent and that is why it is necessary to determine its correlation.

We can start from obvious and empirically tested facts: maximal velocity in traffic flow corresponds to the density near zero, when each one vehicle in not influenced by another one. Then we denote that case as *free traffic flow*. From this we can define *congestion* as a state supplemental to the free flow, which contains some other traffic situations. One of these states is the critical value of density, when the speed of traffic flow drops to zero and the flow moves via small jumps or it stops definitely (headways are too small for safe and useful constant speed). We can see that between the free flow and this critical value the velocity must go down (usually supposed monotonously and continuously). Determination of this dependency is very basic and also very complicated task during investigation of traffic flow.

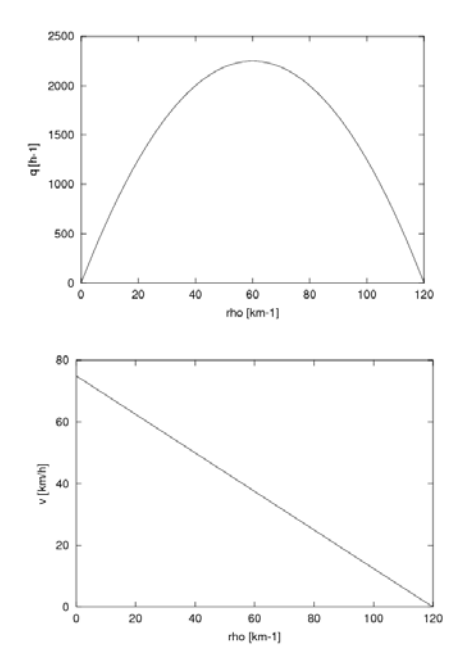


Figure 4. Basic and very simple traffic model according to Greenshields, which comes from strictly linear velocity-density dependency. Maximal traffic intensity is reached in middle velocity for this model.



INTERSECTII

http://www.ce.tuiasi.ro/intersections

T. Apeltauer, P. Holcner, M. Kysely, J. Macur

2.3. Fundamental diagrams

The basic instrument for description of steady flow and its global properties is the fundamental diagram. Its most common type describes dependency of the traffic intensity on the traffic density. In is not obvious from diagram itself that the key correlation between density and velocity is uncertain and efforts to determine it precisely were not successful yet. Nevertheless we can some derive some basic characteristic also from empirically gained average values of traffic quantities. We can use for demonstration data from A5-Nord again (fig. 5).

Contrary from previous entry are now showed all measured values which clearly apportioned into two independent groups. Left part graph appertain to already discussed free flow, the right pat to congestions. The waveform corresponds to reality, when the traffic intensity is able to growth almost linear as far as to the certain critical value. Then be enough so ever minor perturbation to switch free stream into congestion. Traffic density nevertheless doesn't need to necessarily growth and may even temporarily tail off. We can see again the phenomenon of sudden emergency of traffic jams at the same time key feature of complicated systems.

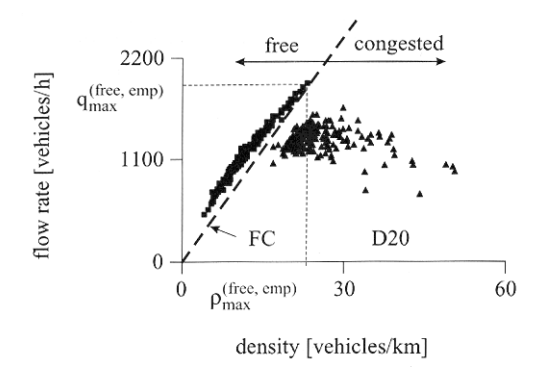


Figure 5. Fundamental diagram of traffic flow, gained from one minute averages traffic density and intensity. Data was collected on A5-Nord on 23. March 2001 between 9.00 - 15.00 via detector D20, it is an average from all three lanes [5].

3. TRAFFIC FLOW SIMULATIONS

It is possible to see dynamic properties of traffic also through the numerical simulation. We have to create a model, which truly describes vehicle behavior and at the same time won't contain unbearable quantity of parameters. As well it is necessary to choose a good simulation method which generates results in a good time. We will present methods at first.

INTERSECTII http://www.ce.tuiasi.ro/inters

http://www.ce.tuiasi.ro/intersections

Non-linear effects in traffic simulations

Till this time plentifully used access are *cellular automata*. Its principle is in dividing the motorway to the finite count of blocks and each block in each computation step contains or does not contain just one vehicle. That is why are cellular automata extreme discreet and then only crudest approximation of the real situation which is balanced by high simulation speed and low hardware exigencies.

Analog models as an opposite access have slow entrance only in last years. In contrast to cellular automata it works with vehicles, which are equipped with moving equations. Evolution of this model looks as moving of bubbles in narrow pipe for example. The model behavior is more realistic but also much more timeconsuming for computational time.

Cellular automata were used for investigation of traffic flow at the beginning of wider focus to this problem. The main reason was relatively low level of computers and quite good results of this model. Especially the first reason is not actual in last

Together with choosing of good method we have to find a good model. This situation is much more transparent, because two main groups of models have difference in the basic principle.

We can consider the traffic flow as a complicated system with separated vehicles. Each vehicle is defined by its features and the main one is dependency between acceleration and the situation around the vehicle. Some used algorithms try to Describe observed properties of a real traffic flow (dynamics, physiological and psychological ability of a driver). These models are known as *microscopic*.

Macroscopic access assume with traffic flow as a continuum defined by the common presumptions. These can be derived by inference from border conditions, measured values in real flow may be based on analogies with physical phenomena, for example from fluxion liquids or gas.

It is often used the third combine approach, when the characteristics macroscopic features are derived from integration of microscopic transport models and presumptions about fluctuations.

The main advantage of the macroscopic access is the ability to describe evolution of traffic flow by one or more differential equations. Is however debatable, if is this presumption of possibilities this unification lawful – analytical complication and venture of this access appears to be also heavy cost behind aesthetics of classical theory.

Users of microscopic models on the other hand can get round of the danger of complicated equations. But it is not all, they early snarl up on crossroad of necessary numeral definition of this model pivotal parameters. About the uncertainty generally witnesses for example historical survey of 23 models defined by "safe distance from previous vehicles in dependency of its speed" and



INTERSECTII http://www.ce.tuiasi.ro/inters

http://www.ce.tuiasi.ro/intersections

T. Apeltauer, P. Holcner, M. Kysely, J. Macur

"responding time" [1]. Response time is between 0 - 2 s, its arithmetic mean is 0.78 s. The maximal value of traffic intensity is 1050 – 4800 vehicles per hour, with the realistic average 2050 vehicles per hour. The vehicle speed, at which is achieved full intensity, is between $10.6 - 55.2 \text{ kmh}^{-1}$, in some cases even growth to infinity (virtually it is necessary to consider about technical or legislative limit). The average (without infinite values) is 29.0 km.h⁻¹. Arithmetic mean itself do not give any help – rather only underscore frustrating motley of models, from which only little is unusable and unfortunately till this time any model is not implicitly good. Perhaps that is just it at projection and scheduling communication meanwhile dominates experiential access, which does not consider behavior inside traffic flow.

3.1. Car following models

Vehicle-following models, exactly Car Following Models (CFM) are investigated nearly for a half century. Determination of the dependency of vehicle acceleration on traffic conditions is in this case fundamental – in the simplest case just on the condition of the previous vehicle (the vehicle driving before). In spite of the fact that this task may appear at the first sight trivial, we did not manage to find a generally respected model which would reflect the reality and would be at the same time sufficiently compact, transparent and especially reasoned until today.

Thus certain general demands were accepted which would meet this proposal without the apparent internal connection of the model with reality. Among these "outer" demands belong especially:

- Non-collision character of simulations performed in the whole spectrum of possible parameters and initial conditions.
- Physically reasonable values of the vehicle velocities and accelerations in course of simulation.
- Asymmetrical character of the model acceleration different from deceleration (usually a stronger deceleration is admissible, e.g. in case of a threatening collision).
- Emergency of global conditions corresponding to the real observation non linear character of the model (waves "stop and go", spontaneous emergency of congestions in case of above critical densities, hysteresis of traffic flow intensity in case of above critical and under critical density etc.).

One of the most often studied models in last time, which partly satisfies the requirements mentioned above, is the so called Intelligent Driver Model (IDM) which was used for experiments of simulation. This model may be considered to be an interpolation of two members for acceleration and deceleration with different shapes in both parts.



INTERSECTII

http://www.ce.tuiasi.ro/intersections

Non-linear effects in traffic simulations

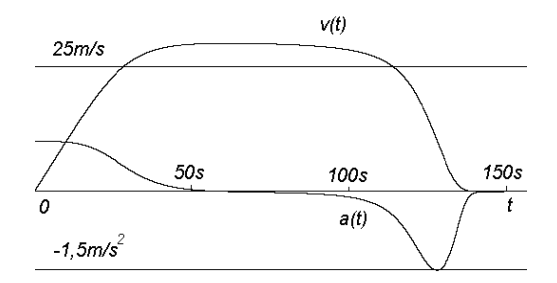


Figure 6. Vehicle velocity and acceleration according to IDM model. Start and stop before an obstacle at the distance 3000 m were used. This kind of test is a good indicator of the model relevance.

Before the simulation we can check for example the first outer demand via the simple experiment, when we test the ability of vehicle to stop ahead the block (fig. 6).

3.2. Model simulations

For the simulation itself we have created a program environment in Java programming language due its easy accessibility, simplicity and portability in internet. Each vehicle is represented by an object with its own parameters and the whole system of vehicles is represented by the so called binded list. In such way it is possible to dynamically change number of vehicles in the system.

For a traffic flow simulation it is advantageous to use the cyclic border conditions which are commonly used for a systems of interacting particles – in this case it means to put vehicles on a circular road with sufficiently large radius. In our case we have chosen the radius 1 km, the total road length is more than 6 km and so we can suppose the system behavior is not rather deformed by correlation between the first and the last vehicle.

3.2.1. System visualization

Direct system animation, when a movement of each vehicle is animated by an object on the circular road, is suitable just for program tuning – it does not bring a good idea about actions in the flow and more over it decelerates the calculation. The representation of time dependent development of density field is more interesting. We unwrap the road in abscissa, where we record each vehicle position by one point. After the selected time interval we similarly indicate a further line of the density field. After sufficiently long interval there arises a model giving a good idea about the development of a vehicle density on the whole road (fig. 7).



INTERSECTII

nttp://www.ce.tuiasi.ro/intersections

T. Apeltauer, P. Holcner, M. Kysely, J. Macur

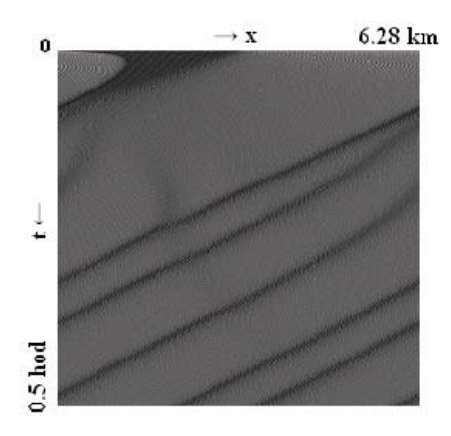


Figure 7. Development of vehicle density. In the beginning vehicles do not move and are homogeneously dislocated in the first half of the road length.

In the mentioned visualization of the density field development there is the distinct quick fixation to the stable state with three synchronized congestions moving upstream. The system moves to stable state with arbitrary initial vehicle distribution. Total number of vehicles in the system is 200.

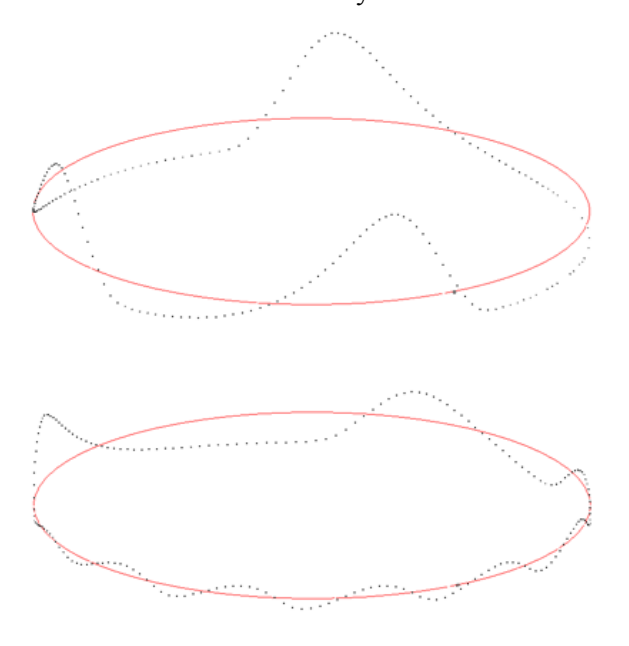


Figure 8. Screen shot from the animation of density distribution in stabilized condition. Full ellipse represents the average density level, which remains constant. The first picture shows the system state after one hour of simulated time, the second one shows the system after seven hours.

INTERSECTII

http://www.ce.tuiasi.ro/intersections

Non-linear effects in traffic simulations

Another type of visualization of system development could be the local density animation (fig. 8). The calculation speed evidently suffers from the animation; however it gives a good idea about mutual interaction of density fluctuations during the stabilization of system and their motion in stabilized condition, which is always upstream.

We can make an interesting conclusion from the simulation: In spite of the fact that congestions in a flow can be unevenly distributed, they have the same form and size which is obviously an expression of vehicles with identical properties.

3.2.2. Obtained results

The main question could be the shape of fundamental diagram. In simulations we used mean values of traffic density and intensity gained from all vehicles on whole road. The final shape of fundamental diagram is too "smooth" and does not show real transient processes in the traffic flow (fig. 9).

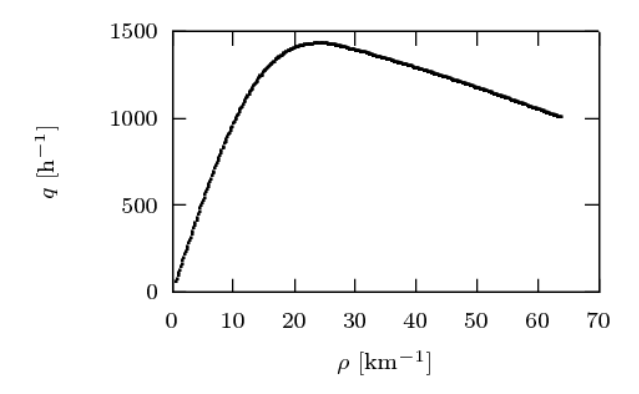


Figure 9. Dependency of simulated traffic intensity on average traffic density.

But we do not have so complex data during the real physical measuring. That is why the real fundamental diagram has so different shape. The main difference in not only in clear reasons: physical measuring do not work with stable traffic flow and vehicles do not have the identical properties. The basic reason is finite time interval, when we measure traffic intensity and density. With the sufficiently long time interval we can obtain similar results in modified simulation experiments, which reflect physical measuring.

It is possible to choose reference point on the simulated road. Each vehicle in each step tests, if it crossed over this point. In positive case the global counter increments with one. By this way we can simply "measure" the traffic intensity in

INTERSECTII

http://www.ce.tuiasi.ro/intersections

T. Apeltauer, P. Holcner, M. Kysely, J. Macur

the selected point for the selected time interval (corresponding number of computational steps).

The same trivial situation is during measuring of corresponding traffic density. This quantity is in real situation derived from measured vehicle speeds and time gaps. Each simulated vehicle has the value of distance from previous vehicle for computing of acceleration.

This value is then possible to use for calculation corresponding local mean density for a period of measuring interval. Then we have to collect to the other counter headways of vehicles, which goes through the reference point.

It is obvious that for traffic densities, when we have stable traffic flow without congestions, we will obtain same values for fundamental diagram as in averaging in the whole system. Totally different situation occurs when we have traffic flow with congestions. Then some few measurements will not give same values, but set of different values on discreet levels of traffic intensities. Dividing into groups is caused by counting only integer over of the vehicle on the bounds of time interval. By this way we will get fundamental diagram which looks more realistic despite of same vehicle properties and stable flow (fig. 10).

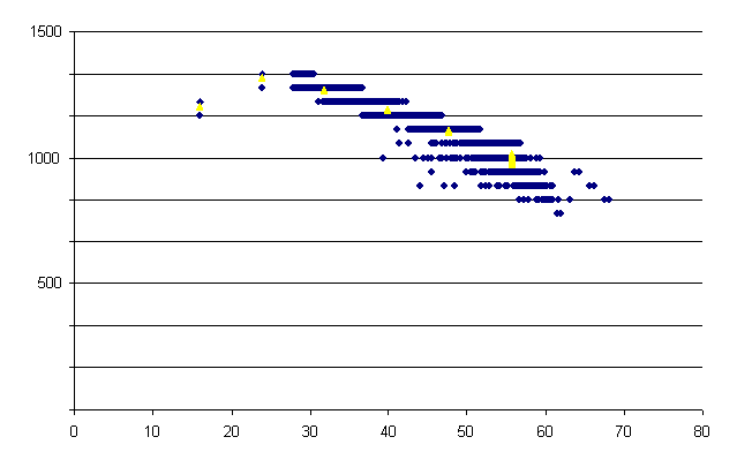


Figure 10. During profile measuring the fundamental diagram looks more realistic as the method of its construction.

From the figure it is apparent that in linear part of diagram is profile measuring concurrent with measuring on the whole system. With emergency of congestions data "blurred" and distances of these levels depends on the period of measuring. We can anticipate that for sufficiently long measuring interval the measured values will converge to values of the whole system.



INTERSECTI

http://www.ce.tuiasi.ro/intersections

Non-linear effects in traffic simulations

3.2.3. Non-linear phenomena

The basic simulation experiment was performed on a system with a maximum number of 400 vehicles, i.e. with density of 63.7 vehicles/km. The flow stabilization was indicated by a stabilization of root-mean-square deviation of distances from an average value. The stabilization was considered as a difference between individual cycles (the passage of reference vehicle through the start) smaller than 10⁻⁵. After each stabilization one vehicle was removed from the system while maintaining the existing states of other vehicles. The gap thus generated was quickly filled, though the existing imbalance was sufficient for the system to jump over into near state with various numbers of congestions. For comparison there an experiment was performed – after each change of the vehicle number, a new initial situation was set (vehicles homogenously distributed along the road without move).

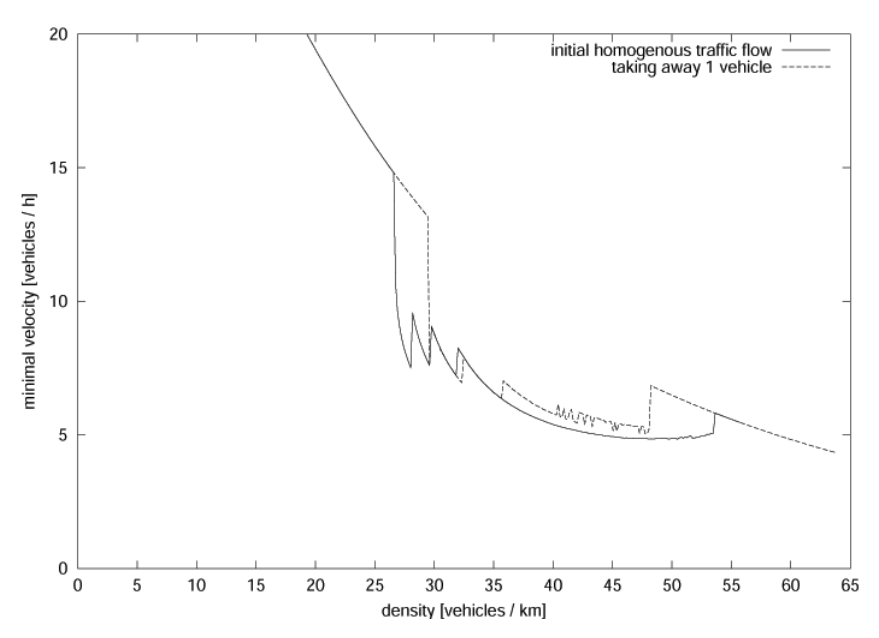


Figure 11. Comparison of dependency of velocities congestion on average density at various strategies of setting initial conditions. Bold line corresponds to the setting of the homogenous traffic flow, thin line to the taking away of the vehicle from the flow without any change of other vehicles states.

From fig. 11 we can see that the disturbance created by taking away the vehicle will be sufficient for the system to overlap into the congestion sooner than it is created by rounding up errors and discretization. In another words in the interval 48 – 53 vehicles/km at least two stable situations exist side by side – homogeneous distribution of vehicles and balanced congestions, while the final situation depends

INTERSECTII

http://www.ce.tuiasi.ro/intersections

T. Apeltauer, P. Holcner, M. Kysely, J. Macur

on the initial conditions. At densities about 45 vehicles per km there are stable situations with various numbers of congestions. During the stabilization from a homogeneous initial situation the system converges alternatively to five or six congestions distributed along the road; with a strategy of taking away vehicles the system stays in a stable state of four congestions. For a lower density the state with six congestions become unstable and extinguishes. A detailed investigation of stable areas of this model is difficult with regard to the fact that space of initial conditions is created among others by the density function.

Together with the state overlapping, occurrence of higher number of stable situations is a typical property of non-linearities.

4. CONCLUSIONS

The outlined microscopic models of traffic flow are only part of a wide spectrum of further models being used. Many of them are not sufficiently theoretically described because they are parts of commercial products, and therefore subject to commercial confidence.

At present a coexistence of models is admitted with some of them describing traffic flow better at higher densities and others at lower densities or other modes. Traffic engineers still wait for a model which would not contain large number of parameters with the necessity of calibration and which would at the same time characterize various traffic modes. Nevertheless it is possible to make a series of interesting conclusions even from the existing models which may be verified in practice – this is what we tried to do in this paper.

References

- Bernard, M., Notes Notes on the Design Concepts for Transport Infrastructure: Past and Future, 4th Swiss Transport Research Conference, Monte Verita, Ascona, 2004.
- Transportation Research Board, Highway Capacity Manual 2000, National Academy of Sciences, USA, 2000.
- 3. Lighthill, M. J., Whitham G. B., Proceedings of the Royal Society A 229, 1955
- 4. Helbing, D., Hennecke, A., Shvetsov, V., Treiber, M., Micro- and Macrosimulation of Freeway Traffic, *Physical Review Letters* 82, 2000
- 5. Kerner, B. S., The Physics of Traffic, Springer, New York, 2004
- Schreckenberg, M., Schadschneider, A., Cellular automaton models and traffic flow, *Journal of Physics A: Mathematical and General* 26 L679-L683, 1993
- 7. Schreckenberg, M., Schadschneider, A., Car-oriented mean-field theory for traffic flow models, *Journal of Physics A: Mathematical and General* 30 **L69-L75**, 1997
- 8. Helbing, D., Traffic and Related self-driven many particle systems, *Reviews of Modern Physics* 73 **1067-1141**, 2001



INTERSECTII http://www.ce.tuiasi.ro/intersections

The Structural Expertise of Steel Cables

Ludovic G. Kopenetz, Ferdinand-Zsongor Gobesz

Department of Structural Mechanics, Faculty of Civil Engineering and Building Services, Technical University of Cluj-Napoca, Cluj-Napoca, 400020, Romania

Summary

Considering the fact, that steel cables are structural elements forming statically determinated systems, their rupture can lead to catastrophe. In this context, the structural assessment of steel cables represents a primary necessity, generated by the requirement to assure security and safety in use.

Generally the main causes which induce degradation/deterioration of cables are: fatigue and corrosion.

The effects of corrosion and fatigue are displayed usually through fiber laceration sequent to a certain service time, after which the number of ruptures and lacerations increases exponentially.

This paper covers some problems of structural expertise along with numerical simulation aspects of corrosion and fatigue, as well as a methodology for the deduction of the presumed service life of steel cables.

KEYWORDS: steel cable, structural expertise, corrosion, fatigue.

1. INTRODUCTION

The irrefutable qualities of bearing cable structures justify, from one part the extension of their application area, from another part the remarkable effort for world-over research concerning a better insight and knowledge about their behavior under corrosion and fatigue, envisioning a safer and more judicious design.

The aim of the authors through the submission of this paper is to present some aspects of their research done by the Faculty of Civil Engineering and Building equipments from the Technical University of Cluj-Napoca.

Since the middle of 70' the pursuit of this kind of research was focused in the following directions:

• Tests carried out in situ (generally considering only statical behaviour, just infrequently considering dynamical too), including the exact quantification of cable structure geometry based on survey techniques. Due to the fact that



those kinds of st applicable survey swing and vibratic

L.G. Kopenetz, F-Zs. Gobesz

those kinds of structures are located usually at considerable heights, the applicable survey techniques have a dynamic character, recording also the swing and vibration of the structure and the movements induced by dynamic loads (wind, functioning equipment, traffic).

- · Laboratory tests, in order to identify the structural materials through physicomechanical and chemical analysis.
- Statical and dynamical analysis and calculus, including the evaluation of the service time for every structural component considering possible future loads and actions over the operative period.

It has to be pointed out the complex and time consuming character of any credible structural expertise in this field, considering the vastity of involved factors which are combined with the unstationary character of the loads (wind, temperature, vibrations from equipment and traffic etc.) [9], [10], [11].



Figure 1. The Agigea Bridge from Romania

INTERSECTII http://www.ce.tuiasi.ro/intersections

The Structural Expertise of Steel Cables

2. CABLES AND TIE-BACKS IN MEMBRANOUS CABLE **STRUCTURES**

Common materials used in cable fabrication during history were: papyrus, camel hair, flax and hemp, until in 1834 when the first cables and ropes from steel wires were made. This new building material soon became indispensable in many fields, due to its special properties - high breaking strain compared to its self weight, great flexibility and durability [17]. In the field of construction, cables were used initially as bearing parts for suspended bridges, and much more lately for covering large areas without intermediate holders [18].

In the last period, in highly corrosive environments, cables made from polypropylene (specific cable weight / specific water weight = 0.91), polyester and nylon (specific cable weight / specific water weight = 1.14) are used.

2.1. Steel qualities and brands for cables and tie-backs [19], [20]

Cables and tie-backs are made from high- and very high-grade steel, with an average carbon content of 0.5% and a breaking strain around 60 daN/mm². Considerable growth of mechanical strength can be obtained through repeated deformations applied on steel rods during the fabrication process of wires. Thus, a cylindrical steel bar is transformed on the drawbench in wire, while its breaking strain rises up to $120 - 200 \text{ daN/mm}^2$. After that, the wire is subdued to a thermal treatment and hereby the material regains its plastic properties. The wire yarns are entwisted on a central wire, in one or more layers, composing strands. At their turn, the strands are coiled around a central core, forming the cable.

Nowadays in Romania two types of steel are used in the fabrication of wires which can be embodied in cables:

- carbon steel with 0.6 0.9% C and 0.3 0.7% Mn,
- thin alloyed steel, usually with manganese and silicon.

From carbon steel are wires with smooth (SBP) or marked (SBPA) surface made, each type in two qualities (I and II). From thin alloyed steel, high strength rods (PC90) are produced, with geometrical, chemical, mechanical and technological properties prescribed by the STAS438/1-74 standard.

The semi-product which is used in the fabrication of strands and cables is the proprietary carbon steel wire (through initial thermal treatment the steel is heated up to 880 - 930 °C, followed by a quick cooling to 450 - 500 °C in a lead bath after which the cooling continues slowly in the air) and drawn SBP type wire (the laminated wires are forced on a drawbench through a smaller hole than the actual diameter of the wire) without final annealing treatment.

The cables can be classified upon several criteria:



INTERSECTII

http://www.ce.tuiasi.ro/intersections

L.G. Kopenetz, F-Zs. Gobesz

- <u>Classification based on shape</u>: The cables can be <u>flat</u> or <u>round</u> shaped. At their turn, round shaped cables can be simple (made from a single strand), double (composed from several strands) or coupled (formed by wrapping double cables around a central core).
- <u>Classification according to the number of strands</u>: Cables can be made from 1, 6, 8, 18 or 36 strands.
- <u>Classification upon the core material</u>: The cable core can be manufactured from vegetal, mineral, metallic or synthetic wires.
- <u>Classification after the quality of fibers</u>: Steel cables can be produced from uncoated (mat) or zinc coated wires.
- <u>Classification upon the laying of strands</u>: The wire yarns can be coiled in a strand towards right (Z) or left (S). At their turn, the strands can be wrapped within a cable towards right (Z) or left (S).

2.2. Bearing structures with cables

From the point of view of structural analysis, bearing structures with cables can be divided in the following two categories:

- isolated cables,
- cable nets and suspended structures.

Considering these structures, cables can be:

- isolated parallel or twisted wires,
- fascicles of stranded wires,
- ropes,
- thin steel rods,
- ribbons,
- chains,

arranged in one direction or in different directions (Fig. 2).

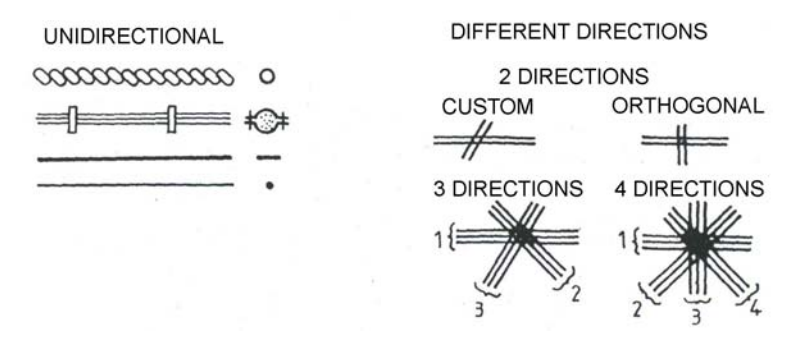


Figure 2. Different cable types

A synthetically exhibition of bearing structures with cables is presented in fig. 3.



INTERSECTI

http://www.ce.tuiasi.ro/intersections

The Structural Expertise of Steel Cables

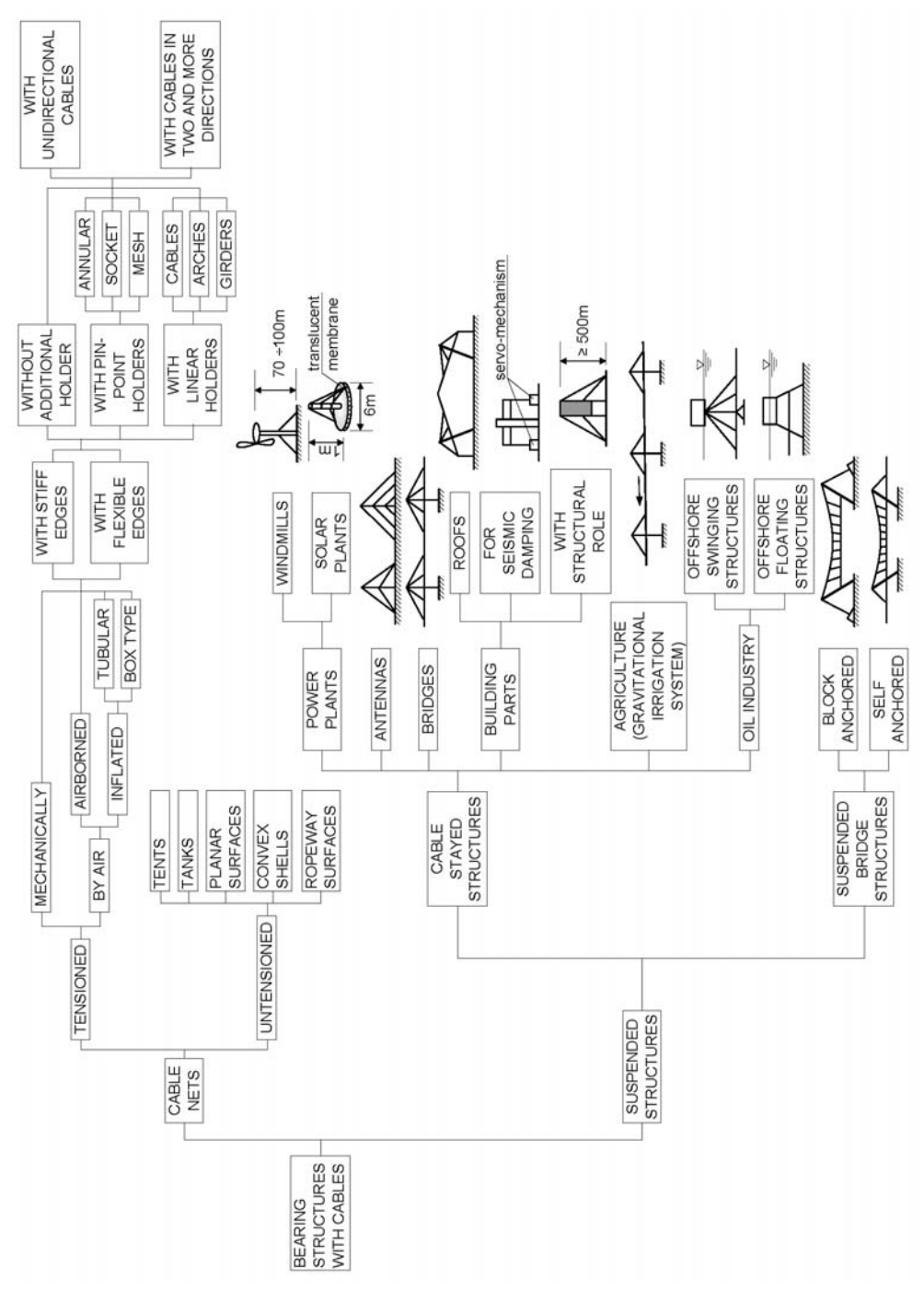


Figure 3. A classification of bearing structures with cables.



INTERSECTII http://www.ce.tuiasi.ro/intersections

L.G. Kopenetz, F-Zs. Gobesz

3. EXAMINATION FACETS FOR STRUCTURAL CABLES

In case of structural cables the problems which are generating noticeable modifications of the structural safety can be grouped in the following classes:

- Problems concerning the quality of the constitutive material (cold flow, brittle or breaking in different manners etc.).
- Fatigue problems due to repeated stress.
- The problem of considerable displacements caused by static and dynamic loads.
- Corrosion and erosion problems.

Bearing structures with cables are characterized by loads which are strongly depending from the basic geometry of the structure, namely by the initial balanced state (including also the geometrical and physical imperfections) induced by the steady and working loads and by eventual pre-stressing.

The expertise and checking of these structures must be done by studying the nonlinear geometrical (eventually physical) behavior and all the factors upon which relies the structural safety. As a decisive element rises in this context the occurrence of corrosion and endurance to oligocyclic fatigue. The resistance to oligocyclic fatigue will be studied from secondary stresses (from vibrations or from daily thermal expansion – contraction) considering the intensity of the stress range.

3.1. Loads on structures with cables

The main loads applied on bearing structures with cables are arising from self weight, wind pressure, temperature, working loads with connected dynamic effects and support displacements.

3.1.1. The influence of weight

The following effects will be considered from dead load, combined also with other loads and forces from different causes:

- active loads, containing self weight and snow build-up, ice (frost);
- inactive loads, containing the self weight of the structural element and other permanent loads.

3.1.2. The influence of wind

This action will be considered in the context of KARMAN vortices, combined from case to case with the phenomena of galloping and fluttering.



INTERSECTII http://www.ce.tuiasi.ro/intersections

The Structural Expertise of Steel Cables

3.1.3. The influence of temperature

The low environmental temperature must be considered in any cases. Structural elements with lower working temperature than 0 °C will be additionally loaded with ice (frost) through the condensation of the moisture from the atmosphere.

In case of cable sustaining tubular structures with closed ends, through the cooling of the built-in gas or steam the inner pressure can drop enough to create vacuum inside the tube. In such case these tubular structural parts must bear up to the external pressure at low temperature.

3.1.4. The influence of dynamic effects

Buildings with structural cables are checked against the detrimal effects of vibrations that can arise from several sources, such as:

- impact forces;
- resonance developing from the operation of equipments (including air conditioning and ventilation appliances, loud musical gears, traffic etc.);
- seismic actions and wind.

3.1.5. The influence of thermal effects (expansion, contraction)

Thermal effects should be considered in combination with loads and forces from other causes:

- thermal actions through constraints and restraints;
- effects due to different coefficients of thermal expansion in case of structures with mixed materials (like steel and aluminum).

3.2. Case of laboratory-tests

The minimal bench tests which are carried out in a laboratory in order to identify the compounding materials of bearing structures with cables are:

- axial extension test, at different velocities;
- repeated bending test;
- torsion test:
- chemical test of the base material;
- simulation of corrosion and fatigue.

3.3. Site investigations [21]

Examining the behavior in time (ageing property) of steel cables is a special assay, imposed primary by the necessity to insure operational safety. In situ tests will pursue:

• Diminution of cable section, namely loss of metallic cross sectional area (LMA) due to corrosion, plastic deformation (afterflow) etc. [22].



INTERSECTII

http://www.ce.tuiasi.ro/intersections

L.G. Kopenetz, F-Zs. Gobesz

- Modification of the shape (geometry).
- Broken wires, laceration and other *local faults* (LF) due to fatigue [22].

In principle the following methods are used for site investigations:

- visual inspection,
- electrochemical (potential, electrochemical sounds, magnetic etc.) methods,
- other nondestructive testing (microscopical examination, gravimetry, infrared thermography, gammagraphy, radiography and radar processing) [23], [24], [25].

For structural cables only a few of these methods give adequate results.

For visual inspection carried out in site, the authors are advising a new method: MOV_CAM (currently under patenting), using sliding digital cameras in order to view and process the image of the cable (fig. 4).

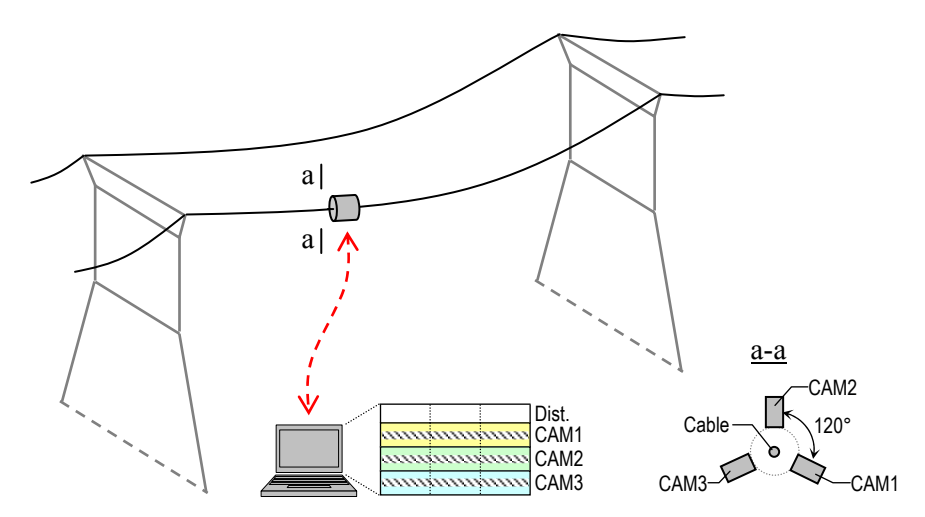


Figure 4. Visual investigation with digital cameras (currently under patenting).

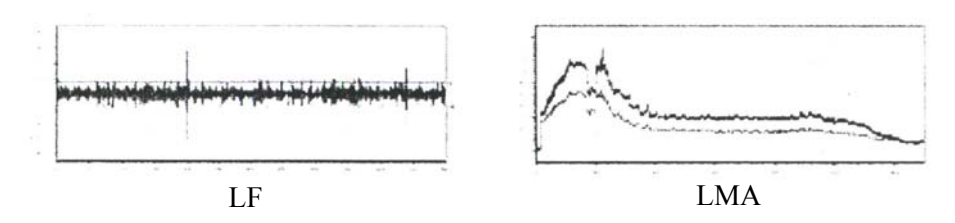


Figure 5. Sample results from LF and LMA testing.



INTERSECTII http://www.ce.tuiasi.ro/intersections

The Structural Expertise of Steel Cables

For LMA and LF type investigations electromagnetic processes are successfully used lately, based on a magnetic head equipped with strong permanent magnets and sensors with distance meter. The software enables to inspect and to display the local faults (LF) and the sectional area diminishments (LMA) in a synthetically manner (fig. 5).

The investigation of the occurrence of corrosion in situ has a peculiar meaning, on one side due to the increasing intensity of the polluting agents in the environment, on the other side due to the requirement regarding the prolongation of the operational service time of cables.

Cables are highly sensitive to corrosion because their self constructional embodiment enables the penetration and stagnation of moisture.

One of the most delicate problems of structural engineering is to track and to keep under control the evolution of degradations caused by corrosion, because this aspect entail in time changes in the physico-mechanical properties and therefore in the strength of materials, leading also to stress redistribution in the structural elements. That is the reason why in the following part a method for monitoring the corrosion of steel cables and the principle of numerical simulation for this process will be described.

The acquisition of primary data about corrosion, in the case of cables, can be done with the method of electric resistance, which is easily applicable in situ. The method of electric resistance is based on the principle that cable corrosion is accompanied by cross sectional reduction. In this way, if there is no intercrystalline corrosion, the raising of electric resistance is produced by the diminution of the cross section.

In case of intercrystalline corrosion, the area of the cross section is not modified significantly, but the specific resistance increases. Thereby, measuring the electric resistance on different portions of a steel cable, considering 500 – 1000 mm long segments, the commencement of corrosion can be promptly recorded. Monitoring the corrosion of steel cables by the means of the electric resistance method enables the undelayed signaling of the occurrence of corrosion, including intercrystalline corrosion. This method is simple, safe and relatively cheap, implying low costs.

4. NUMERICAL SIMULATION OF CABLE CORROSION

The numerical simulation of corrosion can be done in order to study the phenomena in time, using probabilistic degradation functions or data acquired through monitoring. Some of the most frequently encountered fault types are presented in table 1.



INTERSECTII http://www.ce.tuiasi.ro/inters

L.G. Kopenetz, F-Zs. Gobesz

Table 1. Typical patterns of wire rope degradation and failure [25]			
Illustration	Short explanation		
	A "bird cage" caused by sudden release of tension and resultant rebound of rope from overloaded condition. These strands and wires will not return to their original positions.		
	A close-up of a rope subjected to drum crushing. The distortion of the individual wires and displacement from their normal position is noticeable. This is usually caused by the rope scrubbing on itself.		
	A wire rope jumped from a sheave. The rope itself is deformed into a "curl" as if bent around a round shaft. Close examination of the wires show two types of breaks – normal tensile "cup and cone" breaks and shear breaks which give the appearance of having been cut on an angle with a cold chisel.		
	Localized wear over an equalizing sheave. The danger of this type wear is that it is not visible during operation of the rope. This emphasizes the need of regular inspection of this portion of an operating rope.		
÷ €	A wire which has broken under tensile load in excess of its strength. It is typically recognized by the "cup and cone" appearance at the point of the fracture. The necking down of the wire at the point of failure to form the cup and cone indicates that failure occurred while the wire retained its ductility.		
DO STATES TO SERVED IN	An illustration of a wire which shows a fatigue break. It is recognized by the squared off ends perpendicular to the wire. This break was produced by a torsion machine which is used to measure the ductility. This break is similar to wire failures in the field caused by excessive bending.		
	A wire rope which has been subjected to repeated bending over sheaves, under normal loads. This results in "fatigue" breaks in individual wires, these breaks being square and usually in the crown of the strands.		
	An example of "fatigue" failure of a wire rope which has been subjected to heavy loads over small sheaves. The usual crown breaks are accompanied by breaks in the valleys of the strands, caused by "strand nicking" resulting from the heavy loads.		
	A single strand removed from a wire rope subjected to "strand nicking". This condition is the result of adjacent strands rubbing against one another and is usually caused by core failure due to continued operation of a rope under high tensile load. The ultimate result will be individual wire breaks in the valleys of the strands.		

INTERSECTII

http://www.ce.tuiasi.ro/intersections

The Structural Expertise of Steel Cables

The SACOC (*Structural Analysis of Corrosion for Cables*) software package is based on the finite element method and it proved to be very useful in the study of the corrosion of structural cables. A schematic block diagram of this program is presented in figure 6 [21].

The user can take advantage of several available degradation functions simulating cable corrosion in time, or he can use quantifications from site investigations gathered in a data base.

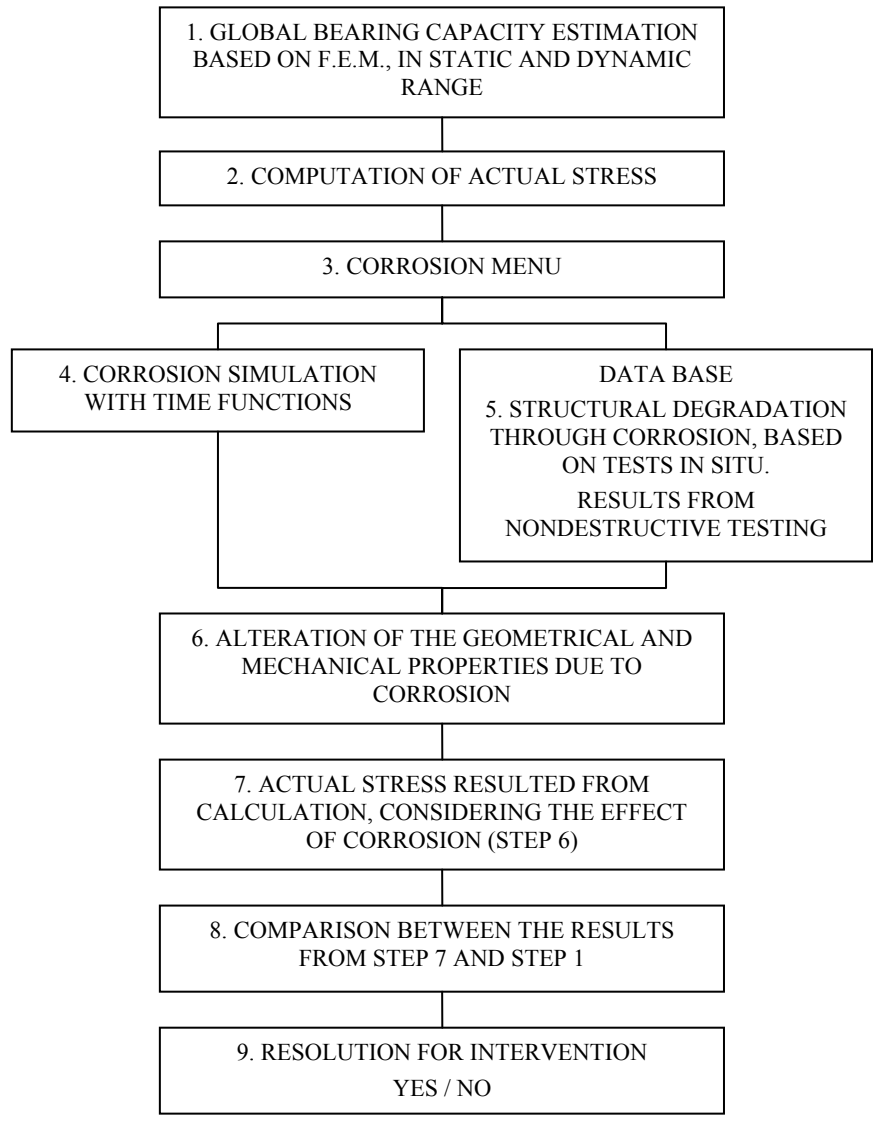


Figure 6. The schematic block diagram of the SACOC software.



INTERSECTII http://www.ce.tuiasi.ro/inters

L.G. Kopenetz, F-Zs. Gobesz

5. CABLE QUALITY CERTIFICATION

The quality of cables is guaranteed by the manufacturer through quality assurance certificates, released for each product range. Deviations in dimensions, properties and shape shall not exceed the prescribed limits from the relevant Romanian technical regulations, nor those stated by the manufacturer. The list of standards for wires and steel cables is presented in table 2.

Table 2 The list of Romanian standards (STAS) in use

Table 2. The list of Romanian standards (STAS) in use			
Pos.	Title	STAS	
1 03.	Title	code	
1	Materials	880-66	
2	Cold-drawn steel wires for drag ropes	1298-80	
3	Steel cables. Concept and classification.	1710-79	
4	Steel cables. Simple structure cables. Shapes and dimensions.	1513-80	
5	Steel cables. Technical requirements.	1352-78	
6	Steel cables. Double cables. Combined structure. Shapes and dimensions	1689-80	
7	Steel cables. Combined cables. Double cables. Ordinary structure. Shapes and dimensions	1535-71	
8	Steel cables. Combined cables. Triple structure. Shapes and dimensions	2693-80	
9	Steel cables. Combined flexible double cables. Shapes and dimensions	1353-80	
10	Steel cables. Flat cables. Shapes and dimensions	1559-80	
11	Alternate bending test for steel wires	1177-74	
12	Testing of metals. Torsion test for wires	1750-80	
13	Testing of metals. Coiling test for wires	6622-70	
14	Testing of metals. Tensile test for wires	6951-76	
15	Testing of metals. Tensile test for steel cables	2172-74	
16	Combined double concentric cables	2590-80	
17	Steel wire for prestressed concrete	6484-77	

6. CONCLUSIONS

Bearing structures with cables are liable to generate unappointed phenomena in comparison with conventional structures. Thus, beside the great displacements originated from their custom designed structural shapes, displacements arise due to the $\sigma_{breaking}$ / E ratio. While this ratio in case of conventional structures, considering OL37 steel is 3700/2100000 = 1/568, in case of using cables becomes 15000 / 1650000 = 1 / 110, namely five times bigger.



INTERSECTII http://www.ce.tuiasi.ro/intersections

The Structural Expertise of Steel Cables

Zinc coated cables are able to withstand to corrosion approx. 10 - 15 years. For this reason, in case of highly corrosive environment should be remembered that high quality ropes and cables made from synthetic materials with outstanding endurance are available too.

The required anchoring of cables must be done by wrapping their end with cast zinc inside threaded pipes instead of using clamps, because the cable may slip out from the clamp at high dynamical stress.

Cables should be prestressed in a jointly manner with their anchors (thus the anchoring is tested) before installation, with a force equal to approx. 1.10 times the computed actual stress, in order to consume the significant remnant elongations and to avoid subsequent loosening and relaxation.

References

- 1. Falk, S., Lehrbuch der Technischen Mechanik, Springer Verlag, Berlin-Heidelberg, 1967.
- Leonhardt, F., Zellner, W., Vergleiche zwischen Hängebrücken und Schrägkabelbrücken für Spannweiten über 600 m, International Association for Bridge and Structural Engineering, vol. 32, 1972
- 3. ***, Bibliography and Data Cable-Stayed Bridges, Journal of the Structural Division, ST10,
- 4. Knut, G., Merkblatt-496, Ebene Seiltragwerke, Beratungstelle für Stahlverwendung, Düsseldorf,
- 5. Kopenetz, L. G., Ionescu, A., Lightweight Roof for Dwellings, International Journal for Housing and its Application, vol. 9, No. 3, Miami, Florida, USA, 1985.
- 6. Haug, E., Engineering Contributions to the Design of Lightweight Structures via Numerical Experiments, 2nd International Symposium Weitgespannte Flachentragwerke, University of Stuttgart, 1979.
- 7. Jensen, J. J., Das Dynamische Verhalten Eines Vorgespannten Kabelnetz, University of Trondheim, Norway, 1972.
- 8. Goschy, B., Dynamics of Cable-Stayed Pipe Bridges, Acier-Stahl-Steel, No. 6, 1961.
- 9. Szabó, J., Kollár, L., Függőtetők számítása, Műszaki Könyvkiadó, Budapest, 1974.
- 10. Otto, F., Das Hängende Dach, Bauwelt Verlag, Berlin, 1959.
- 11. Oden, J. T., Finite Elements of Nonlinear Continua, McGraw-Hill, 1972.
- 12. Krishna Prem, Cable-Suspended Roofs, McGraw-Hill, London & New York, 1979.
- 13. Fuller, B. W., Weathering of neoprene-coated Nylon fabric, E. I. Dupont de Nemours & Co., Report BL-327, 1956.
- 14. Otto, F., Trostel, R., Zugbeanspruchte Konstruktionen II, Ullstein Verlag, Frankfurt-Berlin, 1966.
- 15. O'Brien, T., General Solution of Suspended Cable Problems, Journal of the Structural Division, ST1, Febr. 1967.
- 16. Sofronie, Ramiro, Vertical Deflection of Suspension Bridges, Revue Roumain Scientique Technique-Mécanique Appliqué, Tome 24, No. 3, București, 1979.
- 17. Mollmann, H., A Study in the Theory of Suspension Structures, Copenhagen, 1965.
- 18. ***, Recommendation for Guyed Masts, The Working Group on Guyed Masts of I.A.S.S., 1981.
- 19. Kopenetz, L. G., Cătărig, A., Cabluri structurale, Simpozionul Tehnologie și Siguranță, U.T. Pres, Cluj-Napoca, 2004. (in Romanian)
- 20. Kopenetz, L. G., Cătărig, A., Teoria structurilor ușoare cu cabluri și membrane, U.T. Pres, Cluj-Napoca, 2006. (in Romanian)



INTERSECTII http://www.ce.tuiasi.ro/intersections

L.G. Kopenetz, F-Zs. Gobesz

- 21. Kopenetz, L. G., Cătărig, A., Probleme ale coroziunii cablurilor din oțel, Lucrările celei de a VIIa Conferințe de Construcții Metalice, vol. 2, Timișoara, 1994. (in Romanian)
- 22. ***, GTU Documentation, USA (Nondestructive Testing Technical Diagnostics).
- 23. Knut, G., On the Fatigue Strength of Wires in Spiral Ropes, Journal of Energy Resources Technology, vol. 107, 1985.
- 24. ***, Internal Report, Bethlehem Wire Rope, USA.
- 25. ***, Technical Report No. 107, Wire Rope Corporation, St.Joseph, MO, USA.
- 26. Bârsan, G. M., Kopenetz, L. G., Alexa, P., Theil, S., Gedanken zum Entwurf Leichter Zusamengesetzter Tragwerke, Proceedings of the 4th Conference on Steel Structures, Timisoara, Romania, 1985.

INTERSECTII http://www.ce.tuiasi.ro/intersections

Quality costs in Bridge Engineering

Alina Nicuță, Constantin Ionescu

Faculty of Civil Engineering and Installations, University Gh. Asachi, Iasi, 700050, Romania

Summary

The current paper desires to create an introduction towards the research in quality costs for bridges.

The superior quality of bridges is a matter of great importance. The quality administration is determined by different instruments which are components of ISO 9000 standards. As for Romania the quality in the area of engineering is guided by the Law 10 of quality. The concept of quality costs has the main objective the identification, evaluation and comparison of costs. These costs administration must integrate all the phases of creation and exploitation of a bridge construction.

KEYWORDS: quality costs, bridges, Law 10 – quality law, design, execution and exploitation.

1. INTRODUCTION

The bridges network is ageing and so the agencies take more and more into consideration the maintenance and rehabilitation of the existent infrastructure.

The quality of bridge structures is influenced by different types of factors such as technical, economical, social and natural. Most of the times, their influence isn't an isolated phenomena but a simultaneous one. They interfere on the quality characteristics, creating the rise and fall of the quality general level.

Quality costs are the costs associated with preventing, finding, and correcting defective work. These costs may be huge. Many of these costs can be significantly reduced or completely avoided. One of the key functions of a Quality Engineer is the reduction of the quality total cost associated with a construction work.

2. GENERAL APPROACH OF TRANSPORTATION QUALITY **COSTS**

Considering the transport capacity already valuated, the agencies must focus more than before on the work zones effects on the users.



INTERSECTII

http://www.ce.tuiasi.ro/intersections

A. Nicuță, C. Ionescu

The costs in a different approach can be connected to the transport infrastructure elements quality.

The most common is the traditional approach of the costs regarding the quality. It allows the determination of the source where they appear, the cause and quality costs measurement

A certain time period the quality improvement and the quality costs reduction were considered differently. This problem was settled in 1979, in the paper "Quality is Free" by Ph. Crosby, where the quality costs are analyzed in detail. In its book, Crosby demonstrated the fact that the lack of quality determines complementary expenses. Even if in practice is difficult to identify and divide all the quality costs, an attempt in this direction brings into evidence looses due to the reparations, replacements, stagnation etc.

The determination of quality costs takes to profit increase by the identification of the most proper solutions of costs reduction.

Quality costs are grouped this way:

- 1. prevention
- 2. inspection
- 3. internal costs of unconformity
- 4. external costs of unconformity

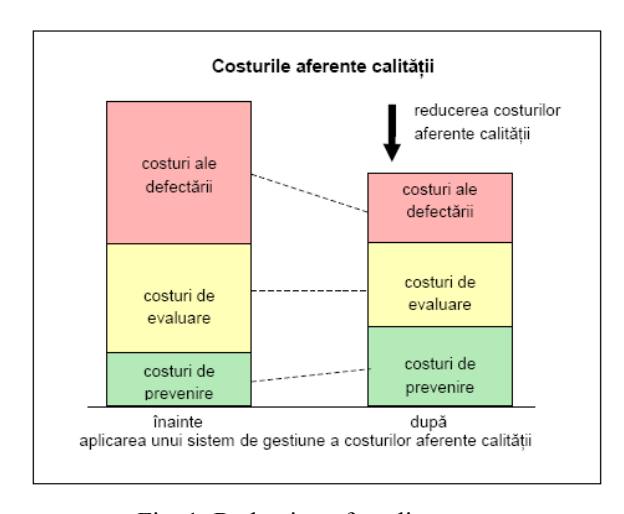


Fig. 1: Reduction of quality costs

Source: Marieta Olaru, "Costurile referitoare la calitate", in "Quality Management" Second Edition

Quality costs have different classifications as seen in Figure 1.



INTERSECTII

http://www.ce.tuiasi.ro/intersections

Quality costs in Bridge Engineering

The prevention costs in the area of bridges represent the investments done before the execution works or maintenance in order to prevent the defection in the next steps. Here are being included also the quality costs determined by the infrastructure impact on the environment. The lately transportation fast development had a great impact on the environment so that the transportation has become the main source of aggression on the environment and human health. The environment pollution due to a bridge structure takes place in two steps: the execution and exploitation.

Evaluation costs are inspection costs (testing, inspection, examinations) and tests which have been considered if the quality requests have been fulfilled. In the bridge area the evaluation costs represent the value of the effort done in order to determine the conformity degree of the construction works with the specified quality.

Internal unconformity costs in bridges execution and maintenance represents the costs of unconformity adjustments discovered after the works creation but before the element exploitation. These are expenditures caused by the fact that certain works quality level doesn't fulfill the specified requests.

External unconformity costs in the bridge area are the expenses determined by the unconformities correction discovered after the execution and maintenance works and after bringing into service the elements. These are costs caused by the fact that the quality level for certain constructions doesn't fulfill the specified requests.

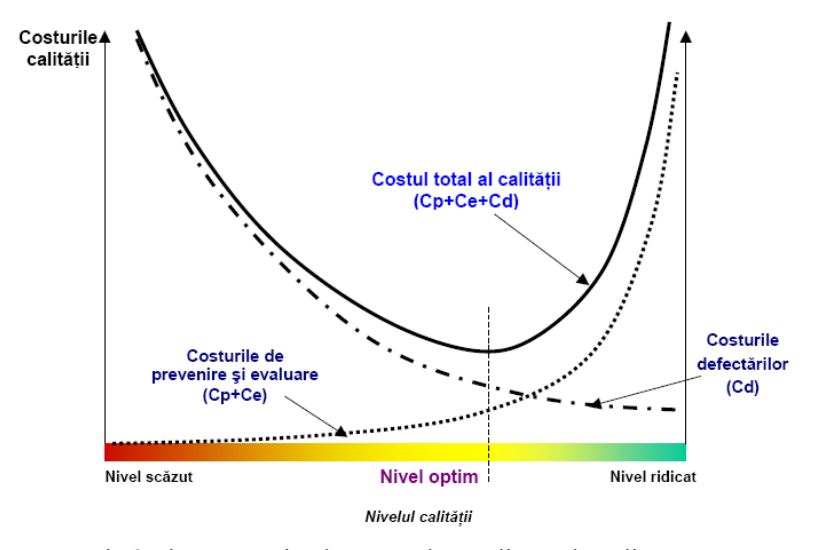


Fig 2 The connection between the quality and quality costs
Source: Marieta Olaru, "Costurile referitoare la calitate", in "Quality Management" Second
Edition



INTERSECTII http://www.ce.tuiasi.ro/intersections

A. Nicuță, C. Ionescu

The connections between the quality costs categories is suggested in fig 2 by the graphical representation of the quality "optimal level". It can be seen that in the situation of a relatively small increase of the investments for the prevention and evaluation measures will result a sensitive reduction of the unconformity costs, so that, totally, the quality costs will decrease. This fact is also presented in the previous figure but with a different structure. On the other hand, in the case of neglecting the preventive quality costs component, can result important increases of the other expenses, considering the internal and external unconformity multiplication.

The decrease of any of the three expenses categories will lead towards the decrease of quality total cost, but the minimal level is in the equilibrium point between these three costs categories. As seen in figure, there is a point on the total expenses curve where these are minimal and this is a result of the combination between the unconformity costs and those of prevention and evaluation.

Being outside the optimal level means obtaining a low quality level, when the quality loses are greater than the investments, or obtaining a high level of quality, when unconformity costs reduction is done with great expenses for the prevention and evaluation and also by more important investments.

The quality costs are interconnected:

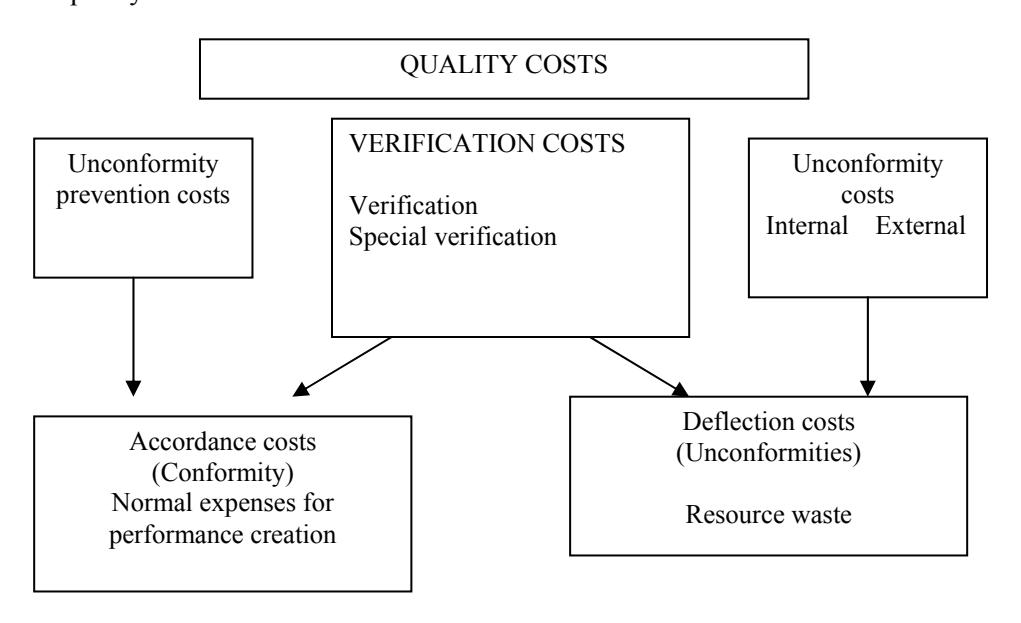


Fig 3 Quality costs



INTERSECTII

http://www.ce.tuiasi.ro/intersections

Quality costs in Bridge Engineering

Identification of the quality costs is necessary for operative and administrative procedures supervision. They are used as a strategic instrument to create projects and for measures argumentation.

Quality costs gathering and calculation is included into a quality management system. It is recommended a preventive treatment of the quality costs.

The basic point in quality costs treatment is represented by the unconformity prevention and costs, in the first steps of the construction and not the unconformities improvement.

A different vision on the quality costs starts from the Law 10 regarding the Quality in Constructions. For a bridge construction work are being taken into consideration as research points not only the quality regarding the bridge construction but also complementary elements such as:

- design
- execution
- exploitation

with the proper expenses for the quality.

If previously in general view, the accent is on the quality costs in the context of construction work exploitation, in the current view are being considered also the quality costs in the phase of design and execution.

3. QUALITY SYSTEM IN BRIDGE ENGINEERING

In accordance with Law no. 10 regarding the quality in construction, the quality system is composed from:

- a. Technical regulation;
- b. Quality of the products used for the construction creation;
- c. Technical agreements for new products and technologies;
- d. Projects verification, works execution and projects and constructions expertise;
- e. Assurance of quality in construction area;
- f. Authorization and accreditation of analysis laboratories and testing in construction activity;
- g. Metrology activity in constructions;
- h. Construction reception;
- i. Behavior in exploitation and time intervention;
- i. Construction post utilization;
- k. State quality control in construction.



INTERSECTII http://www.ce.tuiasi.ro/intersections

A. Nicuță, C. Ionescu

In the area of Bridge Engineering, quality assurance, control and maintenance for a bridge has some particularities, specially, considering the exploitation period, the fact that this is designed, executed and exploited by different companies, by the long time contact with the environment and by its social importance.

This way, for every company must by developed and implemented a quality system with the purpose of realizing the quality policy objectives. In order to achieve the quality objectives are realized the mobilization of all the technical, administrative and human factors which can influence a construction quality. The quality system must be guided towards the reduction, elimination and most important prevention of qualitative deficiencies.

In order to implement the quality policies and deficiencies, in a company must be created proceedings regarding the personnel training, design activities coordination, bridge creation and maintenance.

Also, it is necessary to select all the activities which lead directly towards the assurance, administration and maintenance of the quality, reported to the design, creation and maintenance activities. Based on the specified data there must be determined as right as possible a bridge quality costs on the existence period.

4. AGENTS WHICH DETERMINE THE QUALITY IN BRIDGE **ENGINEERING**

Considering a critical analysis of the quality system components and the existence steps for a bridge such as: design, execution and exploitation can be determined the factors by which it can be assured the quality.

- 4.1. In the design phase, the factors which assure the bridge quality are:
 - The professional level of each member of the design collective (including the collective operational discipline);
 - b. The experience in the area of the design collective (the general experience and the specific experience for the design theme);
 - informational system complexity (standardization, instructions, normative, treaty, similar projects etc.);
 - d. The used computer field system performance (data base, INTERNET, INTRANET, HARD, Soft);
 - The durability of the adopted constructive system (bridge on frames, girder bridge, etc.);
 - The site identification (information, technical and environmental knowledge, etc.);



INTERSECTII

http://www.ce.tuiasi.ro/intersections

Quality costs in Bridge Engineering

- g. The capacity to satisfy the basic requests: resistance, stability, safety in exploitation, environment protection;
- h. Optimization of the adopted constructive solution;
- i. Project inspection, project expertise in the case of frictions between designer and verifier, approval of the internal technical department of the beneficiary.
- 4.2. Factors specific to the bridge construction phase:
 - a. Level of professional background of each and every member of the engineers collective (including the collective operational discipline);
 - b. Experience in the area of bridge execution and experience specific to the designed bridge type;
 - c. The complexity of used information system (standardization, instructions, technological methodologies etc.);
 - d. Performances of the analysis and testing laboratories;
 - e. Information related to the execution project acquired by the executor (relation between designer executor);
 - f. Quality of the products used for the construction;
 - g. Bridge testing (if mentioned in the project);
 - h. Bridge reception.
- 4.3. In the exploitation phase the bridge quality maintenance factors are:
 - a. The level of professional background of each member of the experts collective in bridge maintenance, at beneficiary (including the collective operational discipline);
 - b. Experience in bridge exploitation area and experience specific to the received bridge type;
 - c. The bridge exploitation in accordance with the project specifications (weight, load class etc.);
 - d. Pursuit in exploitation of the received bridge behavior;
 - e. Processing and stocking of data and information from the determination in time of the bridge behavior;
 - f. Intervention in due time on the bridge: maintenance, repairing, consolidation etc.;
 - g. Construction expertise.

5. QUALITY COSTS IN BRIDGE ENGINEERING

Considering the factors specific for the creation of the bridge quality, the quality cost can be detailed in three main costs groups:



INTERSECTII http://www.ce.tuiasi.ro/inters

A. Nicuță, C. Ionescu

- The cost for quality assurance and damages prevention and technological, personnel (constructive training improvement, costs of the used equipments etc.);
- b. Quality cost control (evaluation, remuneration, endowment
- c. Costs of losses due to the non quality (remunerations, replaced elements, costs of intermissions in assembly delivering, looses in exploitation phase etc.).

Total cost of a bridge quality, C_{TC} is:

$$C_{TC} = C_{PA} + C_{C} + C_{I} + C_{P}$$

where:

 C_{PA} - Prevention cost of the damages and assurance of the quality level;

 $C_{\rm \tiny C}$ - Total quality control cost;

C₁ - Maintenance costs at the beneficiary;

C_P - Looses due to the lack of quality.

6. CONCLUSIONS

In order to determine the quality costs it is necessary to study all the factors which influence the quality in a bridge life time, to detail these factors and to distinguish the quality costs considering the other activities costs which fulfill for the bridge edification.

At the bottom of quality costs evaluation we must consider the quality system correlated with the systems engineering concept by which the total creation of a bridge is determined by a system consisting from the design subsystem, creation (construction), exploitation and evaluation of the bridge.

References

- 1. Kelada, J., La gestion intégrale de la qualité. Pour une qualité totale. Edition Quafec, Québec,
- "Quality Costs" in Juran, J.M. & Gryna, F. M. (1988, 4th Ed.), Juran's Quality Control Handbook, McGraw-Hill
- Marieta Olaru, Costurile referitoare la calitate, Managementul calitatii, editia a II-a
- 4. Voicu M., Irina Severin, Inițiere în ingineria calității, Editura Bren, București 2000
- 5. Principles of Quality Costs, ASQC Quality Press, Appendix B, "Detailed Description of Quality Cost Elements.'



ш

Transportation Infrastructure Engineering

INTERSECTII http://www.ce.tuiasi.ro/inters

Sensitivity study of a model for the stability analysis of continuous welded rail

Valentin-Vasile Ungureanu, Marius Comanici Department of Civil Engineering, "TRANSILVANIA" UNIVERSITY, Braşov, Romania

Summary

In 1992÷1999 period the International Union of Railways (UIC) commissioned a research program from European Rail Research Institute (ERRI) about improving the knowledge of continuous welded rail (CWR) track, including switches [2]. This research was necessary for revision and update of Leaflet UIC 720 which regulate the problems concerning the laying and maintenance of CWR track, which was from January 1986 [3]. In the new Leaflet UIC 720 [4], which was from March 2005, was introduced concepts and criteria for the CWR buckling safety assessment and it were shown cases studies which appeal to the two analysis of CWR stability software, one developed at TU Delft (Holland) for ERRI – software called initially CWERRI, and nowadays LONGSTAB - and the other developed at Foster&Miller company for Federal Rail Administration of United States of America (FRA) – software called CWR-BUCKLE [1, 2]. In this context, at Civil Engineering Faculty from Brasov was developed a software for simulation of lost of track stability using a non-linear discrete model for CWR buckling analysis, in presence of thermal and vehicle loads, model called SCFJ [5, 8]. A presentation of SCFJ model can be found in [5].

In this paper is presented a comparison of numerical experiment results which were achieved with SCFJ and CWERRI software.

KEYWORDS: Continuous welded rail, Non-linear stability analysis, Temperature loading, Sensitivity analysis.

1. INPUTS

For this analysis which used the same inputs like in comparative studies of CWERRI and CWR-BUCKLE software presented in [6, 7, 9].

Hereby, it was considered a sector of L=47.5 m in the central zone of a CWR track located in a curve with R=400 m, which has in the middle a misalignment characterized by a half sine wave with a length of $\lambda = 9.144$ m and an amplitude of $\delta = 0.0381$ m (fig. 1). These values are characteristic for USA railway [6, 7, 9]. The track is composed from AREA 136 type rails and reinforced concrete sleepers



INTERSECTII

http://www.ce.tuiasi.ro/intersections

V.V. Ungureanu, M. Comanici

laying at 0,61 m spacing. For the fastenings it was considered a linear-elastic behavior with a torsional resistance of the fastenings $R_t = 11250$ N/rad per meter track. The vertical behavior of railway track is supposed to be linear-elastic with a stiffness of $R_z = 68900$ kN/m per meter track. The longitudinal resistance is supposed to be linear-elastic. The lateral resistance is tri-linear with o pick value F_p which corresponds to W_p displacement and a limit value F_l for W_l displacement. It was supposed that the values of lateral resistance are in function of the vertical force between the sleeper and ballast (fig. 2) generated by the vertical loads on train axle. The model is vertically loaded by a hooper wagon with two bogies, represented by four vertical axle forces of F_z = 293 kN each (fig. 3). The centre spacing between bogies is 12,85 m. The space between the axle in a bogie is 1,78 m. The vehicle is placed on track in such a way that the middle of center spacing between bogies is coincident with the centre of the misalignment. Ori: The vehicle is centered on the misalignment. The value of the friction coefficient between sleepers and ballast is $tan \Phi = 0.86$ – this being an average value for reinforced concrete sleepers.

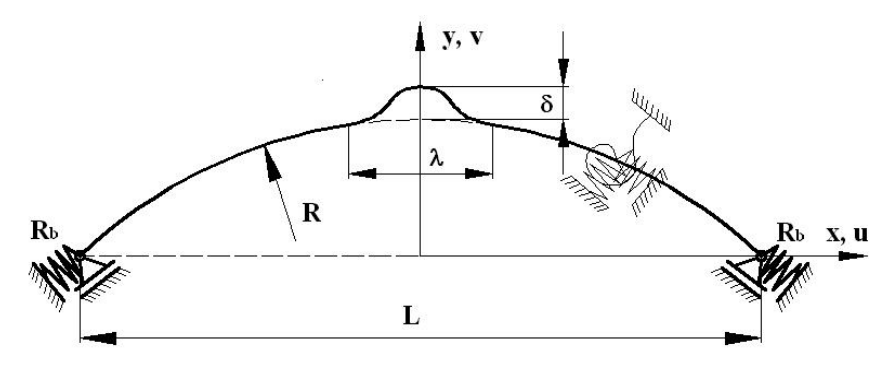


Fig. 1. Plan view of CWR track model

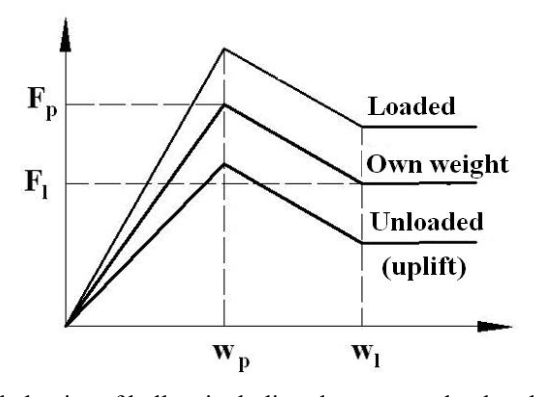


Fig. 2. The lateral behavior of ballast including the corrected value due to vertical loads

INTERSECTII

http://www.ce.tuiasi.ro/intersections

Sensitivity study of a model for the stability analysis of continuous welded rail

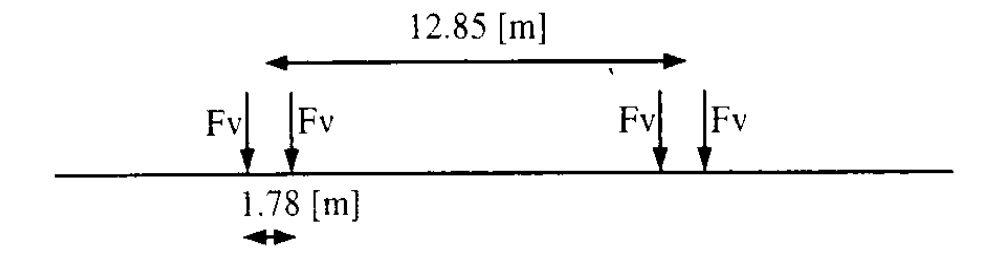


Fig. 3. Vertical axle loads on track

2. THE COMPARISON OF THE RESULTS

In the sensitivity study the quantities of interests are the increases of the superior critical temperature T_{max} , respectively inferior T_{min} , which result from the lateral displacement curve for the middle of the CWR model in function of the increase of the temperature (fig. 4). These were obtained through variation of each parameter in an interval, while the other parameters are remaining constants, as shown in Table 1. It was considered that in the initial position the track is strain free.

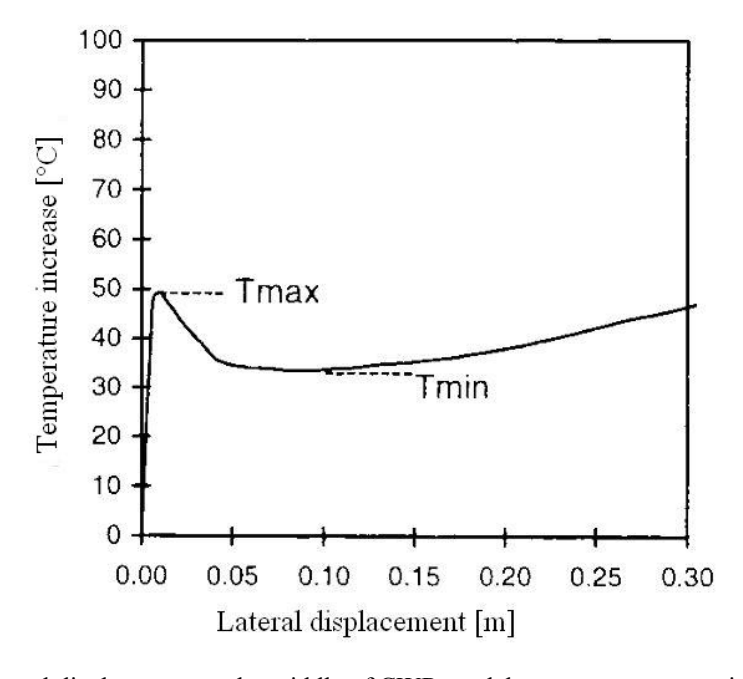


Fig. 4. Lateral displacement at the middle of CWR model versus temperature increasing

INTERSECTI

nttp://www.ce.tuiasi.ro/intersections

V.V. Ungureanu, M. Comanici

Table 1. The parameters of the model for the sensitivity analysis

Parameter		Reference value	Range
Radius (R)	[m]	400	100 ÷ ∞
Lateral peak resistance (F_p)	[N/m track]	17508	8754 ÷ 26262
Lateral limit resistance (F_l)	[N/m track]	9630	4815 ÷ 14445
Longitudinal resistance (R_x)	[N/m/m track]	1,378·10 ⁶	$1,0\cdot10^5 \div 1,0\cdot10^7$
Torsional resistance (R_t)	[Nm/rad/m track]	$1,1125\cdot10^5$	$0.0 \div 3.0 \cdot 10^6$
Misalignment amplitude (δ)	[m]	0,0381	0,008 ÷ 0,05
Wave length of misalignment	[m]	9,144	1,2 ÷ 9,6

It is observed that for the critical temperature increases in function of radius (fig. 5), the difference between SCFJ and CWERRI results is maximum 7%, and the biggest differences are for the smallest radius values.

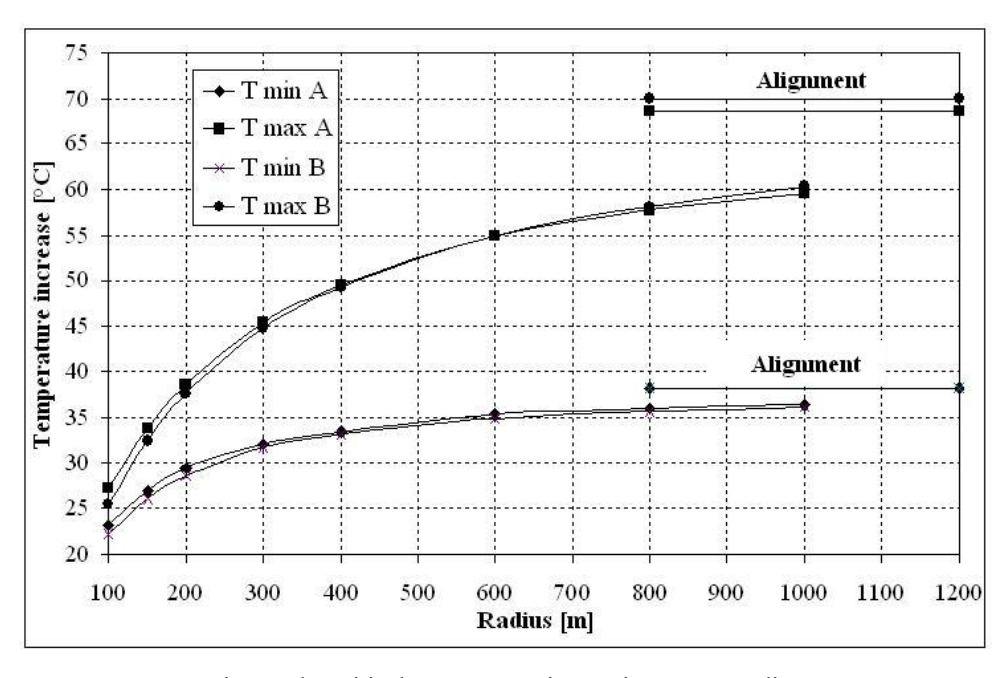


Fig. 5. The critical temperature increasing versus radius

The differences between SCFJ and CWERRI for the critical temperature increasing in function of the lateral peak resistance (fig. 6) are maximum 2,6% when the track is loaded only with thermal loads, therefore in absence of vehicle vertical loads.

INTERSECTII

http://www.ce.tuiasi.ro/intersections

Sensitivity study of a model for the stability analysis of continuous welded rail

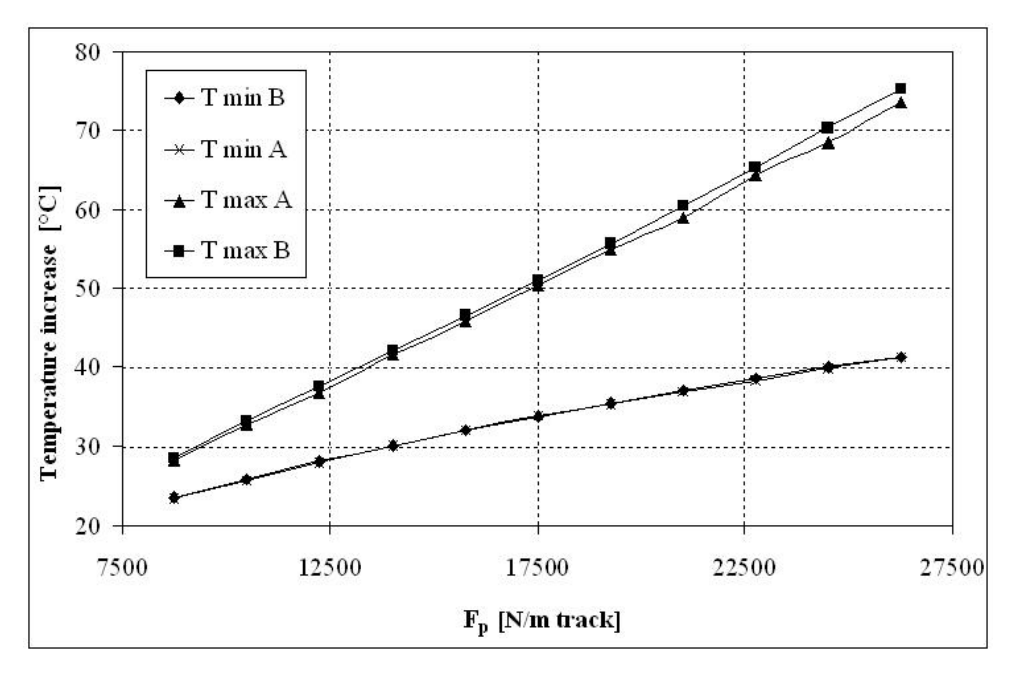


Fig. 6. The critical temperature increasing versus lateral peak resistance (without vertical loads)

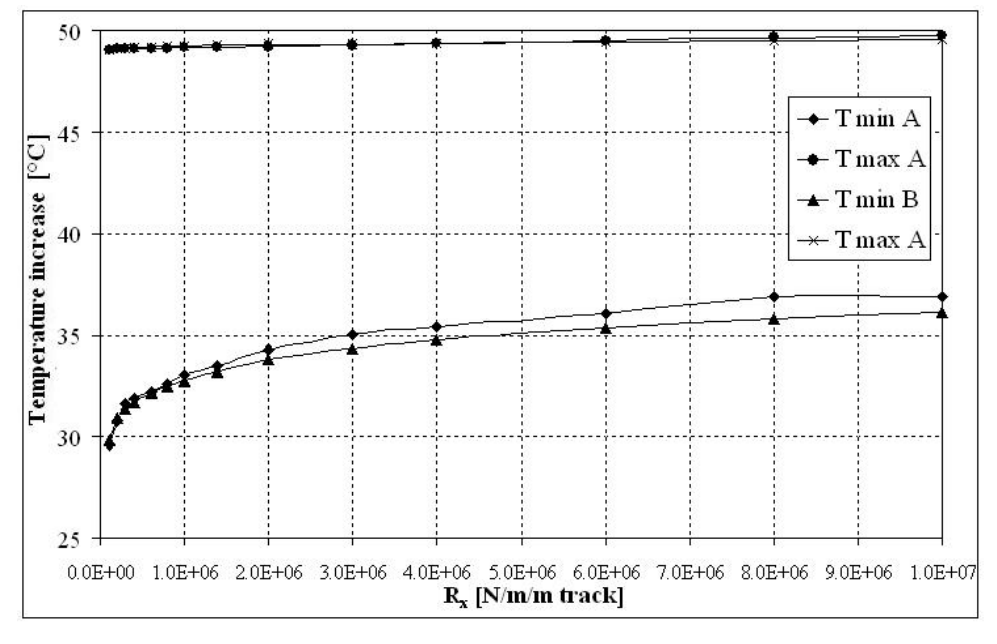


Fig. 7. The critical temperature increasing versus longitudinal resistance



INTERSECTION http://www.ce.tuiasi.ro/inters

V.V. Ungureanu, M. Comanici

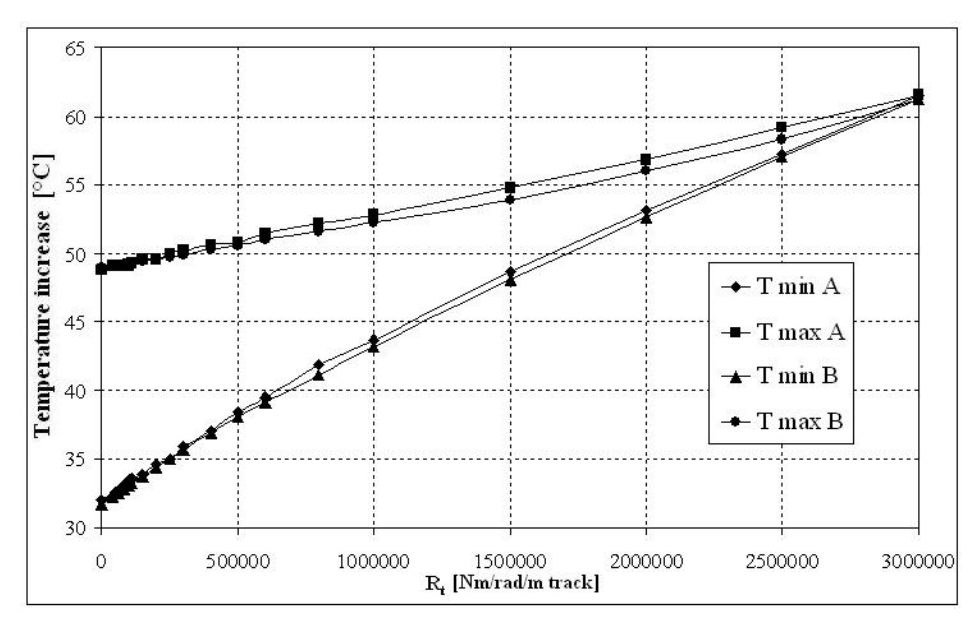


Fig. 8. The critical temperature increasing versus torsional resistance of the fastenings

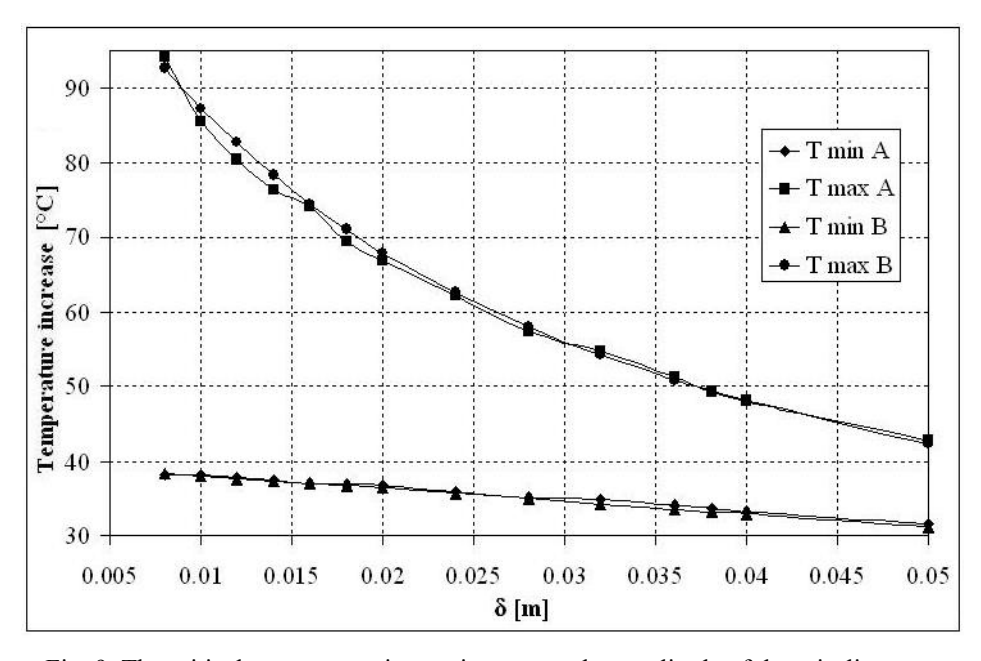


Fig. 9. The critical temperature increasing versus the amplitude of the misalignment



INTERSECTII

http://www.ce.tuiasi.ro/intersections

Sensitivity study of a model for the stability analysis of continuous welded rail

For critical temperature increasing in function of lateral resistance (fig. 7) resulted 3% maximum differences between SCFJ and CWERRI results.

There were analyzed the differences between SCFJ and CWERRI results for critical temperature increasing in function of torsional resistance of the fastenings (fig. 8). It results a maximum difference of 1,7%.

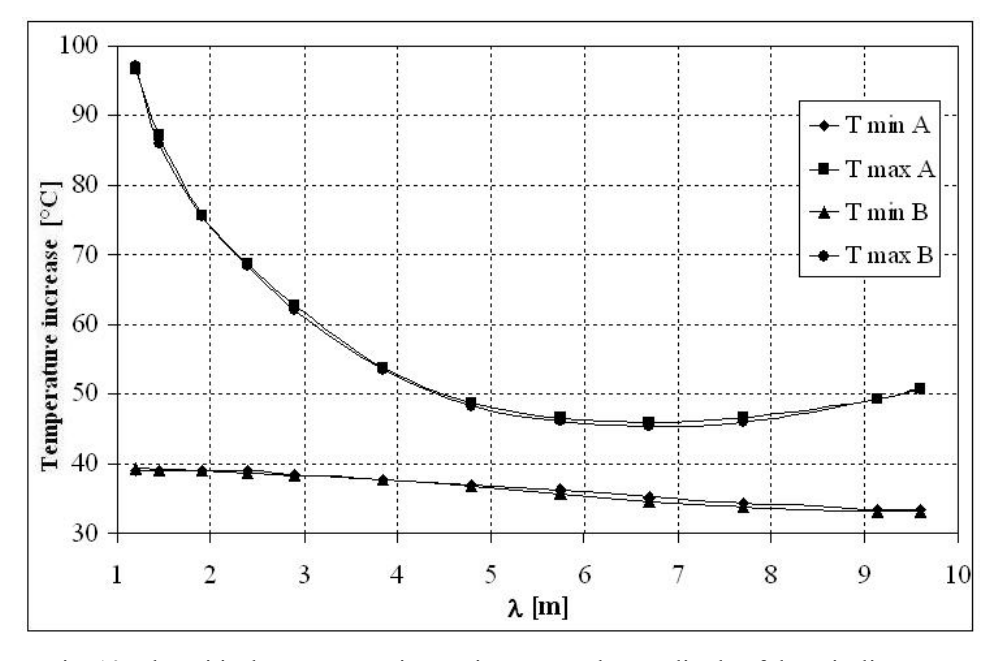


Fig. 10. The critical temperature increasing versus the amplitude of the misalignment

With regards to the amplitude of the misalignment, the differences between SCFJ and CWERRI results for critical temperature increasing (fig. 9), it results a maximum difference of 2,7%.

Finally, it was observed that for the critical temperature increasing in function of the length of initial misalignment (fig. 10), the differences between SCFJ and CWERRI results were maximum 1,9%, if the amplitude is 1/240 of the length of initial misalignment.

In conclusion, it was observed a good correspondence between the results of the two models, therefore the SCFJ model can be used for implementation of Leaflet UIC 720R regulation in Romania or in stability of CWR track analysis with a precision of the results closed to those developed by others.



INTERSECTII

http://www.ce.tuiasi.ro/intersections

V.V. Ungureanu, M. Comanici

References

- 1. *** ERRI D202-RP3 Improved knowledge of forces in CWR track (including switches) -Theory of CWR track stability, European Rail Research Institute, Utrecht, February 1995.
- *** ERRI D202-RP12 Improved knowledge of forces in CWR track (including switches) -Final report, European Rail Research Institute, Utrecht, February 1999.
- *** UIC 720 R Laying and maintenance of CWR Track, 1st edition, January 1986.
 *** UIC 720 R Laying and maintenance of CWR Track, 2nd edition, March 2005.
- Dósa, A., Ungureanu, V.V. SCFJ model discret de pierdere a stabilității căii fără joante, Infrastructuri eficiente pentru transporturi terestre – Zilele Academice Timișene, 24-25 mai 2007, Timisoara.
- 6. Esveld, C. A better understanding of continuous welded rail track, Rail Engineering International, No. 4, 1996.
- 7. Esveld, C. Improved knowledge of CWR track, Delft University Press, 1997.
- Ungureanu, V.V. Modele de pierdere a stabilității căii fără joante, Referatul nr.3 din cadrul stagilului de pregătire pentru doctorat, Universitatea "TRANSILVANIA" din Brașov, Facultatea de Construcții, Brașov, 2006.
- Van, M.A.- Stability of Continuous Welded Rail Track, PhD Thesis, Delft University Press, 1997, ISBN:90-407-1485-1.



INTERSECTII

http://www.ce.tuiasi.ro/intersections

The Generalised Mohr-Coulomb (GMC) Yield Criterion and some implications on characterisation of pavement materials

Mircea Balcu¹, Ştefan Marian Lazăr²

¹Strength of Materials Department, Technical University of Civil Engineering Bucharest, RO-020396, Romania

Summary

In this study a generalization of Mohr-Coulomb Yield Criterion has been developed, implemented, and tested in practice. The practical usefulness of the proposed model is demonstrated with a case study

In the Generalised Mohr-Coulomb (GMC) Yield Criterion one introduces in the Plasticity Mohr-Coulomb Theory the complete three-dimensional stress state $(\sigma_I, \sigma_{II}, \sigma_{III})$, thus generalising the well-known Mohr-Coulomb Theory (σ_I, σ_{III}) . Indirectly, GMC also takes into account the influence of spherical tensor $\tilde{\sigma}$ ", therefore $\tilde{\sigma} = \tilde{\sigma}' + \tilde{\sigma}$ " ($\tilde{\sigma}' = the \ deviatory \ tensor$).

According to Soil Plasticity Theory, and the constitutive characterisation, the material model can be described by the cohesion c and internal friction angle Φ , or, alternatively, by the uni-axial strengths R_c and R_t . In the GMC model, the material is described by the generalised parameters c^* and Φ^* .

KEYWORDS: yield criterion; plasticity; cohesion and internal friction angle; pavement materials

1. INTRODUCTION

The object of the mathematical theory of plasticity is to provide a theoretical description of the relationship between stress and strain for a material which exhibits an elasto-plastic response. In essence, plastic behavior is characterized by an irreversible straining which is not time dependent and which can only be sustained once a certain level of stress has been reached.

In order to formulate a theory which models elasto-plastic material deformation three requirements have to be meet:



²Department of Roads and Railways, Technical University of Civil Engineering Bucharest, RO-020396, Romania

INTERSECTION

http://www.ce.tuiasi.ro/intersections

M. Balcu, Ş.M. Lazăr

- An explicit relationship between stress and strain must be formulated to describe material behavior under elastic conditions, i.e. before the onset of plastic deformation;
- A yield criterion indicating the stress level at which plastic flow commences must be formulated;
- An incremental relationship between stress and strain must be developed for post-yield behavior, i.e. when the deformation is made-up of both elastic and plastic components.

The Mohr-Coulomb yield criterion is a generalization of the Coulomb (1773) friction failure low defined by:

$$\tau = c - \sigma_n t g \Phi \tag{1}$$

where τ is the magnitude of the shearing stress, σ_n is the normal stress (tensile stress is positive), c is the cohesion and Φ is the angle of internal friction.

Graphically Eq. (1) represents a straight line tangent to the largest principal stress circle as shown in Fig. 1 and was first demonstrated by Mohr (1882).

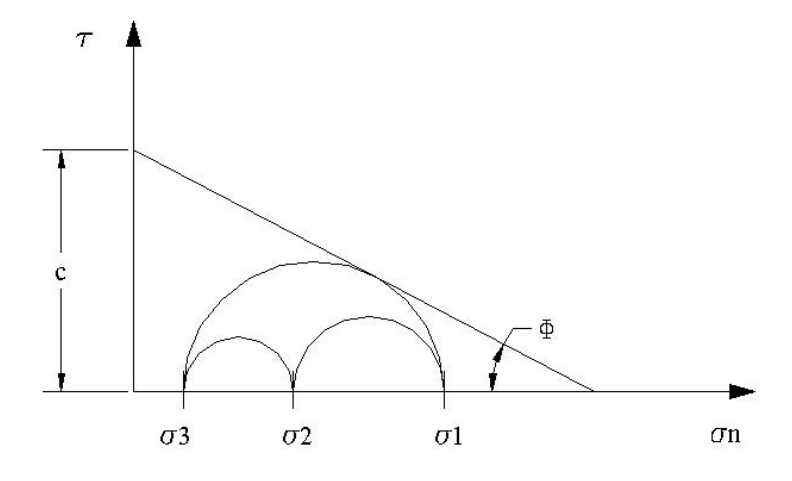


Figure 1. Mohr criterion

From Fig. 2, and for $\sigma_1 \ge \sigma_2 \ge \sigma_3$ Eq. (1) can be written as

$$(\sigma_1 - \sigma_3) + (\sigma_1 + \sigma_3)\sin\Phi = 2 \cdot c \cdot \cos\Phi$$
 (2)



INTERSECTII

http://www.ce.tuiasi.ro/intersections

The GMC Yield Criterion and some implications on characterization of pavement materials

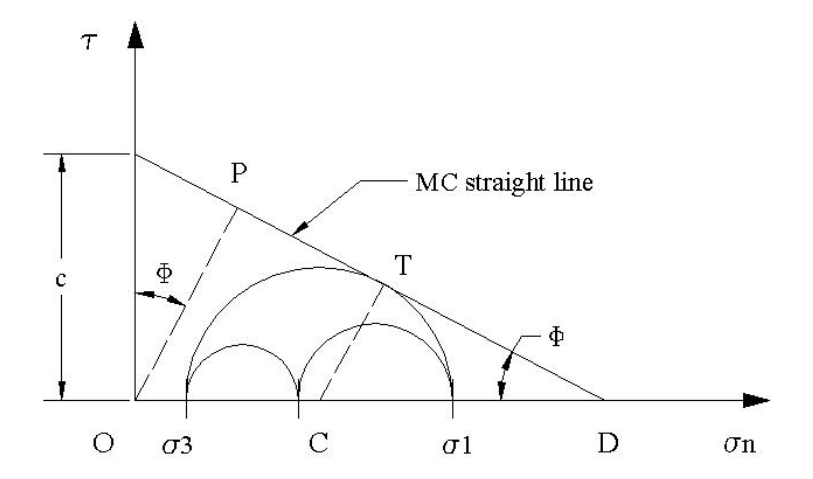


Figure 2. Mohr-Coulomb Yield Criterion

A complete derivation of the Mohr-Coulomb (MC) yield criterion is given in an forcoming paper [2].

2. NOVOZHILOV'S APPROACH OF MC YIELD CRITERION

The equivalent value of MC – yield criterion will now be expressed as follows:

$$\sigma_{ech}^{MC} = c \cdot \cos \Phi \tag{3}$$

or, in a Plasticity Theory format,

$$f(\sigma_1, \sigma_2, \sigma_3, c, \Phi) = \sigma_{ech}^{MC} - c \cdot \cos \Phi = 0$$
 (4)

The use of spheric/deviatoric decomposition of the stress tensor, $\widetilde{\sigma} = \widetilde{\sigma}' + \widetilde{\sigma}''$, yields the following expressions for principal normal stresses used in Eq. (2) (see [2] for details):

$$\sigma_1 = \sigma'' + \frac{1}{3}\overline{\sigma}\left(-\sin\Theta + \sqrt{3}\cos\Theta\right)$$

$$\sigma_3 = \sigma'' + \frac{1}{3}\overline{\sigma}\left(-\sin\Theta - \sqrt{3}\cos\Theta\right)$$

INTERSECTII

http://www.ce.tuiasi.ro/intersections

M. Balcu, Ş.M. Lazăr

Therefore,

$$\sigma_1 - \sigma_3 = \frac{2\sqrt{3}}{3} \overline{\sigma} \cos \Theta$$

$$\sigma_1 + \sigma_3 = 2\sigma'' - \frac{2}{3}\sigma\sin\Theta$$

and σ_{ech}^{MC} writes as:

$$\sigma_{ech}^{MC} = \sigma'' \sin \Phi + \overline{\sigma} \left(\frac{1}{\sqrt{3}} \cos \Theta - \frac{1}{3} \sin \Theta \sin \Phi \right) = c \cdot \cos \Phi$$
 (5)

Comment: The MC - yield criterion is not a pure "shear" theory, because it contains both spherical part σ ", and the "deviatory" part, $\overline{\sigma}$.

3. THE GENERALISED MOHR-COULOMB (GMC) YIELD CRITERION

In Fig. 3 the effective stress σ is given an interesting geometric interpretation, due to V.M. Rosenberg [3].

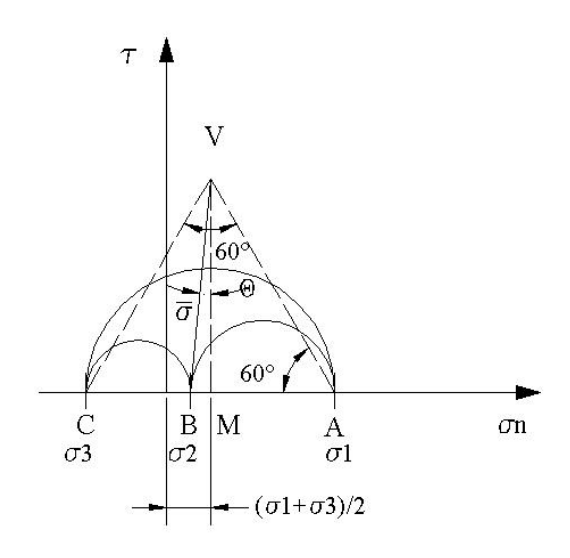


Figure 3. Rosenberg's method: $\overline{\sigma} = ||VB||$; $\Theta = MVB$; $||VM|| = \overline{\sigma}\cos\Theta$

INTERSECTII

http://www.ce.tuiasi.ro/intersections

The GMC Yield Criterion and some implications on characterization of pavement materials

A generalized Mohr-Coulomb yield criterion follows the line of classical MC, with the vortex point V following the straight line equation:

$$\frac{X}{d*} + \frac{Y}{c*} = 1 \tag{6}$$

where (see Fig. 4): c^* and d^* denote the generalized cohesion and generalized abscissas, respectively.

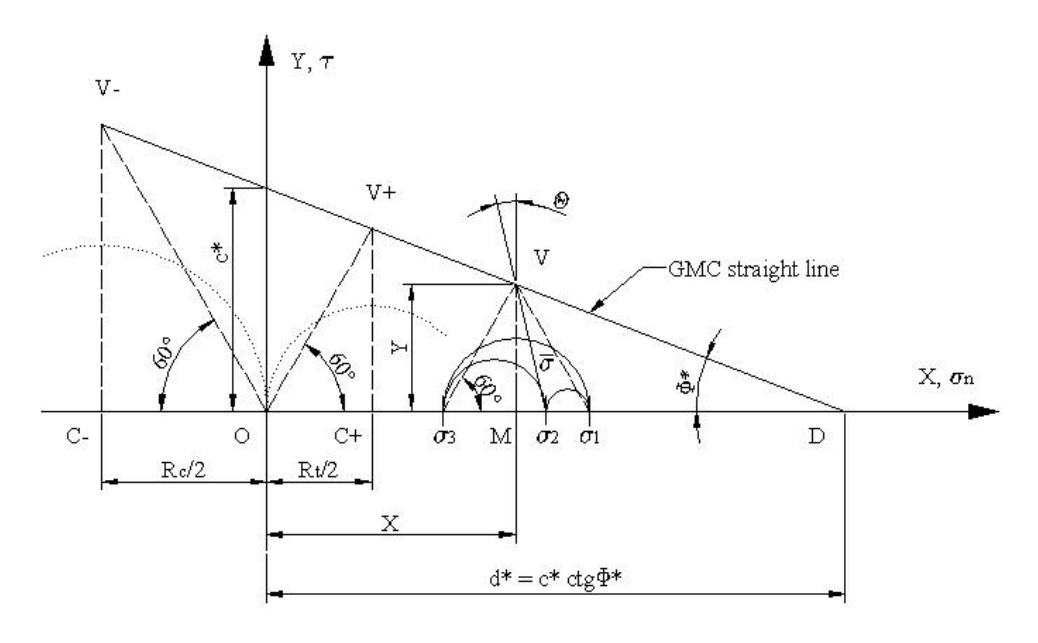


Figure 4. The Generalised Mohr-Coulomb (GMC) Yield Criterion

The Eq. (6) writes, successively, as follows:

$$\frac{\frac{\sigma_1 + \sigma_3}{2}}{c^* c t g \Phi^*} + \frac{\overline{\sigma} \cos \Theta}{c^*} = 1$$

$$\frac{\sigma_1 + \sigma_3}{2} t g \Phi^* + \overline{\sigma} \cos \Theta = c^*$$

$$\frac{\sigma_1 + \sigma_3}{2} \sin \Phi^* + \overline{\sigma} \cos \Theta \cos \Phi^* = c^* \cos \Phi^*$$
(7)

INTERSECTII

http://www.ce.tuiasi.ro/intersections

M. Balcu, Ş.M. Lazăr

Now, following the trigonometric procedure of Novozhilov, one writes successively:

$$\sigma_1 + \sigma_3 = 2\sigma'' - \frac{2}{3}\sigma\sin\Theta$$

and, therefore,

$$\frac{\sigma_1 + \sigma_3}{2} \sin \Phi^* = \left(\sigma'' - \frac{1}{3} - \frac{1}{3} \sin \Theta\right) \sin \Phi^*$$
 (8)

Eq. (7) finally writes as follows:

$$\sigma_{ech}^{GMC} = \sigma'' \sin \Phi * + \overline{\sigma} \left(\cos \Phi * \cos \Theta - \frac{1}{3} \sin \Theta \sin \Phi * \right) = c * \cdot \cos \Phi * \tag{9}$$

To compare, one observes that σ_{ech}^{GMC} (Eq. (9)) is a generalization of σ_{ech}^{MC} (Eq. (5)).

4. APPLICATION – CASE STUDY: ASPHALT MIXTURES

Laboratory tri-axial tests enable one to find out the intrinsic material characteristics of an asphalt mixture MASF 16 in the ambient temperature T = 23 °C, lateral pressure $\sigma_3 = 2$ to 4 daN/cm², and a vertical loading in a regime of v = 0,46 mm/min.

The following MC – parameters were found:

$$\Phi = 36,90^{\circ}$$

$$c = 2.02 \text{ daN/cm}^2$$

Following the Generalized Mohr-Coulomb theory (GMC) the corresponding values are found as follows:

$$\Phi^* = arctg(\sqrt{3}\sin\Phi) = arctg(\sqrt{3}\sin 36.90) = 46.12^{\circ}$$

$$c^* = \sqrt{3} \cdot c \cdot \cos \Phi = \sqrt{3} \cdot 2,02 \cdot \cos 36,90 = 2,80 \text{ daN/cm}^2$$



INTERSECTII

http://www.ce.tuiasi.ro/intersections

The GMC Yield Criterion and some implications on characterization of pavement materials

5. CONCLUSIONS

For yield criteria with non-smoothly intersecting multiple yield surfaces e.g. Mohr-Coulomb (MC) and Generalized Mohr-Coulomb (GMC), a good return scheme has to be supplemented by proper care to account for the non-regular regions in the yield surface. The problem of determining if multiple yield surfaces are active, has recently received some attention. If these predictor-corrector algorithms have to incorporate the Koiter's generalization [4], some singularities should be taken into account [2].

References

- 1. Owen, D.R.J., Hinton, E., *Finite elements in Plasticity: Theory and Practice*, Pineridge Press. Limited, Swansea, U.K., 1980.
- 2. Balcu, M., Lazăr, Ş.M., A Generalised Mohr-Coulomb (GMC) Plasticity Theory for solving non-linear analysis of pavement materials and structures, *Buletinul Ştiinţific al UTCB*, nr. 4, 2007. (in English and Romanian)
- 3. Smirnov-Aliaev, G.A., Rozenberg, V.M., *Theory of plastic deformations in metals*, Lenizdat, 1951. (in Russian)
- 4. Koiter, W.T., Stress-strain relations, uniqueness and variational theorems for elastic-plastic materials with a singular yield surface, *Q. Appl. Math.*, vol. 11, 350-354, 1953.



INTERSECTII http://www.ce.tuiasi.ro/inters

The use of the bispectrum for analysis dynamic parameters of rail fastening

Jaroslav Smutny¹, Lubos Pazdera²

¹Department of Railway Constructions and Structures, Faculty of Civil Engineering, University of Technology Brno, Brno, 602 00, Czech Republic ²Department of Physics, Faculty of Civil Engineering, University of Technology Brno, Brno, 602 00, Czech Republic

Summary

"Higher Order Statistics" (HOS) is extension of second-order characteristics such as the auto-correlation function and power spectrum. HOS analysis is emerging as a new powerful technique in signal analysis, offering insight into non-linear coupling between frequencies and potential applications in many areas where traditional linear analysis provides insufficient information. This contribution describes the HOS theory and possibilities application to experimental data acquisition from measurements of rail fastening parameters.

KEYWORDS: Higher Order Statistics, Cumulants, Bispectrum, Railway Superstructure

1. INTRODUCTION

The basic claim put in particular components of the railway track is their functional reliability and the interrelated minimum costs of their manufacturing, repair and maintenance. Each part of the rail structure is exposed to an extensive static and dynamic stresses. This fact is of great importance especially in the design and construction of high-speed railway lines.

Different methods and various criteria have been applied to test the railway superstructure, and different mathematical methods are used to evaluate the signals measured. The method exciting the structure by a mechanical impact is often used in dynamic tests. The excitation by impact is advantageous for the determination of proper frequencies of a given system. Another possibility is the loading of the structures specimens by a continuous excitation by means of vibrators. This makes it possible to focus attention on certain frequencies or to the interval of the frequencies. For the evaluation, frequency spectra transfer functions, frequency response functions, etc. have been composed. From the viewpoint of the railway operation security, it is expedient to focus our attention also on new methods that will offer the information about the quality of particular components (or of the



INTERSECTII http://www.ce.tuiasi.ro/inters

http://www.ce.tuiasi.ro/intersections

The use of the bi-spectrum for analysis dynamic parameters of rail fastening

whole structure) both from the viewpoint of different failures and from the assembly viewpoint.

It should be said that until the present time practical applications of the evaluation of the results of measuring by "elementary" methods such as typical statistic and frequency analyses have prevailed. At the present time, there exist a number of mathematical methods through which discrete data may be processed and which are especially suitable for processing the signal measured. However, in the technological practice these methods appear only rarely although these may offer more information about the signals measured and also about the structure tested. These methods could not be used because of low efficiency of the hardware and the technology of measuring. At the present time, these methods are not fully utilized owing to the insufficient awareness of technologists.

2. THEORETICAL BACKGROUND

"Higher Order Statistics" (HOS) is extension [1, 2] of second-order characteristics such as the auto-correlation function and power spectrum to higher orders. HOS analysis is emerging as a new powerful technique in signal analysis, offering insight into non-linear coupling between frequencies and potential applications in many areas where traditional linear analysis provides insufficient information.

The second-order analyses work fine if the signal has a Gaussian (Normal) probability density function, but many real-life signals are non-Gaussian. The easiest way to introduce the HOS measures is just to show some definitions so that the reader can see how they are related to the familiar second-order measures. In the text to follow, are definitions for the time-domain and frequency-domain thirdorder HOS measures, moments, cumulants, high-order spectra or polyspectra, etc. [3, 4].

2.1 Moments

The time process x(n) can be characterized in many ways, for example by its amplitude, its energy or its waveform. The probability density function (pdf) of the process provides detailed information about the distribution of the amplitudes of the process which can be used to characterize the process. A set of quantities which describes the shape of this "pdf" are the moments. The first-order moment m_1 of process x(n) is just its mean, and it provides a measure of location of the "pdf". The second-order moment is the variance, a measure of the spread of the "pdf". Higherorder moments exist too, such as the skewness and kurtosis. Now, moments are statistical measures which characterize signal properties. The first four moments of the process are defined by the following equations:



INTERSECTII http://www.ce.tuiasi.ro/inters

J. Smutny, L. Pazdera

$$m_1 = E\{x_n\} \tag{1}$$

$$m_{2}(\tau) = E\{x(n) \cdot x(n+\tau)\}\tag{2}$$

$$m_3(\tau_1, \tau_2) = E\{x(n) \cdot x(n + \tau_1) \cdot x(n + \tau_2)\}. \tag{3}$$

$$m_4(\tau_1, \tau_2, \tau_3) = E\{x(n) \cdot x(n+\tau_1) \cdot x(n+\tau_2) \cdot x(n+\tau_3)\}$$

$$\tag{4}$$

2.2 Cumulants

Cumulants are specific non-linear combinations of these moments. The first-order cumulants of process is the mean. The second, third and fourth-order cumulants of process are defined by the following equations [5]:

$$c_2 = m_2 - m_1^2 \tag{5}$$

$$c_3 = m_3 - 3 \cdot m_2 \cdot m_1 + 2 \cdot m_1^3. \tag{6}$$

$$c_4 = m_4 - 4 \cdot m_3 \cdot m_1 + 3 \cdot m_2^2 + 12 \cdot m_2 \cdot m_1^2 - 6 \cdot m_1^4 \tag{7}$$

2.3 Polyspectra

This term is used to describe the family of all frequency-domain spectra, including the those of the 2nd order. Most HOS work based on polyspectra and focus their attention on the bispectrum (third-order polyspectrum) and the trispectrum (fourthorder polyspectrum). Polyspectra consist of higher order moment spectra and cumulant spectra and can be defined for both the deterministic signal and random processes. Moment spectra can be very useful in the analysis of deterministic signals (transient and periodic), whereas cumulant spectra can play a very important role in the analysis of stochastic signals. The kth-order polyspectrum [3, 5] is defined as the Fourier transform of the corresponding cumulant sequence:

$$C_2(f) = \sum_{k=-\infty}^{\infty} c_2(k) e^{-i2\pi jk}$$
 (8)

$$C_3(f_{1,}f_2) = \sum_{k=-\infty}^{\infty} \sum_{l=-\infty}^{\infty} c_3(k,l) e^{-i2\pi f_1 k} \cdot e^{-i2\pi f_2 l} . \tag{9}$$

$$C_4(f_1, f_2, f_3) = \sum_{k = -\infty}^{\infty} \sum_{l = -\infty}^{\infty} \sum_{m = -\infty}^{\infty} c_4(k, l, m) \cdot e^{-i2\pi(f_1k + f_2l + f_3m)}$$
(10)



INTERSECTII http://www.ce.tuiasi.ro/inters

The use of the bi-spectrum for analysis dynamic parameters of rail fastening

which are the power spectrum, respectively the bispectrum and trispectrum. These can be estimated in a way similar to the power spectrum, but more data is usually needed to get reliable estimates. Note that the bispectrum is a function of two frequencies, whereas the trispectrum is a function of tree frequencies. In contrast to the power spectrum which is real-valued and non-negative, bispectrum and trispectrum are complex valued and contain a phase information.

Bispectrum a technique that is often used, can be estimated in a way similar to Welch periodogram method for the power spectrum estimation but the lengths of data required to obtain consistent estimates are longer than those required for the power spectrum estimation.

The variance of the estimate can still be reduced by averaging over multiple segments of data. To extract an information from the non-normalized bispectrum is often difficult because the variance of the bispectrum estimate at a particular frequency pair (k,l) depends not only on the data length but also on the power of the signal at frequencies k, l and k+l. The bicoherence is a useful normalized bispectrum. The bicoherence at any frequency pair k, l can be interpreted as a fraction of power at frequency k+l which is a phase coupled to the component at k+l. Bicoherence is estimated as [4]

$$b(f_1, f_2) == \frac{\left| C_3(f_1, f_2) \right|^2}{P(f_1) \cdot P(f_2) \cdot P(f_1 + f_2)}$$
(11)

where $C_3(f_1, f_2)$ is the estimate of the bispectrum, and P(f) is the estimate of the power spectrum.

3. EXPERIMENTAL RESULTS

The text to follow presents an example of the laboratory measurements and the analyses of the dynamic parameters of the rail fastening specimen. The measurements were carried out mainly with respect to the transfer properties of this fastening of rails under different assembly and operational states (the effects of tightening and releasing).

The test specimen was assembled of a part of the concrete sleeper B 91, on which a rail of structural shape UIC 60 using the elastic fastening of VOSSLOH SKL14 type was fastened.

To test the specimen of the rail grid, the method of measuring the response to the random excitation was used. The excitation was implemented in the horizontal direction towards the rail head by means of an efficient vibration exciter B&K

INTERSECTII http://www.ce.tuiasi.ro/inters

http://www.ce.tuiasi.ro/intersections

J. Smutny, L. Pazdera

4818. The frequency range of the observed area was determined ranging from 5 Hz to 1500 Hz.

The measuring system PULSE 3560C by the firm Brüel& Kjaer was used for the experiment control. The acceleration responses were measured by an accelerometric sensing unit fixed to the sleeper 10 cm from the fastening. Let us remark that the acceleration sensing unit was fixed to the structure measured by means of the bee-wax.

The measurement resulted in the scanned and digitally recorded electrical signal proportional to the instantaneous value of the acceleration in place of the sensing unit fixation. Frequency spectra and bicoherence were developed from the time responses.

The graphs in Figures 1 and 3 represent a dynamic response of the rail fastening with the standard tightened bolts.

Figure 1 shows a graph of the amplitude spectrum calculated by means of a direct application of Fourier's transformation to the signal measured. Significant components on frequencies 15 Hz, 20 Hz, 75 Hz, 95 Hz, 150 Hz, 220 Hz and 550 Hz may be read from this graph. It is evident from this graph that particular frequency peaks are relatively uniformly distributed in the frequency region. Figure 3 shows the graph of the bicoherence. There are no distinctive maximum values noticeable here.

The graphs in Figures 2 and 4 represent dynamic responses of the rail fastening with loosened bolts. Figure 2 represents a frequency spectrum, and Figure 4 the bicoherence graph. From graph on Figure 2, significant components in frequencies 15 Hz, 75 Hz, 100 Hz, 160 Hz, 210 Hz and 550 Hz may be read. So, if the graphs of frequency spectra (Figures 1 and 2) are compared, it may be stated that the spectra are almost identical and the differences in significant components are not excessively important.

On the contrary, great differences are evident if the graphs of bicoherence in Figures 3 and 4 are compared. In the graph in Figure 4, significant components in and frequency pairs of 15 Hz, 75 120 Hz, 150 Hz, and 190 Hz are evident. Compared with the graph in Figure 2, there are significant maximum values in the graph in Figure 4.

These results from the fact that the nonlinearity of the transmission of vibration waves from the rail to the sleeper increases in the specimen with the rail improperly fixed. Thus, this phenomenon is very well detected by the calculated bicoherence.



INTERSECTII

http://www.ce.tuiasi.ro/intersections

The use of the bi-spectrum for analysis dynamic parameters of rail fastening

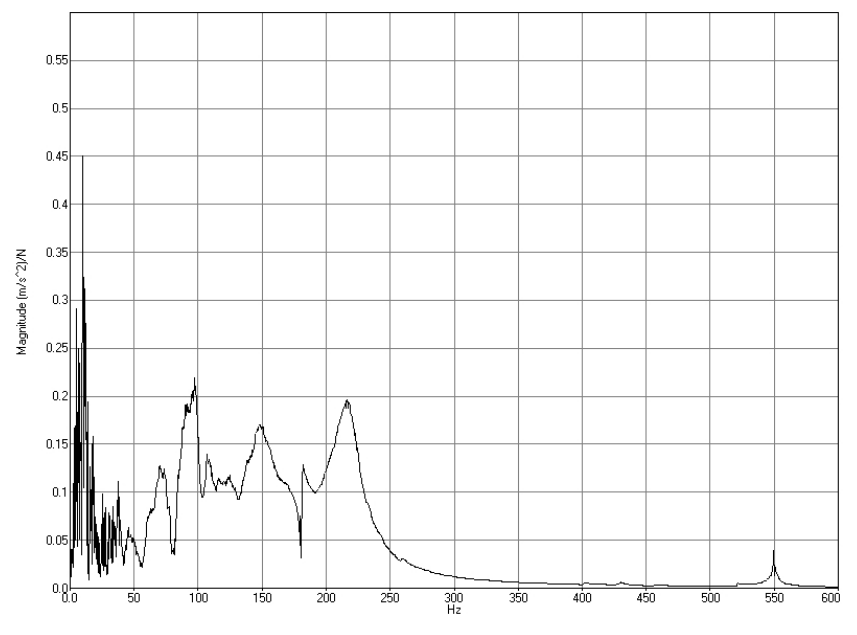


Figure 1 Frequency response function, rail fastening with the standard tightened bolts

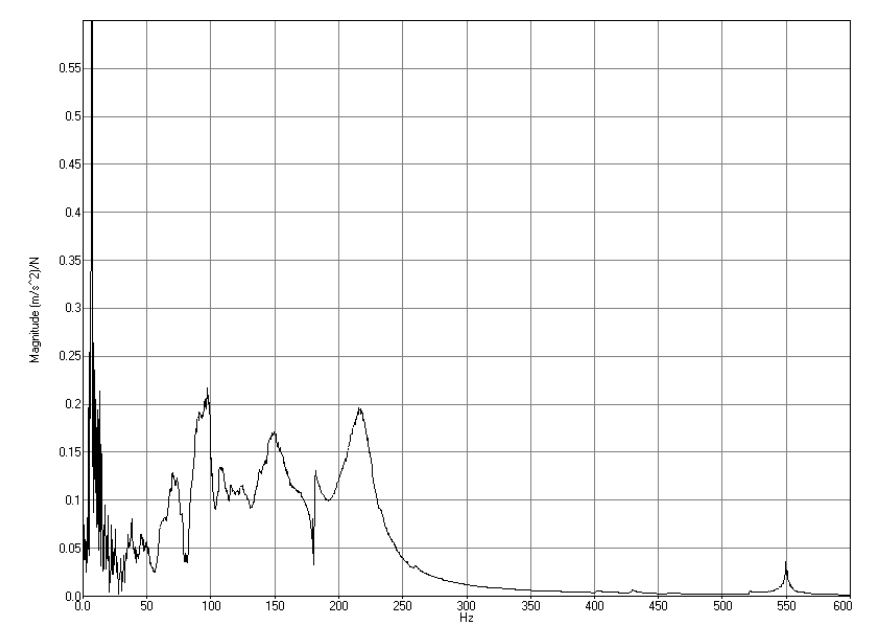


Figure 2 Frequency response function, rail fastening with loosened bolts



INTERSECTII

http://www.ce.tuiasi.ro/intersections

J. Smutny, L. Pazdera

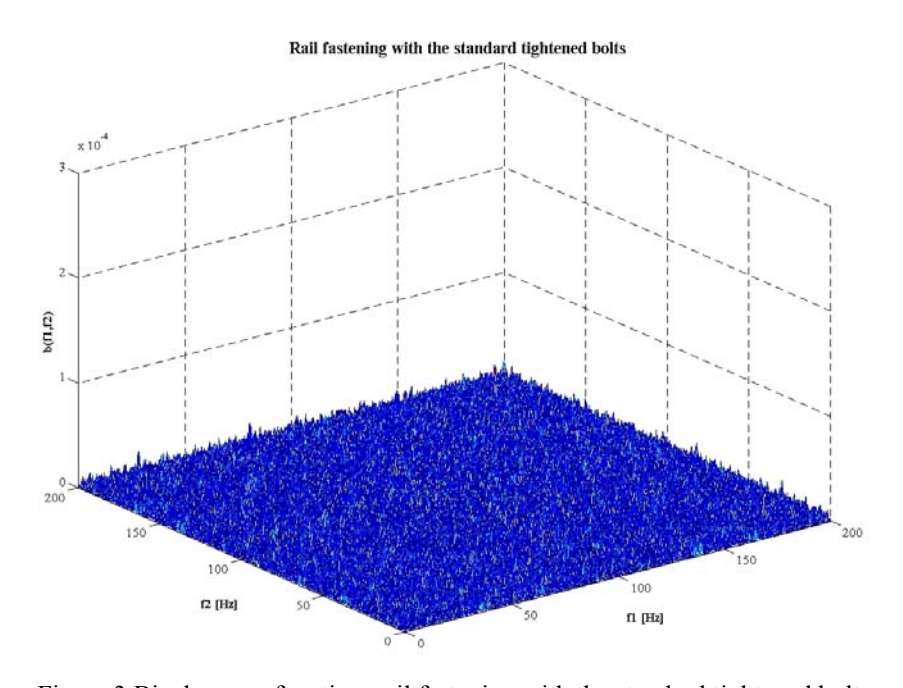


Figure 3 Bicoherence function, rail fastening with the standard tightened bolts

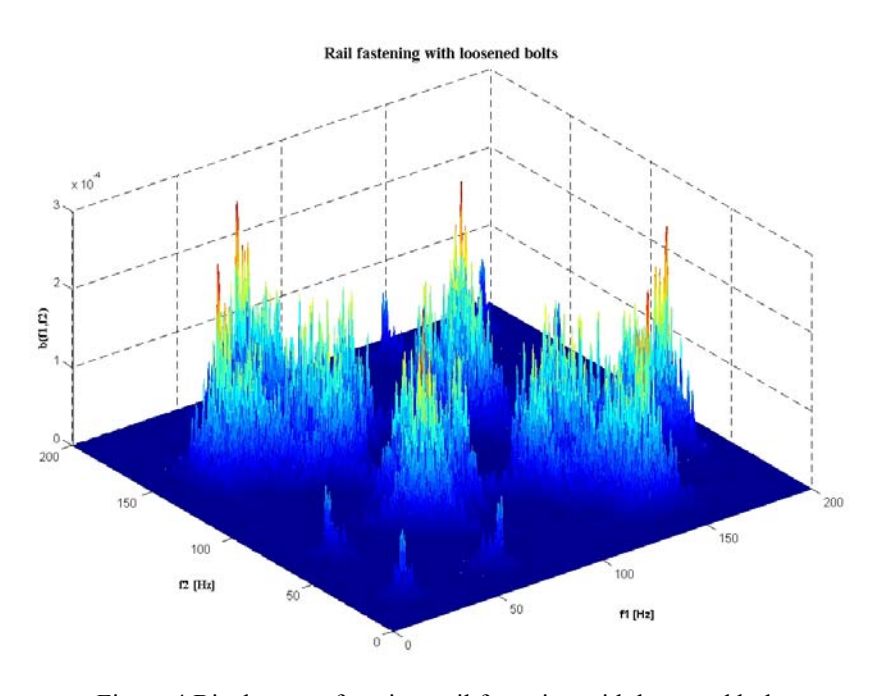


Figure 4 Bicoherence function, rail fastening with loosened bolts



INTERSECTII

http://www.ce.tuiasi.ro/intersections

The use of the bi-spectrum for analysis dynamic parameters of rail fastening

4. CONCLUSION

In conclusion, it may be stated, based upon the measurements and analyses carried out that the experiment carried out successfully verified the possibilities of utilizing the given method for assessing the quality of particular components of the rail structure. It follows from the text mentioned above that the method of higher order spectra may play an important role in future when analyzing railway structures.

The results obtained show that this method proves to be prospective for the analysis of the reaction of the rail fastening under different technological (constructional) state to the dynamic load, then in detecting different types of defects in fastening rails, sleepers and also the defects of rails proper.

Another important fact is that this method can be used to detect structural defects and to assess the quality of the superstructure, which is not essentially made possible when both the calculation models and the typical methods used until now are applied. Laboratory tests should also be verified by measurements in the field.

Based upon the results obtained, it may be assumed that the method presented is feasible in the region of the railway traffic. For example this method may be used in continuous diagnostics of various components of the rail structure or in the creation of a diagnostic system directly applied to commercial railway carriages etc.

Acknowledgements

This research has been supported by the research project 103/07/0183 ("The investigation of dynamic effects due to the rail transport by the method of quadratic time and frequency invariant transformations") and by research project MSM 0021630519 ("Progressive reliable and durable load-bearing structural constructions")

References

- 1. G. Bessios, C. L. Nikias, FFT-Based Bispectrum Computation on Polar Rasters, IEEE Transactions on Signal Processing, 39 (11), pp. 2535-2539, 11/1991
- M. L. Williams: The use of the bispectrum and other order statistics in the analysis of one dimensional signals, PhD Thesis, Imperial College of Science, Technology and Medicine, University of London, 1992
- J. W. A. Fackrell, S. McLaughlin: Quadratic phase coupling detection using Higher Order Statistics, IEE Colloquium on Higher Order Statistics, Savoy Place London, 1995
- 4. Wang W. Y., Harrap M. J.: "Condition monitoring of ball bearings using envelope autocorrelation technique," Machine Vibration, Vol. 5, pp. 34-44, 1996
- 5. Rivola A., White, P. R.: "Bispectral Analysis of the Bilinear Oscillator with Application to the Detection of Fatigue Cracks," Journal of Sound and Vibration, Vol. 216(5), pp. 889-910, 1998



INTERSECTII

http://www.ce.tuiasi.ro/intersections

Parametrical study of the effect of the torsional resistance of the fastenings on the stability of continuous welded rail

Valentin-Vasile Ungureanu, Adam Dósa Department of civil engineering, "TRANSILVANIA" UNIVERSITY, Braşov, Romania

Summary

This work contains a parametrical study on the stability of continuous welded rail (CWR), taking in account the torsional resistance effect which appears between rail and sleepers through fastenings system. The effect of the torsional resistance was analyzed in the presence and in the absence of vehicle loading. It was considered both linear and nonlinear behavior of the fastenings. The analysis was done using a simplified bi-dimesional model of CWR, with beam elements and nonlinear lateral, longitudinal and torsional spring elements.

It was shown the influence of the different parameters which governs the behaviour of the fastenings on the stability of CWR.

KEYWORDS: Continuous welded rail, Track stability, Fastening system.

1. GENERALITIES FOR THE TORSIONAL RESISTANCE OF FASTENINGS

The continuous welded rail track is loaded by vehicles and weather factors, especially by temperature variations. These loads generate vertical, transversal and longitudinal displacements and deformations of railway track panels. Each of these displacements and deformations are restricted by one or more resistances. All of these resistances are of friction forces kind. The rotation of rail in the fastenings is restricted, mainly by the torsional stiffness of fastenings. In the literature the resistant moment of fastenings is marked by $M_{\rm o}$ or $M_{\rm r}$.

This moment is experimentally determined in laboratory by graduate loading of a rail clamped in fastening with a force F placed at a a distance from the fastening axis, which generate a θ rotation of the rail [1, 2, 8, 10, 11]. The resistant moment and the rotation are determined by following relations:

$$M_o = F \cdot a$$
 (1)

$$\theta = \Delta/b \tag{2},$$



INTERSECTII

http://www.ce.tuiasi.ro/intersections

Parametrical study of the effect ... on the stability of continuous welded rail

where b is the distance between fastening axis and the gauge which measure Δ displacement of the rail (fig. 1).

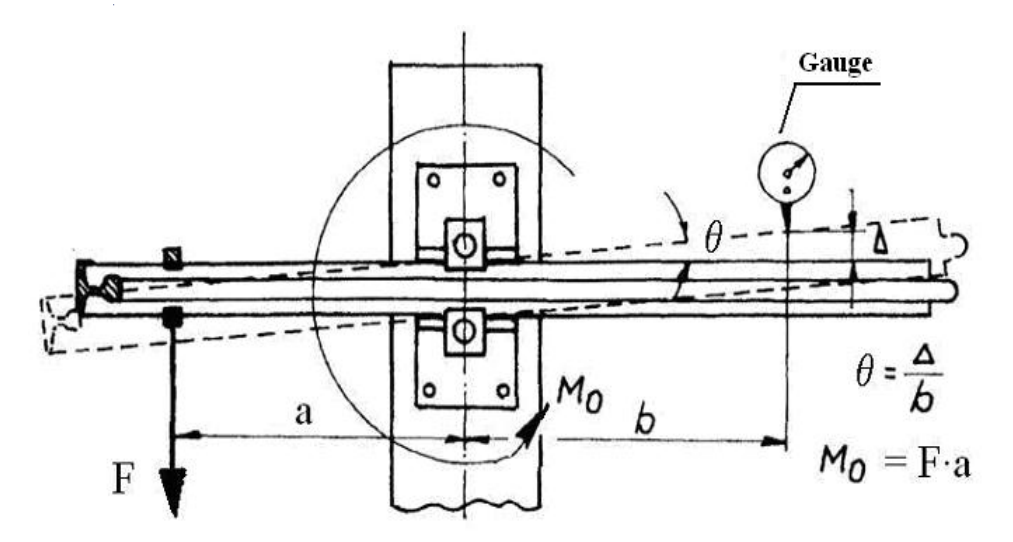


Fig. 1. Experimental determination of the torsional resistance of the fastenings $M_0[1, 2, 8]$.

The torsional resistance (M_o) – rotation (θ) diagram, called characteristic curve of fastener, can have different shapes (fig. 2), depending on the relative position of the rail in fastening.

So, if the rail is oblique positioned (1st case by fig.2), between rail and the lateral shoulder of fastening do not exist clearances, the rail is tangent to lateraly shoulder of fastening – for example like a K type indirect fastening – the fastening will be restrict the rotation until the fastening elements will be destroyed, and the characteristic curve will be linear. When the rail is in the normal position in fastening (2nd case by fig.2), between rail and the lateral shoulder of fastening exist equal clearances to both sides of rail, for small rotations will be mobilized the rotational friction resistances between rail foot and seating plate, as well as between rail foot and K clamping claw fastening, and the concordant branch will be approximate linear. If all of these resistances will be integral mobilised it will be remarked increases of rail rotation for small increases of rotational moment, until the clearances between rail and lateraly shoulder of fastening will be passed off, and the characteristic curve will be approximate constant on this branch. After the rail will be tangent to the lateral shoulder of the fastening, the fastening will be restrict the rotation until the fastening elements will be destroyed, and the characteristic curve will be linear, again. The size of the branch whichever the characteristic curve is constant is a function of the size of clearance between the rail and the lateral shoulder of fastening. Hereby, if the rotation of rail in fastening will be in that direction which lead the rail from oblique to normal position, it will

INTERSECTII

http://www.ce.tuiasi.ro/intersections

V.V. Ungureanu, A. Dósa

obtain the maximum size of the level of the characteristic curve, for the situation in which the rail is tangent to the lateral shoulder of fastening and it exist maximum values of clearances between the rail foot and the lateraly shoulder of fastening (3rd case by fig. 2).

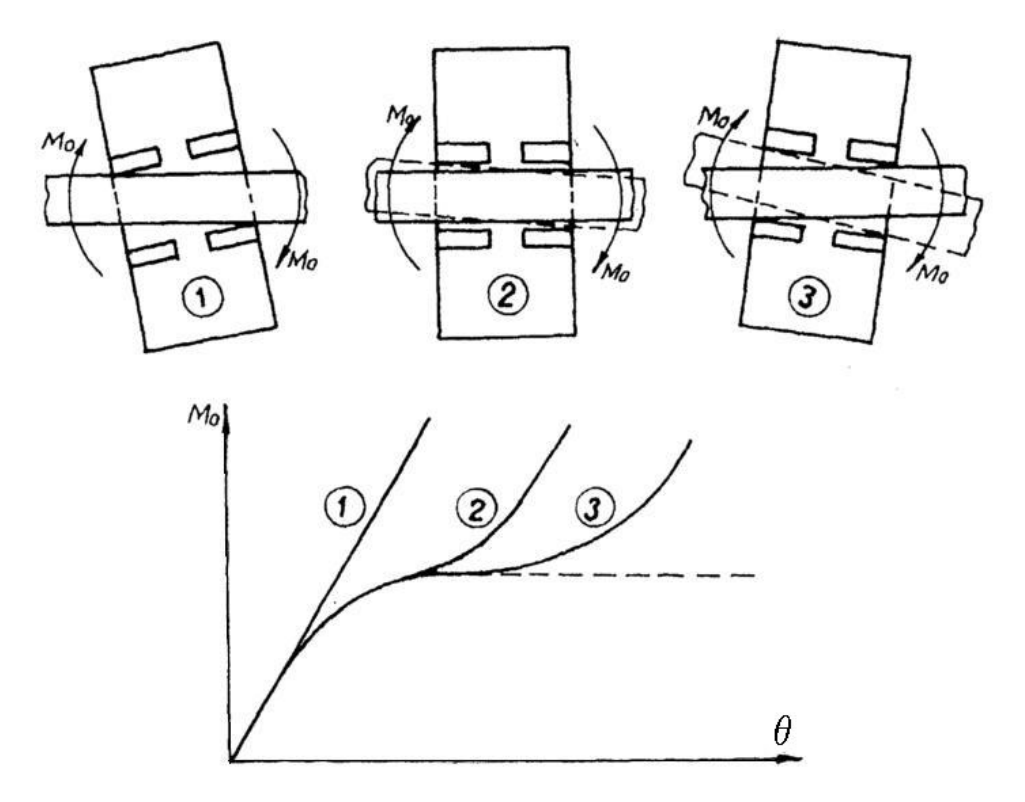


Fig. 2. The torsional resistance (M_o) – rotation (θ) diagram for diverse relative positions of the rail in the fastening [4, 8, 10].

The value of resistent moment M_o , for which the characteristic curve of fastening is constant depends on the vertical force with wich the fastening push on the rail foot by fastening elements (for example, by the clamping claw, in case of K type fastening), it being directly proportional with the size of this vertical clamping force. In the fig. 3 is shown one example for this situation [8, 11].

The regulations and some authors consider a linear characteristic curve of fastening which result by linearisation of the first branch of characteristic curve [1, 2, 5, 6, 7, 8, 11]. The explanation for this supposition is that, for the allowed values of misalignment, the rotation of rail in the fastening does not exceed the characteristic values of the first branch of the experimental characteristic curve.

INTERSECTION

nttp://www.ce.tuiasi.ro/intersections

Parametrical study of the effect ... on the stability of continuous welded rail

However, for the common fastenings used in Romania, a tri-linear characteristic curve is most proper for the real behaviour of the fastening.

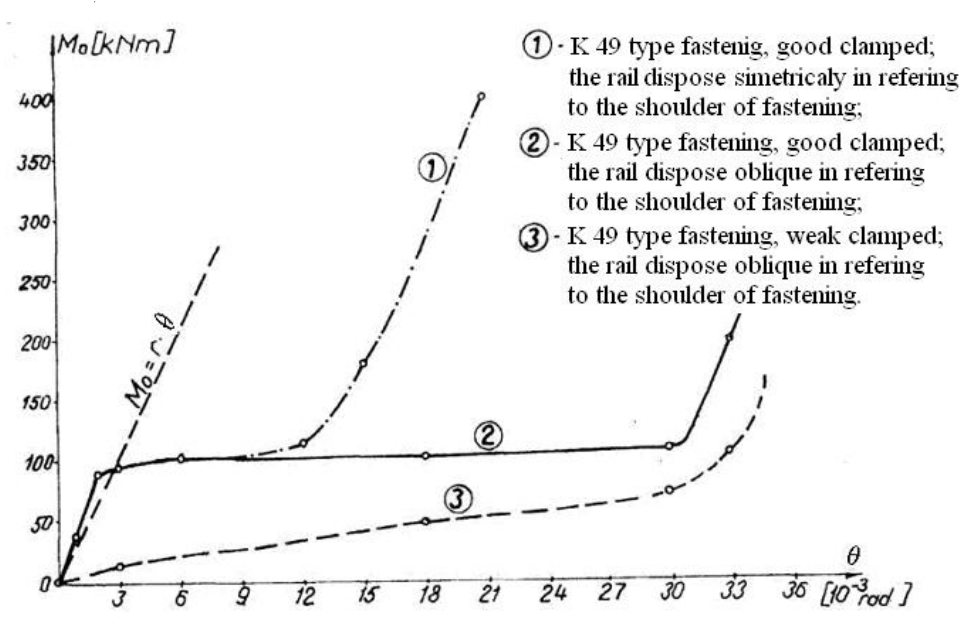


Fig. 3. Characteristic curves of K 49 type fastening [10, 11].

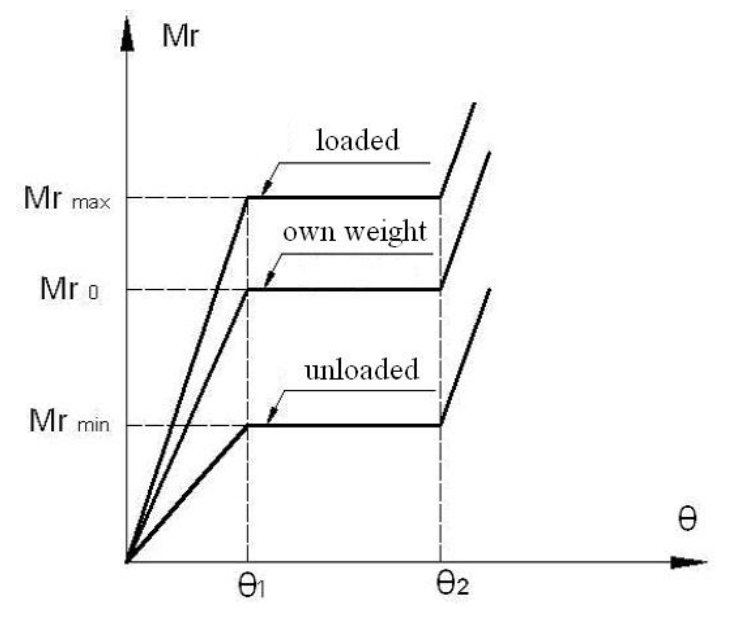


Fig. 4. Characteristic curve of the fastening in function of vertical load due to vehicle [12].

INTERSECTII

http://www.ce.tuiasi.ro/intersections

V.V. Ungureanu, A. Dósa

2. THE MODELING OF TORSIONAL RESISTANCE OF FASTENINGS

The majority of models consider a linar variation of characteristic resistent moment – rotational angle of rail in the fastening (fig. 5 a), but exist models in which it is considered a bi-linear, tri-linear (fig. 5 b) or multi-linear characteristic curve [2].

All linear [2, 6, 7, 13], bi-linear [3] or tri-linear [4, 8, 9, 10, 11] common models are not taking in account the influence of vehicle vertical load on the rotation of the rail in the fastenings, but in the model given in [5, 12] it is included. The behaviour of fastening to rail rotation can be appropriately corrected according to this model [5, 12], taking account of the pushing force on sleeper, as it is shown in fig. 4. Such as approach is more close to the real behaviour of the fastening and it allows the estimation of the influence of other parameters of fastening, which are not considered in the other models.

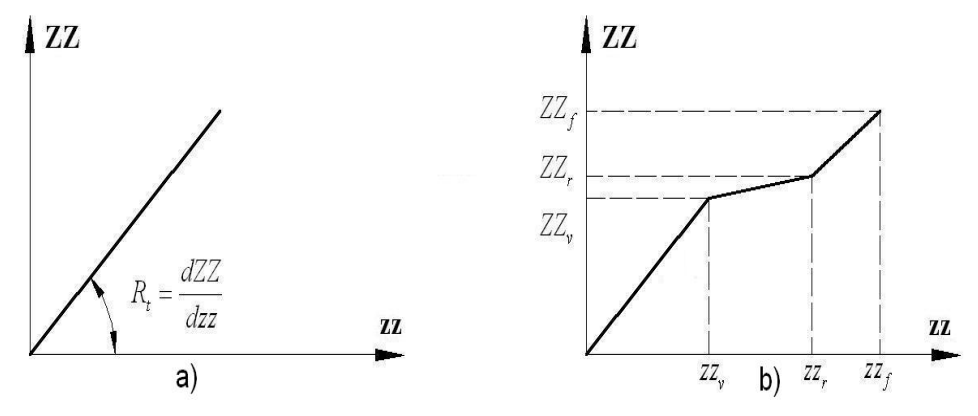


Fig. 5. Torsional resistance of fastenings [5].

Hereby, the resistance to rotation of rail in fastening will be Mr_o for unloaded railway track into the tri-linear model, and for the loaded railway track it will be with values between Mr_{max} , concordantly with the most vertical loaded sleeper, and Mr_{min} , concordantly with the less vertical loaded sleeper or unloaded sleeper – which is on the sector of railway track between the most distant axle where coming on the upplift of track.

The SCFJ model was presented in [5] and it was used in numerical experiments depicted in the following. It allowes the use of a linear or tri-linear characteristic curves (fig. 5).

INTERSECTION

http://www.ce.tuiasi.ro/intersections

Parametrical study of the effect ... on the stability of continuous welded rail

3. THE COMPARISON OF THE RESULTS WITH THOSE PROVIDED BY THE OTHER SIMILAR MODELS

The values of critical temperature are very important in the analysis of the stability of continuous welded rail (CWR), i.e. the maximum increase of temperature T_{max} over which the buckling of CWR will be surely coming on - and the minimum increase of temperature T_{min} – under which the buckling of CWR will surely not be coming on [2, 3, 5, 6, 7, 12, 13].

The numerical experiment shown in [6, 7, 13] for testing of the SCFJ model – in wich the torsional resistance of fastenings is linear and it is independent of the vertical vehicle load – was repeated. It resulted maximum 1,5 % difference in regard to the other models for the torsional resistance of fastening like in [7].

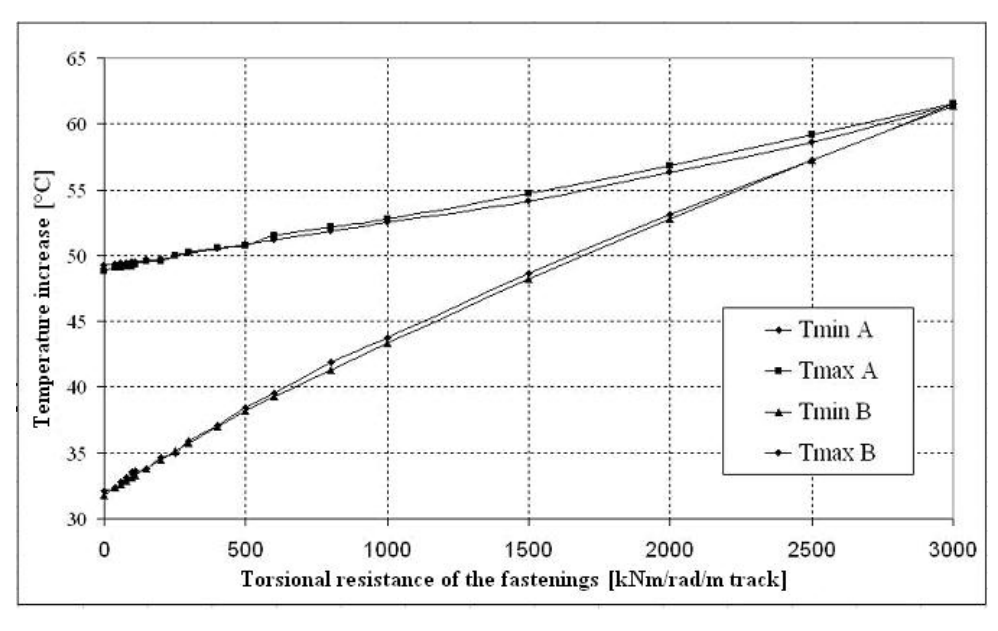


Fig. 6. The increases of critical temperature versus the torsional resistance of the fastenings [6, 7, 13].

A graphical representation of the results is shown in fig. 6, where the maximum and minimum critical temperatures by [7] were marked by $T_{min\ A}$ and $T_{max\ A}$, and the maximum and minimum critical temperatures by SCFJ were marked by $T_{min\ B}$ and $T_{max\ B}$, respectively. It results a very good correspondence between both results. Torsional resistance of fastenings increase, minimum critical temperature T_{min} increase more than maximum critical temperature T_{max} .



INTERSECTION

http://www.ce.tuiasi.ro/intersections

V.V. Ungureanu, A. Dósa

The explanation of this behaviour is that the rotations and transversal dispacements of rails are smaller for minimum critical temperature T_{min} , while maximum critical temperature T_{max} have more important values, therefore the mobilization of torsional resistance of fastenings is bigger for minimum critical temperature T_{min} . It is important to point out that the common values of torsional resistance of fastenings are in the range of $0 \div 500 \text{ kNm/rad/m}$ track.

4. THE INFLUENCE OF THE TORSIONAL RESISTANCE OF FASTENINGS ON THE STABILITY OF CWR TRACK

For former example the vehicle was eliminated to distinguish the influence of torsional resistance of fastenings when the track is loaded only with temperature variations. The analises of results relieve, in absence of vehicle load, a growth of T_{min} with about 2%, and a growth of T_{max} with about 3,5%, comparatively with the results obtained in presence of vehicle loads.

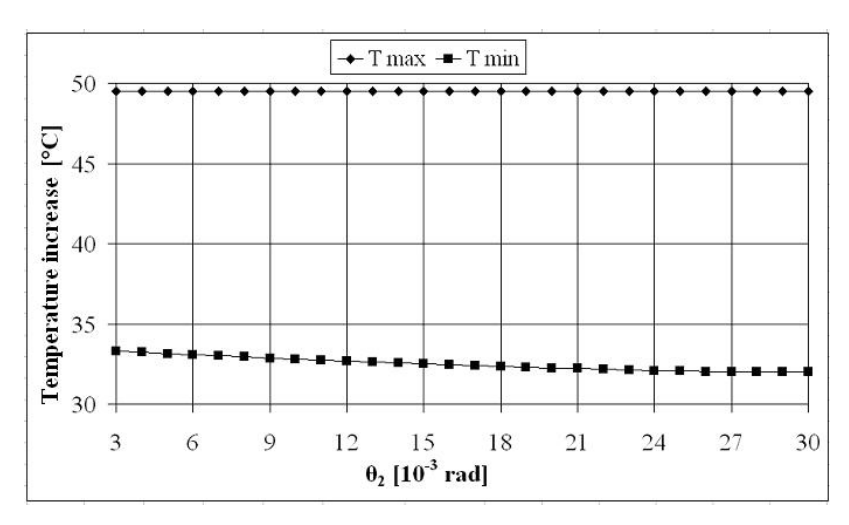


Fig. 7. The variation of critical temperature versus the value of rotation angle of rail in fastenings θ_2 for a constant value $\theta_1 = 3 \cdot 10^{-3}$ rad.

It was analyzed the influence of level $\theta_1 \div \theta_2$ size, for that the value of torsional resistance of fastenings is constant, on the value of the critical temperature is increasing. It was considered a reference value of resistant moment $M_o = 333.75$ Nm/rad/m track, adjusted in terms of vertical load from vehicle. It was considered that the value of fastening stiffness for the rotations of rail in fastening which exceed θ_2 is equal with the stiffness for the first branch – i.e. it is that which characterizes the rotations between 0 and θ_1 . It was obtained the results shown in

INTERSECTII

http://www.ce.tuiasi.ro/intersections

Parametrical study of the effect ... on the stability of continuous welded rail

fig. 7, for a constant value $\theta_1 = 3 \cdot 10^{-3}$ rad – which correspond at a K type fastening – and for values of θ_2 in range $3 \cdot 10^{-3} \div 30 \cdot 10^{-3}$ rad. The values of θ_2 were considered for a step by $1 \cdot 10^{-3}$ rad. It was observed that T_{max} stays constant, the corresponding rotation being less than θ_1 , and T_{min} decreases with about 4% for $\theta_2 = 28 \cdot 10^{-3}$ rad, thereupon the value of T_{min} being constant because the appropriate rotation is smaller than θ_2 , i.e. it can say that the behavior of model is bi-linear, not tri-linear.

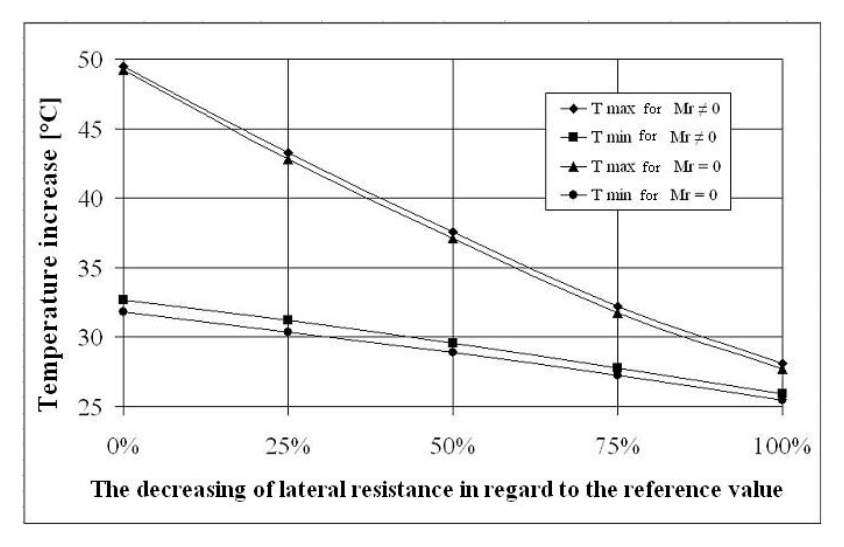


Fig. 8. The variation of critical temperature versus the decrease of lateral resistance.

In order to mark out the effect of torsional resistance of fastenings on stability of CWR track it was also analyzed the situation with reduced lateral resistance on the central zone of the misalignment. Hereby, it was investigated the situation in which the lateral resistance is reduced up 100%, 75%, 50% and 25% at 4 sleepers placed on central zone of the misalignment, as for the situation in which the torsional resistance is zero, as for the situation in which that has the same values like in the previous numerical experiment. It was considered $\theta_1 = 3 \cdot 10^{-3}$ rad and $\theta_2 = 12 \cdot 10^{-3}$ rad. The results of this numerical experiment are shown in fig. 8. Though the influence of torsional resistance is small, if the results are compared it can be observed that T_{min} is more influenced by the torsional resistance of the fastenings than T_{max} .

Almost all developed models neglect the influence of torsional resistance because they are taking in account the small influence this parameter.

However, it was observed in numerical and laboratory experiments that in some cases the torsional resistance of the fastenings can have a significant influence on the track stability. Therefore a more trusty analysis of the track stability must take in account the effect of this factor, also.



INTERSECTII http://www.ce.tuiasi.ro/intersections

V.V. Ungureanu, A. Dósa

References

- 1. *** ERRI D170-RP5 Track component dimensions. Standardisation of characteristics and acceptance tests. Study of fastening system characteristics and test methods, European Rail Research Institute, Utrecht, September 1994.
- *** ERRI D202-RP3 Improved knowledge of forces in CWR track (including switches) -Theory of CWR track stability, European Rail Research Institute, Utrecht, February 1995.
- 3. Bao, Y. L. Three-dimensional stability/lateral shift analysis of continuous welded rail (CWR) track and innovative methods to enhance CWR track performance, PhD Thesis, University of Illinois at Urbana-Champaign, Urbana, Illinois, 1998.
- 4. Chatkeo, Y. Die Stabilität des Eisenbahngleises im Bogen mit engen Halbmessern bei hohen Axialdruckkräften, Mitteilungen des Prüfamtes für Bau von Landverkehrswegen der TU München, Heft 46,1985.
- 5. Dósa, A., Ungureanu, V.V. SCFJ model discret de pierdere a stabilității căii fără joante, Infrastructuri eficiente pentru transporturi terestre – Zilele Academice Timisene, 24-25 mai 2007, Timişoara.
- 6. Esveld, C. A better understanding of continuous welded rail track, Rail Engineering International, No. 4, 1996.
- 7. Esveld, C. Improved knowledge of CWR track, Delft University Press, 1997.
- 8. Herman, A. Contribuții la calculul căii fără joante, Teză de doctorat, Universitatea "Politehnica" Timișoara, Facultatea de Construcții, Timișoara, 1998.
- Radu, C., Poștoacă, S., Sianu, C. Unele aspecte privind stabilitatea căii fără joante, Consfătuirea pe țară a lucrătorilor de drumuri, poduri și căi ferate - vol. II, Tușnad, 1982.
- 10. Rangosch, R. S. Lagestabilität lückenloser Meterspurgleise in kleinen Bogenradien, Dissertation ETH Nr. 11322, Schriftenreihe des IVT Nr. 108 Zürich, Oktober 1995.
- 11. Rădulescu M. Calea fără joante Stabilitatea și calculul eforturilor, Editura Transporturilor și Telecomunicațiilor, București, 1963.
- 12. Ungureanu, V.V. Modele de pierdere a stabilității căii fără joante, Referatul nr.3 din cadrul stagilului de pregătire pentru doctorat, Universitatea "TRANSILVANIA" din Brașov, Facultatea de Construcții, Brașov, 2006.
- 13. Van, M.A.- Stability of Continuous Welded Rail Track, PhD Thesis, Delft University Press, 1997, ISBN:90-407-1485-1.

